THE ROLE OF KIRREL3 IN HIPPOCAMPAL MOSSY FIBER SYNAPSE DEVELOPMENT

by

Elizabeth Anne Martin

A dissertation submitted to the faculty of
The University of Utah
in partial fulfillment of the requirements for the degree of

Doctor of Philosophy

Department of Neurobiology and Anatomy

The University of Utah

December 2018

The University of Utah Graduate School

STATEMENT OF DISSERTATION APPROVAL

The dissertation of **Elizabeth Anne Martin**

has been approved by the following supervisory committee members:

Megan E. Williams	, Chair	**10/8/18** Date Approved
Jan Christian	, Member	**10/8/18** Date Approved
Michael Deans	, Member	**10/8/18** Date Approved
Adam Douglass	, Member	**10/8/18** Date Approved
Erik Jorgensen	, Member	**10/8/18** Date Approved

and by **Monica L. Vetter**, Chair/Dean of

the Department/College/School of **Neurobiology and Anatomy**

and by David B. Kieda, Dean of The Graduate School.

ABSTRACT

Synaptic target specificity, whereby neurons make distinct types of synapses with distinct target cells, is critical for proper brain function, yet the molecules driving this process are poorly understood. This work demonstrates that, contrary to established dogma, wildtype hippocampal mossy fiber (MF) filopodia do not synapse exclusively onto GABA neurons as previously thought, but instead synapse with similar frequency onto GABA neurons and CA3 neurons in developing mice. Moreover, loss of transmembrane cell adhesion molecule Kirrel3 selectively reduces MF filopodial synapses onto GABA neurons but not those made onto CA3 neurons nor DG-GABA en passant synapses. Consequently, Kirrel3 loss robustly increases CA3 neuron activity during development. In addition, rare Kirrel3 variants found in individuals with neurodevelopmental disorders reduce both cell-cell aggregation and specific synapse formation. In sum, the selective loss of MF filopodial synapses with GABA neurons likely underlies the hippocampal activity imbalance observed in Kirrel3 knockout mice and may impact neural function in patients with Kirrel3-dependent neurodevelopmental disorders. These findings demonstrate that subtle synaptic changes during development can greatly impact circuit function, solidify Kirrel3 as a bona fide synapse specificity molecule, and provide the first insight toward understanding the basis of Kirrel3-dependent neurodevelopmental disorder.

This dissertation is dedicated to Will, Watney, Tiz, and Tom,

the best family a girl could have.

TABLE OF CONTENTS

LIST OF FIGURES

ACKNOWLEDGEMENTS

I would first like to thank the members of the Williams lab for their support and encouragement. My mentor, Dr. Megan Williams, took a chance on a graduate student with little background in research science and spent the time, resources, and patience on crafting me into the scientist I am today. I am endlessly grateful for the opportunities she has given me, as well as for the life coaching she has also provided. My fellow graduate students, Dr. Raunak Basu and Matthew Taylor, were everything I could have hoped for in science compatriots. I am indebted to them for their constant willingness to think together to solve problems and work hard to accomplish our goals. I also want to thank Jennifer Hunter, Dr. Randi Rawson, Dr. Shruti Muralidhar, and Kara Graves for their assistance in lab projects and their constant optimism. Lastly, I would like to thank Derek Woodruff, Allison Schneggenburger, and Keegan Teeter for their assistance tracing mossy fiber synapses. Without their aid, I would still be working on that project.

I would next like to thank the members of my dissertation committee, Dr. Jan Christian, Dr. Erik Jorgensen, Dr. Michael Deans, and Dr. Adam Douglass, for their helpful insights contributing to my project, and for always answering the ceaseless stream of Doodle polls necessary to schedule meetings. I would also like to thank the administrative staff, including Nicole Caldwell, Neha Kushan, Liz Woolsey, Mark Nielson, and Todd Bjorklund, who were supportive at all time points of my graduate

school career, but especially in helping me successfully negotiate the use of my grants. Thanks also to Dr. Monica Vetter for championing the Neurobiology and Anatomy Department at the University of Utah and making it what it is today.

I want to also thank my funding sources. I was privileged to receive several grants in my graduate school career that opened up so many opportunities to me. The Autism Speaks Weatherstone Predoctoral Fellowship, The NIH Developmental Biology Training Grant, and the John Weis Memorial Graduate Student Award each were huge milestones guiding my professional development. I would also like to thank every person who helped me write these grants, as well as the drafts for numerous other grant submissions, paper submissions, and other pieces of writing throughout graduate school.

Finally, I wish to thank my husband, Will Martin. He helped me decide that to be happy, I needed to change my career to fulfill my desire to investigate the world through science. He has offered continuous support to me to help overcome self-doubt and accomplish my goals, and has been my constant companion in the ups and downs of life.

CHAPTER 1

INTRODUCTION

The brain is considered to be the most complex object in the known universe. Billions of cells must elegantly come together to create trillions of specialized cell-cell junctions called synapses that communicate every thought and action of our lives. There are many types of brain cells, or neurons, and they must form specific types of synapses between each other for proper brain function to occur. However, the rules governing how specific types of neurons form specific types of synapses are still relatively unknown. Moreover, disrupting one type of synapse but not others can alter the balance of neural activity within the brain, resulting in disease. Neurodevelopmental disorders are increasingly thought to be synaptopathies, or disorders of the synapse, but the fundamental molecular players failing to synthesize these precise circuit connections in disease are yet to be understood. One such fundamental player is Kirrel3, which regulates a particular kind of synapse within the hippocampus, a region of the brain necessary for learning and memory. In this introduction, I will present the concept of synapse specificity, followed by background on synaptic molecules and disease, and conclude with a primer on Kirrel3.

What is synapse specificity?

During development, an axon from one type of neuron must contact a dendrite from another type of neuron, and build a particular kind of synapse. This must occur trillions of times over to accomplish proper brain connectivity. These synapses can be categorized by their size, molecular composition, and localization. For instance, CA3 pyramidal neurons within the hippocampus make three distinct types of excitatory synapses along their dendritic length; and each of these synapse types can be

distinguished based on their morphology, presynaptic partner, and distinct molecular properties (Rawson, Martin, & Williams, 2017).

One theory to explain this precise organization is the existence of molecular identification tags expressed by specific populations of neurons. These molecules are thought to also localize to particular regions of the neurons. These factors would instruct incoming axons to specific neuronal subregions to make specific types of synapses (Sperry, 1963). For example, a CA3 dendrite makes distinct synapses with axons from dentate granule (DG) neurons, CA3 neurons, and entorhinal cortex (EC) neurons in particular subregions. In support of Sperry's theory, loss of cell adhesion molecule Cadherin-9 disrupts specifically DG synapses onto CA3 dendrites (Williams et al., 2011). This theory requires a diversity of synapse specificity molecules to act within particular temporal and spatial windows to specify each synapse type. By examining the molecular composition of synapses, it has been hypothesized that trans-synaptic cell adhesion molecule (CAM) families are good candidates for this role (Sanes & Yamagata, 2009).

Synaptic cell adhesion molecules

Cell adhesion molecules (CAMs) are proteins present on the cell surface that act to bind other cell surface molecules on other cells, or extracellular matrix molecules, to facilitate cell-cell binding. There are a multitude of CAMs expressed in various cell types. Cadherins, Leucine-Rich Repeat Transmembrane (LRRTM) proteins, neurexins, neuroligins, ephrins, teneurins, and many others are CAMs that have emerged as necessary players in synapse specificity (Basu, Taylor, & Williams, 2015; Leamey & Sawatari, 2014; Shapiro, Love, & Colman, 2007; Südhof, 2008; Südhof, 2017). These

proteins are composed of an extracellular domain that binds with transcellular partners to mediate cell-to-cell contacts, a transmembrane domain, and an intracellular domain thought to contact the necessary scaffolding molecules for synapse formation and function.

In addition, these molecules can be alternatively spliced to generate even larger numbers of potential specificity molecules (Shapiro et al., 2007). For example, the Down syndrome cell adhesion molecule (Dscam) gene of the immunoglobulin superfamily of CAMs can express more than 38,000 different mRNAs via 95 alternative exons in flies, resulting in over 19,000 discrete extracellular domains. These numerous isoforms are developmentally regulated, can be found in distinct brain regions, and display isoform-specific binding (Celotto et al., 2001; Wojtowicz et al., 2004). These characteristics are well-suited for molecules driving specific wiring of the brain. Thus, it is valuable to determine the molecules present in and around synapses that contribute to the brain's ability to wire itself.

Synaptic molecules and disease

In the search for the etiology of neurodevelopmental disorders, hundreds of genes encoding for synaptic proteins have been identified as containing damaging copy number variations, deletions, and point mutations. These findings have inspired the theory that synapses and their dysfunction are the root cause of these disorders, now commonly called synaptopathies (Torres, Vallejo, & Inestrosa, 2017). Introduction of these genetic variants to stable systems are found to impact synapses in numerous ways. For example, Neuroligins (NLGN) are a set of five genes (NLGN1, 2, 3, 4, 4Y) encoding for

transmembrane cell adhesion postsynaptic proteins that serve as heterophilic partners for presynaptic Neurexins. These neuronal complexes are thought to mediate synapse development and/or remodeling in either excitatory or inhibitory neurons depending on the protein type (Chih, 2004; Rawson et al., 2017; Südhof, 2017). As both Neuroligins and Neuerxins are commonly linked with autistic disorders, mutations of these proteins have been investigated for altered function. When mutation NLGN3 R451C is transfected into COS cells and tested for surface biotinylation, reduced surface expression is observed. Subsequent cellular localization assays suggest the mutated protein is sequestered in the endoplasmic reticulum (Chih et al., 2004). Additionally, when overexpressed, wildtype Neuroligin localizes to dendritic spines and increases synapse number. However, when observing the mutated protein in cultured hippocampal neurons, very little is observed in dendritic spines. However, this again appears to be primarily because of cellular sequestration and not a defect in the ability to induce synapse formation as the few proteins able to make it to the spine do appear to recruit presynaptic elements (Chih et al., 2004). Thus, examining the point mutations found in individuals suffering from neurodevelopmental disease can identify critical protein domains as well as help us understand the root causes of neurodevelopmental disease.

Another way synaptic protein alterations are thought to contribute to neurodevelopmental disorders is through perturbation of the excitation/inhibition (E/I) balance. A properly functioning brain reaches a stable circuit homeostasis between excitatory and inhibitory neurons to orchestrate precise neuronal firing patterns. If a population of excitatory or inhibitory synapses is lost or never formed, the E/I balance can shift, resulting in altered circuit function.

It was suggested in 2003 that autism spectrum disorders (ASD) might result from an increase in cortical circuit excitation via reduced inhibition (Rubenstein & Merzenich, 2003). Since this proposition, evidence has been found for both increases and decreases in excitation over inhibition in relation to ASD. This suggests that rather than whole brain shifts towards excitation or inhibition, it is more likely that individual circuits are uniquely altered. It is also probable that primary circuit imbalances can drive secondary effects. For example, reduced excitation can lead to increased inhibition in one circuit, which then subsequently causes either increased or reduced excitation in a second circuit depending on the output from the originating circuit. This also illustrates how it can be difficult to distinguish primary circuit defects from a large pool of possible secondary effects (Nelson & Valakh, 2015).

Thus, while E/I imbalances are now generally attributed to ASD, little is known about the specific source of the imbalance (Nelson & Valakh, 2015). Sadly, much of the evidence for such imbalances results from the use of imprecise methods such as FMRI (functional magnetic resonance imaging), which can only identify regions of gross imbalances. A single FMRI voxel contains more than a million synapses, thus precise circuit imbalances cannot be identified from this type of investigation. As a result, very little is known about specific circuit imbalances that could lead to disease, and even less about the molecules driving synapse formation and stabilization that organize these circuits. Therefore, it becomes critical to identify these molecules whose dysfunction leads to specific E/I imbalances to tease apart the true etiology of these disorders.

Kirrel3

Kirrel3 is a member of the immunoglobulin superfamily with five extracellular immunoglobulin domains, a single-pass transmembrane protein, and an intracellular domain with a single PDZ-binding motif located at its C-terminal tip. The PDZ-binding domain implies binding with a number of synaptic molecules including PSD-95 and ZO-1 (Huber et al., 2003; Lee & Zheng, 2010). Three Kirrel family members exist called Kirrel 1, 2, and 3 corresponding to Neph1, Neph 3, and Neph2, respectively. Previously, these molecules had been examined for their ability to drive specific cell-cell contact through extracellular homophilic binding. Neph2/Kirrel3 has been investigated for its role in kidney slit diaphragm formation in which it is thought to interact intracellularly with ZO-1 and podocin to manage renal filtration by guiding podocyte foot processes (Gerke et al., 2005). In the brain, Kirrel3 was identified to regulate axonal fasciculation of odorant sensory neurons expressing the same odorant receptor onto specific glomeruli located within the olfactory bulb (Serizawa et al., 2006).

In terms of synapses, Kirrel3's ortholog SYG-1 has been studied for its role in directing specific synapse formation at HSN neurons in *C. elegans*. Here, it heterophilically binds SYG-2, otherwise known as nephrin. Loss of SYG-1 results in fewer synapses onto correct target cells and an increase in synapses onto improper targets (Shen & Bargmann, 2003; Shen, Fetter, & Bargmann, 2004). However, prior to our investigation of Kirrel3, no lab had examined Kirrel3's role in mammalian synapse formation.

Kirrel3 and disease

Kirrel3 is repeatedly linked to neurodevelopmental disorders through several copy number variations, deletions, and exonic missense point mutations identified in patients with autism spectrum disorders (Ben-David & Shifman, 2012; Cheng, Quinn, & Weiss, 2013; De Rubeis et al., 2014; Iossifov et al., 2012; Kalsner et al., 2017; Michaelson et al., 2012; Neale et al., 2012; Talkowski et al., 2012), intellectual disability (Bhalla et al., 2008; Kaminsky et al., 2011; Talkowski et al., 2012), and Jacobsen syndrome (Guerin et al., 2012). Jacobsen syndrome is caused by the loss of the tip of chromosome 11 where the Kirrel3 gene is located. It is a developmental disorder that is often found to be comorbid with ASD, epilepsy, and intellectual disability (Guerin et al., 2012). Several of these Kirrel3 variants are proposed to be pathogenic; however, the nature of this pathogenicity is unknown. The exonic point mutations are found both in the extracellular and intracellular domains, and have low minor allele frequency (MAF) scores that identify them to be extremely rare variants within the population.

With these links to disease, Kirrel3 knockout mice have been independently generated and tested for behavioral abnormalities by three research groups (Choi et al., 2015; Hisaoka et al., 2018; Prince et al., 2013). The first group examined Kirrel3 knockout mice solely in coordination with a study on Kirrel3's role in the olfactory bulb. They used a resident-intruder assay in which mice use urine pheromonal cues to respond aggressively to intruders in their territory and found Kirrel3 knockout mice displayed reduced male-male aggression (Prince et al., 2013).

The next two studies were both more comprehensive and tested Kirrel3 knockout mice in a battery of behavioral assays. Choi et al. examined adult mice in the open field

test, elevated plus maze test, three-chamber social interaction test, buried food test, self-grooming, novel object recognition test, Morris water maze test, contextual fear conditioning and extinction, contextual discrimination, radial arm maze test, and for 24 hour movement (2015). They report Kirrel3 knockouts are hyperactive in a familiar environment, but not a novel environment. In addition, they find impaired novel object recognition indicating potential dysfunction in the hippocampus, the center for learning and memory in the brain (Choi et al., 2015). These tests were all completed in adult animals and the behavior of younger Kirrel3-deficient animals was not examined.

The most recent analysis of Kirrel3 knockouts by Hisaoka et al. (2018) examined the mice in the three-chambered social approach test, social recognition test, USV recording test (which examines alterations in ultrasonic vocalizations), open field test, light-dark transition test, rotarod test, elevated plus maze test, and ASR and PPI tests (a set of startle response assays that examine hearing defects). The researchers reported that adult Kirrel3-deficient animals spend far less time investigating novel mice in their home environment compared with wildtype mice, which they interpret as a defect in social investigation and social recognition memory. They also report several social communication defects. They find Kirrel3-deficient pups increase the number of ultrasonic calls upon separation from the mother, adult male mice make fewer calls to oestrous female mice, and in the resident-intruder assay, they find both Kirrel3 knockout male and female pairs make fewer calls to intruders, failing to establish a social dominance hierarchy. In agreement with Choi et al., they find increased hyperactivity within the home cage, but only during the light phase. Rearing was also found to be increased as was motor learning as tested by rotarod. They report Kirrel3-deficient

animals were less sensitive to both acoustic startle and pain stimuli tests as Kirrel3 knockouts required greater stimuli in both to respond, which indicates deficits in hearing. Finally, their findings for the male-male aggression resident-intruder assay were consistent with the previous report from Prince et al. that described reduced aggression in Kirrel3 knockout animals (Hisaoka et al., 2018).

These studies support a role for Kirrel3 in both social behavior and memory. Thus, it will be valuable to examine Kirrel3 for altered synaptic function in brain regions known to regulate these behaviors, such as the hippocampus. In addition, human and mouse Kirrel3 are 98% identical and most, if not all, Kirrel3 variant sites are conserved. Connecting Kirrel3 gene variants to impaired neuronal function is imperative for clarifying how Kirrel3 contributes to healthy brain formation and for generation of specific and effective therapies to combat Kirrel3-dependent developmental disorders.

Dissertation overview

In this chapter, I have discussed synaptic specificity and the potential for a Kirrel3-specific mechanism of synapse formation important for social behavior and memory. In Chapter 2, I will describe research investigating the role of Kirrel3 in hippocampal synapse formation. In Chapter 3, I will describe research into how Kirrel3 alters the synaptic landscape of mossy fiber filopodia as well as describe my findings regarding the profile of wildtype mossy fiber circuitry in developing animals. In Chapter 4, I will describe my findings of how particular Kirrel3 variants alter Kirrel3 function. Finally, in Chapter 5, I will discuss potential mechanisms by which Kirrel3 acts within the hippocampus to drive synapse development.

References

Basu, R., Taylor, M. R., & Williams, M. E. (2015). The classic cadherins in synaptic specificity. *Cell Adhesion & Migration, 9*(3), 193-201. doi:10.1080/19336918.2014.1000072

Ben-David, E., & Shifman, S. (2012). Networks of neuronal genes affected by common and rare variants in autism spectrum disorders. *PLoS Genetics, 8*(3). doi:10.1371/journal.pgen.1002556

Bhalla, K., Luo, Y., Buchan, T., Beachem, M. A., Guzauskas, G. F., Ladd, S., . . . Srivastava, A. K. (2008). Alterations in CDH15 and KIRREL3 in patients with mild to severe intellectual disability. *The American Journal of Human Genetics, 83*(6), 703-713. doi:10.1016/j.ajhg.2008.10.020

Cheng, Y., Quinn, J. F., & Weiss, L. A. (2013). An eQTL mapping approach reveals that rare variants in the SEMA5A regulatory network impact autism risk. *Human Molecular Genetics, 22*(14), 2960-2972. doi:10.1093/hmg/ddt150

Chih, B., Afridi, S. K., Clark, L., & Scheiffele, P. (2004). Disorder-associated mutations lead to functional inactivation of neuroligins. *Human Molecular Genetics, 13*(14), 1471-1477. doi:10.1093/hmg/ddh158

Choi, S., Han, K., Cutforth, T., Chung, W., Park, H., Lee, D., . . . Kim, E. (2015). Mice lacking the synaptic adhesion molecule Neph2/Kirrel3 display moderate hyperactivity and defective novel object preference. *Frontiers in Cellular Neuroscience, 9*. doi:10.3389/fncel.2015.00283

De Rubeis, S., He, X., Goldberg, A. P., Poultney, C. S., Samocha, K., Cicek, A. E., . . . Buxbaum, J. D. (2014). Synaptic, transcriptional and chromatin genes disrupted in autism. *Nature, 515*(7526), 209–215. http://doi.org/10.1038/nature13772

Gerke, P. (2005). NEPH2 is located at the glomerular slit diaphragm, interacts with nephrin and is cleaved from podocytes by metalloproteinases. *Journal of the American Society of Nephrology, 16*(6), 1693-1702. doi:10.1681/asn.2004060439

Guerin, A., Stavropoulos, D. J., Diab, Y., Chénier, S., Christensen, H., Kahr, W. H., . . . Chitayat, D. (2012). Interstitial deletion of 11q-implicating the KIRREL3 gene in the neurocognitive delay associated with Jacobsen syndrome. *American Journal of Medical Genetics Part A, 158A*(10), 2551-2556. doi:10.1002/ajmg.a.35621

Hisaoka, T., Komori, T., Kitamura, T., & Morikawa, Y. (2018). Abnormal behaviours relevant to neurodevelopmental disorders in Kirrel3-knockout mice. *Scientific Reports, 8*(1). doi:10.1038/s41598-018-19844-7

Huber, T. B., Schmidts, M., Gerke, P., Schermer, B., Zahn, A., Hartleben, B., . . .

Benzing, T. (2003). The carboxyl terminus of neph family members binds to the PDZ domain protein zonula occludens-1. *Journal of Biological Chemistry, 278*(15), 13417-13421. doi:10.1074/jbc.c200678200

Iossifov, I., Ronemus, M., Levy, D., Wang, Z., Hakker, I., Rosenbaum, J., . . . Wigler, M. (2012). De novo gene disruptions in children on the autistic spectrum, *74*(2), 285–299. http://doi.org/10.1016/j.neuron.2012.04.009

Kalsner, L., Twachtman-Bassett, J., Tokarski, K., Stanley, C., Dumont-Mathieu, T., Cotney, J., & Chamberlain, S. (2017). Genetic testing including targeted gene panel in a diverse clinical population of children with autism spectrum disorder: Findings and implications. *Molecular Genetics & Genomic Medicine, 6*(2), 171-185. doi:10.1002/mgg3.354

Kaminsky, E. B., Kaul, V., Paschall, J., Church, D. M., Bunke, B., Kunig, D., . . . Martin, C. L. (2011) An evidence-based approach to establish the functional and clinical significance of CNVs in intellectual and developmental disabilities. *Genetics in Medicine, 13*, 777–784. doi: 10.1097/GIM.0b013e31822c79f9

Leamey, C. A., & Sawatari, A. (2014). The teneurins: New players in the generation of visual topography. *Seminars in Cell & Developmental Biology, 35*, 173-179. doi:10.1016/j.semcdb.2014.08.007

Lee, H., & Zheng, J. J. (2010). PDZ domains and their binding partners: Structure, specificity, and modification. *Cell Communication and Signaling, 8*(1), 8. doi:10.1186/1478-811x-8-8

Michaelson, J., Shi, Y., Gujral, M., Zheng, H., Malhotra, D., Jin, X., . . . Sebat, J. (2012). Whole-genome sequencing in autism identifies hot spots for de novo germline mutation. *Cell, 151*(7), 1431-1442. doi:10.1016/j.cell.2012.11.019

Neale, B. M., Kou, Y., Liu, L., Ma'ayan, A., Samocha, K. E., Sabo, A., . . . Daly, M. J. (2012). Patterns and rates of exonic de novo mutations in autism spectrum disorders. *Nature, 485*(7397), 242–245. doi: 10.1038/nature11011

Nelson, S., & Valakh, V. (2015). Excitatory/Inhibitory balance and circuit homeostasis in autism spectrum disorders. *Neuron, 87*(4), 684-698. doi:10.1016/j.neuron.2015.07.033

Prince, J. E., Brignall, A. C., Cutforth, T., Shen, K., & Cloutier, J. (2013). Kirrel3 is required for the coalescence of vomeronasal sensory neuron axons into glomeruli and for male-male aggression. *Development, 140*(11), 2398-2408. doi:10.1242/dev.087262

Rawson, R. L., Martin, E. A., & Williams, M. E. (2017). Mechanisms of input and output synaptic specificity: Finding partners, building synapses, and fine-tuning communication. *Current Opinion in Neurobiology, 45*, 39-44. doi:10.1016/j.conb.2017.03.006

Rubenstein, J. L., & Merzenich, M. M. (2003). Model of autism: Increased ratio of excitation/inhibition in key neural systems. *Genes, Brain and Behavior, 2*(5), 255-267. doi:10.1034/j.1601-183x.2003.00037.x

Sanes, J. R., & Yamagata, M. (2009). Many paths to synaptic specificity. *Annual Review of Cell and Developmental Biology, 25*(1), 161-195. doi:10.1146/annurev.cellbio.24.110707.175402

Serizawa, S., Miyamichi, K., Takeuchi, H., Yamagishi, Y., Suzuki, M., & Sakano, H. (2006). A neuronal identity code for the odorant receptor-specific and activity-dependent axon sorting. *Cell, 127*(5), 1057-1069. doi:10.1016/j.cell.2006.10.031

Shapiro, L., Love, J., & Colman, D. R. (2007). Adhesion molecules in the nervous system: Structural insights into function and diversity. *Annual Review of Neuroscience, 30*(1), 451-474. doi:10.1146/annurev.neuro.29.051605.113034

Shen, K., & Bargmann, C. I. (2003). The immunoglobulin superfamily protein SYG-1 determines the location of specific synapses in C. elegans. *Cell, 112*(5), 619-630. doi:10.1016/s0092-8674(03)00113-2

Shen, K., Fetter, R. D., & Bargmann, C. I. (2004). Synaptic specificity is generated by the synaptic guidepost protein SYG-2 and its receptor, SYG-1. *Cell, 117*(4), 553. doi:10.1016/s0092-8674(04)00407-6

Sperry, R. W. (1963). Chemoaffinity in the orderly growth of nerve fiber patterns and connections. *Proceedings of the National Academy of Sciences, 50*(4), 703-710. doi:10.1073/pnas.50.4.703

Südhof, T. C. (2008). Neuroligins and neurexins link synaptic function to cognitive disease. *Nature, 455*(7215), 903-911. doi:10.1038/nature07456

Südhof, T. C. (2017). Synaptic neurexin complexes: A molecular code for the logic of neural circuits. *Cell, 171*(4), 745-769. doi:10.1016/j.cell.2017.10.024

Talkowski, M., Rosenfeld, J., Blumenthal, I., Pillalamarri, V., Chiang, C., Heilbut, A., . . . Gusella, J. (2012). Sequencing chromosomal abnormalities reveals neurodevelopmental loci that confer risk across diagnostic boundaries. *Cell, 149*(3), 525-537. doi:10.1016/j.cell.2012.03.028

Torres, V. I., Vallejo, D., & Inestrosa, N. C. (2017). Emerging synaptic molecules as candidates in the etiology of neurological disorders. *Neural Plasticity, 2017*, 1-25. doi:10.1155/2017/8081758

Williams, M., Wilke, S., Daggett, A., Davis, E., Otto, S., Ravi, D., . . . Ghosh, A. (2011). Cadherin-9 regulates synapse-specific differentiation in the developing hippocampus. *Neuron, 71*(4), 640-655. doi:10.1016/j.neuron.2011.06.019

Wojtowicz, W. M., Flanagan, J. J., Millard, S., Zipursky, S., & Clemens, J. C. (2004). Alternative splicing of drosophila dscam generates axon guidance receptors that exhibit isoform-specific homophilic binding. *Cell, 118*(5), 619-633. doi:10.1016/j.cell.2004.08.021

CHAPTER 2

THE INTELLECTUAL DISABILITY GENE KIRREL3 REGULATES TARGET-SPECIFIC MOSSY FIBER SYNAPSE DEVELOPMENT IN THE HIPPOCAMPUS

Reprint of: Martin, Muralidhar et al. (2015). The intellectual disability gene Kirrel3 regulates target-specific mossy fiber synapse development in the hippocampus. eLife. Reprinted with permission.

eLIFE elifesciences.org

SHORT REPORT

The intellectual disability gene Kirrel3 regulates target-specific mossy fiber synapse development in the hippocampus

E Anne Martin[1†], Shruti Muralidhar[1†], Zhirong Wang[1], Diégo Cordero Cervantes[1], Raunak Basu[1], Matthew R Taylor[1], Jennifer Hunter[1], Tyler Cutforth[2], Scott A Wilke[3], Anirvan Ghosh[4], Megan E Williams[1*]

[1]Department of Neurobiology and Anatomy, University of Utah School of Medicine, Salt Lake City, United States; [2]Department of Neurology, Columbia University, New York City, United States; [3]Neurobiology Section, Division of Biological Sciences, University of California, San Diego, San Diego, United States; [4]Neuroscience Discovery, Roche Innovation Center Basel, F. Hoffmann-La Roche, Basel, Switzerland

Abstract Synaptic target specificity, whereby neurons make distinct types of synapses with different target cells, is critical for brain function, yet the mechanisms driving it are poorly understood. In this study, we demonstrate Kirrel3 regulates target-specific synapse formation at hippocampal mossy fiber (MF) synapses, which connect dentate granule (DG) neurons to both CA3 and GABAergic neurons. Here, we show Kirrel3 is required for formation of MF filopodia; the structures that give rise to DG-GABA synapses and that regulate feed-forward inhibition of CA3 neurons. Consequently, loss of Kirrel3 robustly increases CA3 neuron activity in developing mice. Alterations in the Kirrel3 gene are repeatedly associated with intellectual disabilities, but the role of Kirrel3 at synapses remained largely unknown. Our findings demonstrate that subtle synaptic changes during development impact circuit function and provide the first insight toward understanding the cellular basis of Kirrel3-dependent neurodevelopmental disorders.
DOI: 10.7554/eLife.09395.001

***For correspondence:** megan.williams@neuro.utah.edu

[†]These authors contributed equally to this work

Competing interests: The authors declare that no competing interests exist.

Funding: See page 13

Received: 12 June 2015
Accepted: 13 October 2015
Published: 17 November 2015

Reviewing editor: Graeme W Davis, University of California, San Francisco, United States

Introduction

Executing cognitive tasks requires coordination among neural circuits. Therefore, neurons usually send and receive neural information with different synaptic partners. One way neurons differentially regulate activity among partners is by forming different types of synapses with each partner (***Williams et al., 2010***; ***Emes and Grant, 2012***). This kind of synaptic target specificity is exquisitely exemplified by hippocampal mossy fiber (MF) synapses. MF synapses connect glutamatergic dentate granule (DG) neurons to glutamatergic CA3 neurons and GABAergic interneurons (GABA neurons). The main DG-CA3 synapse consists of a giant presynaptic bouton apposed to a multi-headed CA3 spine called a thorny excrescence (TE). In addition, filopodia project from the main bouton and synapse with nearby GABA neurons (***Frotscher, 1989***; ***Acsády et al., 1998***). Filopodial MF synapses mediate feed-forward inhibition of CA3 neurons and are essential for hippocampal function during learning and memory tasks (***Torborg et al., 2010***; ***Ruediger et al., 2011***). Although main bouton and filopodial MF synapses are physically linked, they have different molecular and functional properties (***Toth et al., 2000***; ***McBain, 2008***). This suggests DG neurons utilize specific cues to construct different types of synapses with CA3 and GABA neurons, but the identity of the target-specific cues is unknown.

eLife digest Nerve cells in the brain connect to each other via junctions called synapses to form vast networks that process information. Much like streets can be joined with stop signs, traffic lights, or exit ramps depending on the flow of traffic, different types of synapses control the flow of information along nerves in distinct ways.

In a region of the brain called the hippocampus, nerve cells called DG neurons are connected to other neurons by two different types of synapses. One type of synapse allows the DG neurons to activate CA3 neurons, while the second type allows the DG neurons to activate GABAergic neurons. These same GABAergic neurons can then inhibit the activity of the CA3 neurons. Therefore, through these two different types of synapses, DG neurons can both increase and decrease the activity of the CA3 neurons. This delicate balance of activity across the two types of DG synapses is very important for the hippocampus to work properly, which is critical for our ability to learn and remember.

Mutations in the gene that encodes a protein called Kirrel3 are associated with autism, Jacobsen's syndrome, and other disorders that affect intellectual ability in humans. Kirrel3 is similar to a protein found in roundworms that regulates the formation of synapses, but it is not known if it plays the same role in humans and other mammals. Now, Martin, Muralidhar et al. studied the role of Kirrel3 in mice.

The experiments show that Kirrel3 is produced in both the DG neurons and the GABAergic neurons, but not the CA3 neurons. Young mutant mice that lacked Kirrel3 made fewer synapse-forming structures between DG neurons and GABAergic neurons than normal mice, but the synapses that connect DG neurons to CA3 neurons formed normally. This disrupted the balance of activity across the two types of DG synapses and the CA3 neurons in the mutant mice were over-active.

Together, Martin, Muralidhar et al.'s findings show that altering the levels of Kirrel3 can alter the balance of synapses in the hippocampus. This may explain how even very small changes in synapse formation during brain development can have a big impact on nerve cell activity. The next challenge is to understand exactly how Kirrel3 helps build synapses, which may lead to the development of new drugs that help to rebalance brain activity in people that lack Kirrel3.

DOI: 10.7554/eLife.09395.002

Kirrel1, 2, and 3 (also known as Neph1, 3, and 2, respectively) are transmembrane immunoglobulin superfamily members (***Figure 1D***). In mice, Kirrels have been studied during formation of the kidney slit diaphragm, an adhesive cell junction for filtering blood (***Donoviel et al., 2001***; ***George and Holzman, 2012***) and in axon targeting of the olfactory and vomeronasal systems (***Serizawa et al., 2006***; ***Prince et al., 2013***). In humans, copy number variations and exonic point mutations in the Kirrel3 gene are associated with intellectual disability, autism, and Jacobsen's syndrome, a rare developmental disorder that often includes intellectual disabilities (***Bhalla et al., 2008***; ***Guerin et al., 2012***; ***Michaelson et al., 2012***; ***Neale et al., 2012***). The Kirrel ortholog SYG-1 regulates synapse formation and axon branching in *Caenorhabditis elegans* (***Shen and Bargmann, 2003***; ***Chia et al., 2014***), but the role of Kirrel3 in mammalian synapse development is unknown. Here, we demonstrate Kirrel3 is a target-specific cue at MF synapses. Kirrel3 specifically regulates development of DG-GABA MF filopodia, which are necessary to constrain excitatory drive to CA3 neurons after DG stimulation.

Results

Kirrel3 is a homophilic, synaptic adhesion molecule

Given the association between Kirrel3 mutations and intellectual disabilities, we investigated the role of Kirrel3 in hippocampal circuits, which are critical for learning and memory, and may be impaired in patients with intellectual disabilities. Kirrel3 protein is enriched in synaptosomes prepared from hippocampal lysates with greatest enrichment at postnatal day (P) 21 (***Figure 1A***). Next, we obtained Kirrel3 knockout mice, which were recently described (***Prince et al., 2013***) and prepared

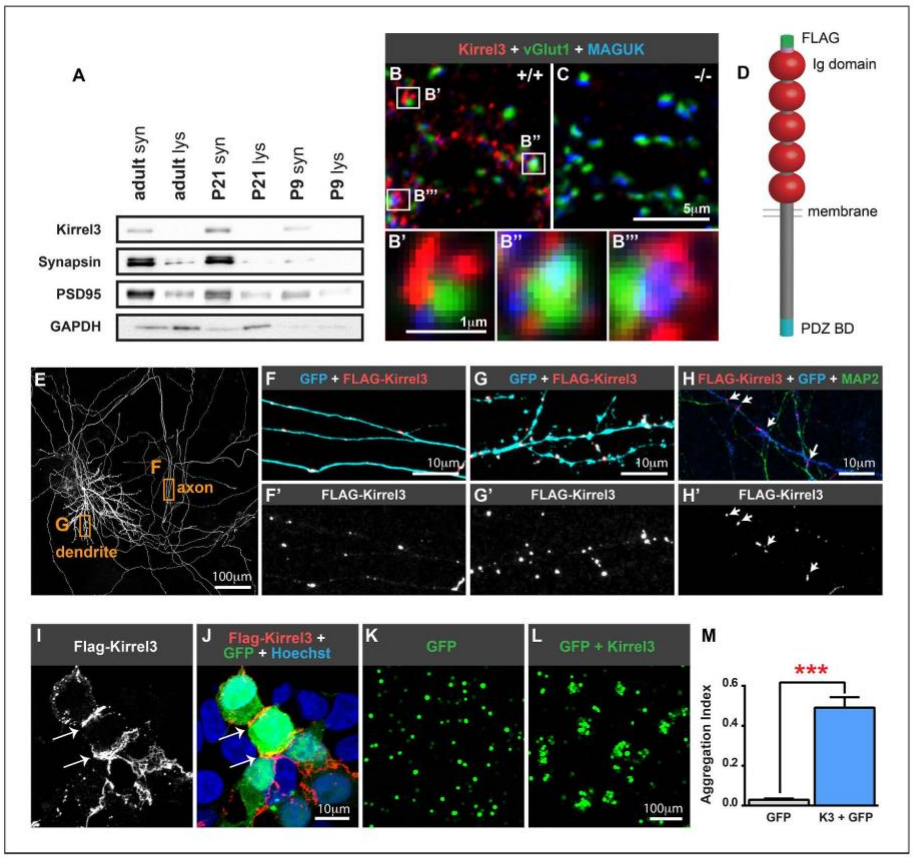

Figure 1. Kirrel3 is a synaptic molecule that mediates homophilic, trans-cellular adhesion. (**A**) Synaptosomes from mouse hippocampi from P9, P21, and adult (P55) were immunoblotted for indicated proteins. lys; lysate. syn; synaptosome. 2 µg protein per lane. (**B**, **C**) 14 days in vitro (DIV) cultured hippocampal neurons immunostained with antibodies against Kirrel3 (red), vGlut1 (green), and MAGUK proteins (blue). Boxed regions in **B** are magnified below in **B′**, **B″**, and **B‴**. Neurons from Kirrel3 knockout mice have no Kirrel3 signal (**C**). (**D**) Diagram of Kirrel3 protein and location of inserted FLAG tag. Ig; immunoglobulin. (**E**–**H**) Cultured hippocampal neurons were co-transfected with FLAG-Kirrel3 and GFP and immunostained for indicated proteins. Anti-FLAG antibodies were added prior to fixation to label only surface Kirrel3. Note surface Kirrel3 is seen as puncta on axons and dendrites after synapse formation in 14DIV neurons (**E**–**G**) and prior to synapse formation in 4DIV neurons (**H**). **H** shows that surface Kirrel3 also clusters at axon–dendrite crossings. Boxed regions in **E** are shown magnified in **F** and **G**. FLAG signal alone is shown in lower panels **F′**, **G′**, and **H′**. (**I**, **J**) Kirrel3 clusters at cell junctions. 293HEK cells were co-transfected with GFP and FLAG-Kirrel3, immunostained for GFP and FLAG, and nuclei labeled with Hoechst. (**K**–**M**) CHO cells transfected with either GFP control or GFP and Kirrel3 were tested for adhesion. Only cells expressing Kirrel3 formed aggregates. Aggregation index was calculated by dividing the total GFP fluorescence in cell aggregates by the total GFP fluorescence in the well. Mean ± SEM are shown, n = 3, *** indicates p = 0.001 by two-tailed t-test.

DOI: 10.7554/eLife.09395.003

The following figure supplements are available for figure 1:

Figure supplement 1. Kirrel1 and 2 are not expressed in the hippocampus.

DOI: 10.7554/eLife.09395.004

Figure supplement 2. Kirrel3 undergoes homophilic binding in cells.

DOI: 10.7554/eLife.09395.005

hippocampal neuron cultures from newborn wild-type and knockout mice. In hippocampal neurons cultured for 14 days in vitro (DIV), Kirrel3 localizes to puncta adjacent to the pre- and post-synaptic markers vGlut1 and MAGUK in wild-type but not knockout neurons (***Figure 1B,C***). This suggests that, like cadherins, Kirrel3 localizes to perisynaptic adhesion zones rather than the synaptic cleft. To determine if Kirrel3 is axonal, dendritic, or both, we analyzed the distribution of surface-expressed FLAG-Kirrel3 (***Figure 1D***) in sparsely transfected neurons using live labeling. Surface FLAG-Kirrel3 is seen as puncta on axons and dendrites of 14DIV neurons (***Figure 1E–G***). Moreover, even prior to synaptogenesis in 4DIV neurons, FLAG-Kirrel3 already has a punctate distribution in axons and dendrites and clusters at axon–dendrite contact points (***Figure 1H***).

Kirrels can function via homophilic binding or heterophilic binding to nephrin, another Ig superfamily member (***Gerke et al., 2003***; ***Serizawa et al., 2006***). However, neither nephrin nor the other Kirrel family members, Kirrel1 and Kirrel2, have appreciable expression in the hippocampus (***Putaala et al., 2001***) (***Figure 1—figure supplement 1***). We noticed Kirrel3 clusters at cell junctions (***Figure 1I,J***) and therefore we directly tested the adhesive ability of Kirrel3 homophilic interactions using a cell aggregation assay. We demonstrate Kirrel3 mediates trans-cellular homophilic binding (***Figure 1K–M*** and ***Figure 1—figure supplement 2***). Taken together, our data indicate Kirrel3 is present at early axon–dendrite contacts, localizes at or near synapses, and is a bona fide homophilic adhesion molecule, all of which implicate Kirrel3 in synapse development.

Hippocampal DG and GABA neurons express Kirrel3

Next, we determined which hippocampal neurons express Kirrel3. In developing P14 and adult hippocampi, Kirrel3 mRNA is present in two cell types: (1) DG neurons and (2) scattered cells of the hilus and area CA3 (***Figure 2A–D*** and ***Figure 2—figure supplement 1A***). Correspondingly, Kirrel3 protein is present in the molecular and stratum lucidum layers of the hippocampus, containing DG dendrites and axons, respectively (***Figure 2E***). It is also present in scattered cells of the hilus and area CA3 (***Figure 2F***) and faintly in the stratum lacunosum-moleculare, which contains axons from entorhinal cortex. No Kirrel3 signal was detected in knockout mice (***Figure 2G,H*** and ***Figure 2—figure supplement 1B***). Instead, Kirrel3 knockout mice have farnesylated GFP in frame after exon 1 so they express membrane-associated GFP instead of Kirrel3 (***Prince et al., 2013***). Examination of GFP expression in knockout mice indicates that again, Kirrel3 is selectively expressed by DG neurons and scattered cells of area CA3 (***Figure 2I–O***). Notably, we never observe GFP expression in CA3 neurons (***Figure 2—figure supplement 1C–E***).

The scattered Kirrel3-positive cells reside mainly outside the pyramidal layer and have GFP-labeled arbors. This suggests they may be GABAergic interneurons. To test this, we co-stained P14 Kirrel3 heterozygous and knockout mice with antibodies against GFP to identify Kirrel3-expressing cells and GABA to identify GABAergic interneurons (***Figure 2I–S*** and ***Figure 2—figure supplement 2***). We find that nearly all Kirrel3-expressing cells express GABA (***Figure 2S***). Conversely, about 20% of all GABA neurons in area CA3 express Kirrel3 (***Figure 2S***). We also co-stained with several common GABA neuron markers and find that two thirds (about 67%) of Kirrel3/GABA neurons express calbindin (***Figure 2P–S***) and these Kirrel3-positive neurons make up about half of all calbindin-positive interneurons. Notably, glutamatergic DG neurons also highly express Kirrel3 and calbindin, providing a shared molecular profile between these neuronal populations. Kirrel3 cell populations are similar in P14 Kirrel3 heterozygous and knockout mice (***Figure 2—figure supplement 2***), suggesting that complete loss of Kirrel3 does not change cell fate or induce cell death of the neurons examined. Taken together, we find that, in the hippocampus, DG neurons and a subset of calbindin-positive GABA neurons selectively express Kirrel3.

Kirrel3 regulates MF filopodia development

Because Kirrel3 is a homophilic molecule expressed by DG and GABA neurons, we hypothesized Kirrel3 homophilic interactions may specifically regulate formation of MF filopodia connecting DG axons to GABA dendrites during development (***Figure 3A***). To test this, we analyzed MF presynaptic morphology in Kirrel3 wild-type and knockout mice at P14, the peak of MF synaptogenesis. DiI crystals were placed in the DG cell body layer of fixed brains. After 1 week, dye diffuses along DG axons and labels MF presynaptic terminals (***Figure 3B–G***). We discovered Kirrel3 knockout mice have significantly fewer and shorter filopodia than wild-type (***Figure 3B–M*** and ***Figure 3—figure***

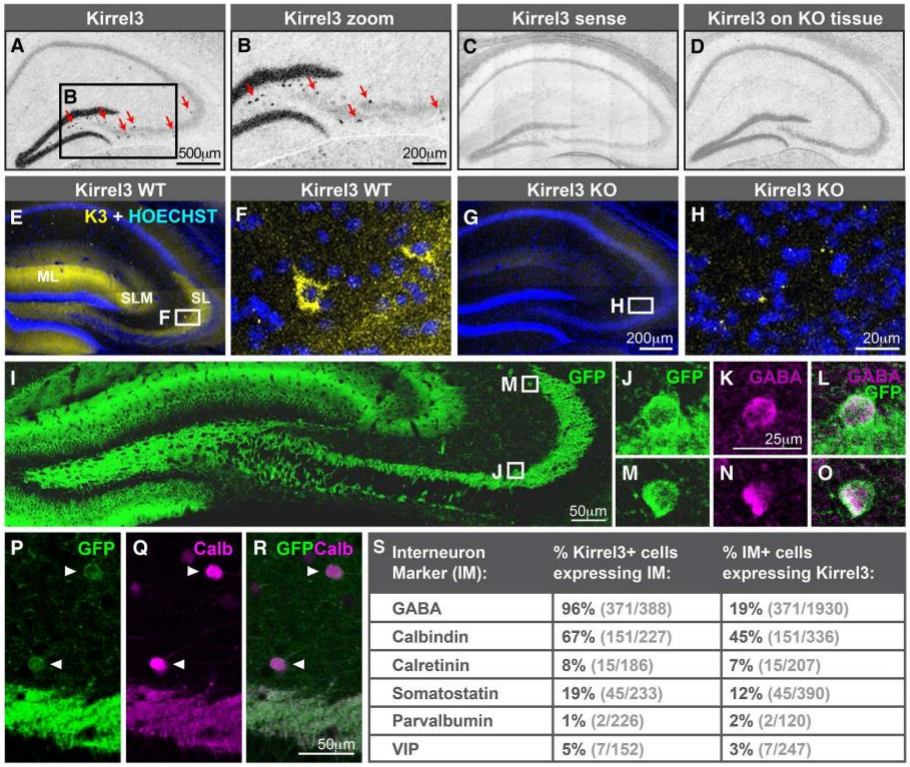

S Interneuron Marker (IM):	% Kirrel3+ cells expressing IM:	% IM+ cells expressing Kirrel3:
GABA	96% (371/388)	19% (371/1930)
Calbindin	67% (151/227)	45% (151/336)
Calretinin	8% (15/186)	7% (15/207)
Somatostatin	19% (45/233)	12% (45/390)
Parvalbumin	1% (2/226)	2% (2/120)
VIP	5% (7/152)	3% (7/247)

Figure 2. Hippocampal DG and GABA neurons express Kirrel3. (**A–D**) In situ hybridizations for Kirrel3 mRNA on adult P60–P70 hippocampal sections from WT (**A–C**) and KO (**D**) mice. A negative control sense probe on WT tissue is shown in **C**. Red arrows in boxed region of **A** point to scattered Kirrel3-expressing cells shown magnified in (**B**). (**E–H**) Hippocampal sections from Kirrel3 WT (**E**, **F**) and KO (**G**, **H**) mice were immunostained with anti-Kirrel3 antibodies (yellow) and Hoechst (blue). **F** and **H** are magnified images of boxed regions in **E** and **G**. (**I–O**) P14 Kirrel3 KO mice with farnesylated GFP inserted in the Kirrel3 locus were immunostained with anti-GFP antibodies to identify Kirrel3-expressing cells (green). Dentate granule (DG) dendrites and their mossy fiber (MF) axons are brightly labeled (**I**) as well as GABA-expressing cells (magenta) in area CA3. (**P–R**) P14 Kirrel3 KO mice were immunostained for GFP (green) and calbindin (Calb, magenta). (**S**) Analysis of Kirrel3-positive cells in P14 Kirrel3 KO mice co-expressing interneuron markers. Abbreviations: wild-type, WT; knockout, KO; molecular layer, ML; stratum lucidum, SL. Stratum lacunosum-moleculare, SLM. Images in **A–D**, **E**, **G**, and **I** are tiled.

DOI: 10.7554/eLife.09395.006

The following figure supplements are available for figure 2:

Figure supplement 1. Kirrel3 is not expressed by CA3 neurons.

DOI: 10.7554/eLife.09395.007

Figure supplement 2. Kirrel3 is expressed by mainly calbindin-positive GABA neurons.

DOI: 10.7554/eLife.09395.008

supplement 1). In contrast, the main bouton area and perimeter are not affected by loss of Kirrel3 (***Figure 3J,K***). To examine the main synapse in more detail, we analyzed postsynaptic CA3 TE spines by filling CA3 neurons with Alexa568 dye (***Figure 3N,O***). TE spine head density and length are similar between P21 Kirrel3 wild-type and knockout mice (***Figure 3P,Q***). Thus, Kirrel3 knockout mice have significant morphological defects in MF filopodia but not in pre- or post-synaptic structures of

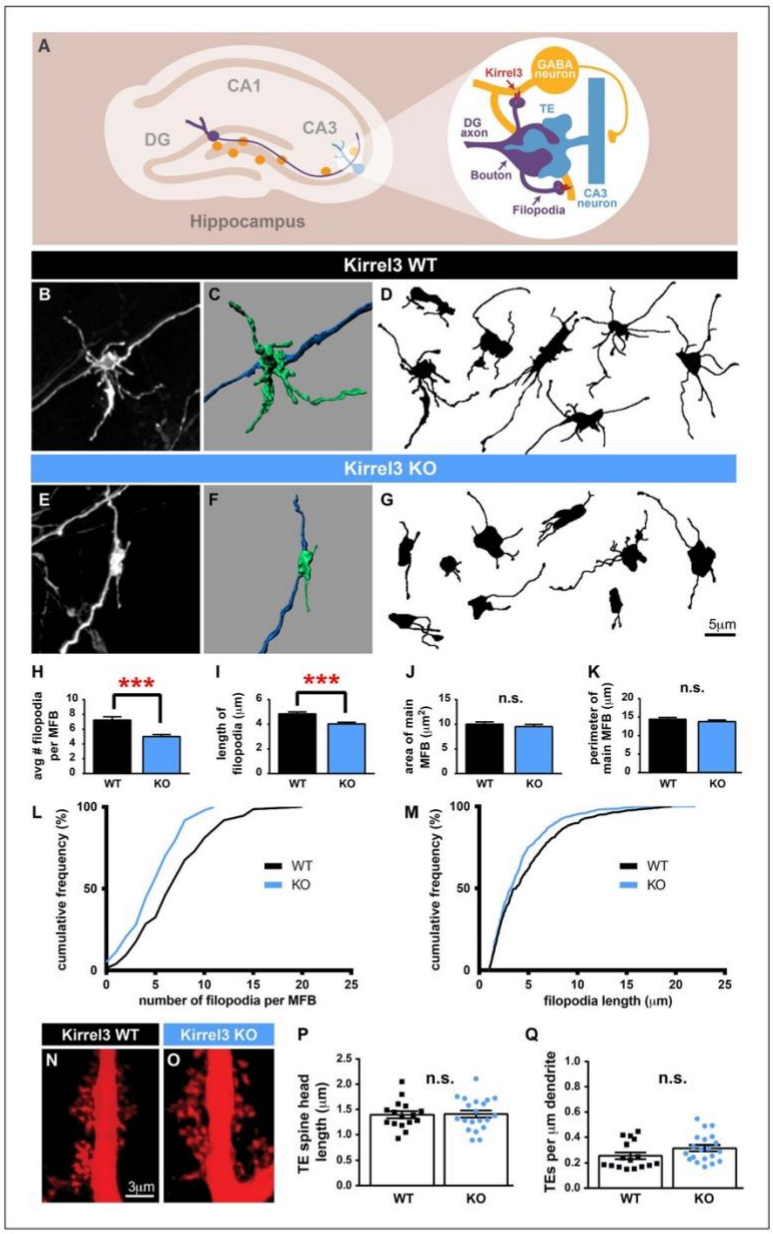

Figure 3. Kirrel3 regulates MF synapse form and function during development. (**A**) MF synapse diagram. TE; thorny excrescence. (**B**, **E**) DiI-labeled MF synapses from P14 Kirrel3 WT and KO mice. (**C**, **F**) 3D renderings of synapses in (**B**, **E**). (**D**, **G**) Tracings of representative DiI-labeled MF synapses. (**H**–**M**) MF synapse morphology quantification. The number of filopodia per MF bouton (**H**, **L**) and filopodia length (**I**, **M**) are reduced in Kirrel3 KO

Figure 3 continued on next page

Figure 3 continued

mice. L and M are cumulative histograms of data shown in H and I, respectively. Area (J) and perimeter (K) of the main MF bouton are unaffected by genotype. n = 74 WT and 97 KO MF synapses from four mice of each genotype. Two-tailed t-tests: in H, *** = $p < 0.001$ and in I, *** = $p = 0.0001$. (N, O) Examples of P21 CA3 TE spines labeled by iontophoresis. (P, Q) Quantification of P21 spine morphology. No significant differences as determined by two-tailed t-tests. n = 16 WT neurons from four animals and 20 KO neurons from three animals. All bar graphs show mean ± SEM.

DOI: 10.7554/eLife.09395.009

The following figure supplement is available for figure 3:

Figure supplement 1. Kirrel3 is required for normal development of MF filopodia.

DOI: 10.7554/eLife.09395.010

main MF synapses, suggesting that the number of DG synapses onto GABA neurons is reduced in Kirrel3 knockout mice.

Kirrel3 regulates CA3 neuron excitability driven by MF input

If Kirrel3 knockout mice have fewer DG-GABA synapses, there should be reduced excitation to GABA neurons, particularly to Kirrel3-positive GABA neurons. Unfortunately, Kirrel3-positive GABA neurons cannot be identified in wild-type mice making it impossible to target them for direct electrophysiological studies at this time. However, reducing DG-GABA synapses in area CA3 is expected to decrease feed-forward inhibition and thereby increase excitation of CA3 neurons after DG stimulation. To test this, we recorded excitatory and inhibitory currents evoked in CA3 neurons after DG stimulation in acute slices (***Figure 4A***). As predicted by our model, P14–P16 Kirrel3 knockout mice have a significantly increased excitatory/inhibitory (E/I) ratio compared to wild-type mice (***Figure 4B***). We confirmed evoked responses were due to MF stimulation by applying DCG-IV, a metabotropic glutamate receptor agonist that selectively inhibits MF release (***Figure 4A***) (***Kamiya et al., 1996***; ***Yoshino et al., 1996***; ***Torborg et al., 2010***).

To test if Kirrel3 knockout mice have increased CA3 activity in an awake and behaving animal, we analyzed cFos, an immediate early gene marking recently activated neurons (***Kawashima et al., 2014***), in P14 Kirrel3 wild-type and knockout mice. Mice were either removed from the home cage for immediate fixation (no stim) or allowed to explore an enriched environment for 25 min prior to fixation (stim). At this age, basal, unstimulated cFos expression is low regardless of genotype, but with stimulation, P14 knockout mice have a twofold increase in cFos-positive CA3 neurons compared to wild-type (***Figure 4C,D***). As a control, mice were recorded and exploration was comparable between genotypes (***Figure 4—figure supplement 1***). Interestingly, the number of cFos-positive neurons did not significantly increase in wild-type mice after stimulation but this is consistent with previous reports (***Waters et al., 1997***) and likely reflects that at P14 the CA3 is dominated by inhibition (***Figure 4B***, note wild-type E/I ratio is <1) (***Torborg et al., 2010***). Because Kirrel3 is expressed by entorhinal cortex axons that innervate the hippocampus, we also generally examined inputs to CA3 and DG neurons by recording miniature excitatory postsynaptic currents (mEPSCs). No significant differences between wild-type and Kirrel3 knockout neurons in mEPSC amplitude or frequency were found for either cell type (***Figure 4—figure supplement 1***). Together, our functional data support the hypothesis that Kirrel3 selectively regulates formation of filopodial DG-GABA MF synapses.

Morphological defects in MF synapses persist in Kirrel3 knockout mice

MF synapse complexity peaks at P14 and is refined such that adult synapses have fewer filopodia and a larger main bouton (***Wilke et al., 2013***). To investigate MF synapse maturation under sustained loss of Kirrel3, we analyzed MF morphology in adult (P60–P75) wild-type and knockout mice. Both genotypes have fewer filopodia as adults than at P14 (compare ***Figure 4E*** and ***Figure 3H***), suggesting age-dependent filopodia refinement is Kirrel3-independent. However, while P14 knockout mice have fewer filopodia with a normal main bouton, adult knockout mice have fewer filopodia and a smaller main bouton (***Figure 4E–J***). Thus, MF synapse defects worsen with age in Kirrel3 knockout mice. It is possible Kirrel3 is directly required for main bouton maturation or maintenance, but Kirrel3 is not expressed by CA3 neurons. Another possibility is that defects in the main bouton in adult knockout mice result from compensatory mechanisms enacted to dampen the dramatic increase in

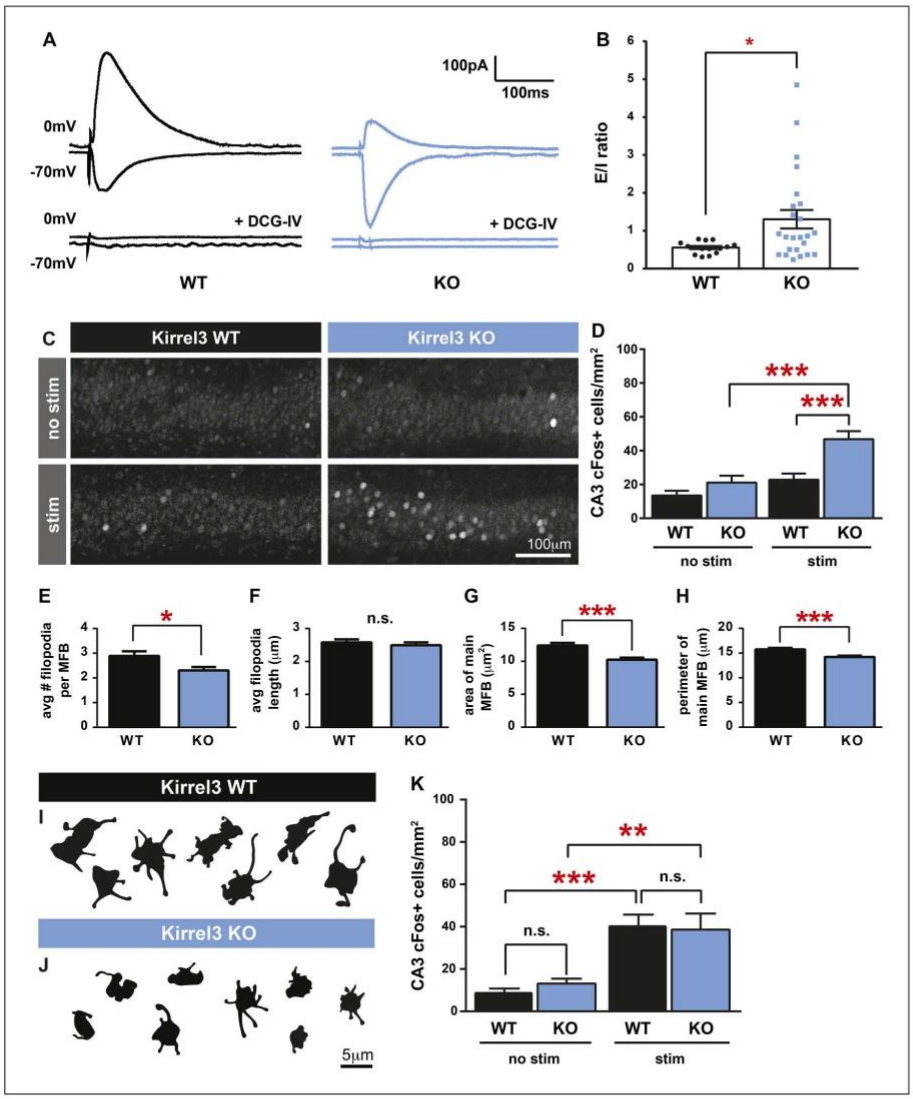

Figure 4. Kirrel3 regulates the activity of CA3 neurons during development. (**A**) Evoked responses at −70 and 0 mV of a CA3 neuron after stimulation of the MF pathway in Kirrel3 WT and KO mice. Lower traces show responses of the same cells after perfusion of 0.5 µm DCG-IV. (**B**) Average excitatory/inhibitory (E/I) ratio for CA3 neurons recorded from P14–P16 WT and KO mice. n = 15 cells from five WT animals and 24 cells from five KO animals. p = 0.02 with unpaired t-test. (**C**) Examples of anti-cFos staining in CA3 neurons from P14 mice. Note increased cell staining in Kirrel3 KO mice after 25 min stimulation (stim) in a novel, enriched environment. (**D**) Quantification of cFos-positive CA3 neurons at P14. n = 14 (WT no stim), 15 (WT stim), 15 (KO no stim), and 15 (KO stim) sections from three mice per condition. Two-way ANOVA indicates there is a significant difference among condition (no stim vs stim) and genotype. p values from post-tests are 0.0001 (KO no stim vs KO stim) and 0.0004 (WT stim vs KO stim). (**E–H**) Quantification of MF synapse structure in adult mice. n = 115 WT and 131 KO synapses from three mice per genotype. Two-tailed t-tests indicate p = 0.01 (**E**), p < 0.0001 (**G**), and p = 0.002 (**H**). (**I**, **J**) Tracings of representative DiI-labeled MF synapses from adult (P60–P75) Kirrel3 WT and KO mice. (**K**) Quantification of cFos-positive cells in area CA3 of adult mice. n = 14 (WT no stim), 14 (WT stim), 16 (KO no stim), and 16 (KO stim) sections from three different mice per condition.

Figure 4 continued on next page

Figure 4 continued

Two-way ANOVA indicates there is a significant difference among condition (no stim vs stim) but not genotype. p values from post-tests are 0.0005 (WT no stim vs WT stim) and 0.003 (KO no stim vs KO stim). All graphs show mean ± SEM.

DOI: 10.7554/eLife.09395.011

The following figure supplement is available for figure 4:

Figure supplement 1. Spontaneous mEPSC activity of CA3 and DG neurons is normal in the absence of Kirrel3.

DOI: 10.7554/eLife.09395.012

CA3 neuron excitability during development. To test this, we analyzed cFos expression in adult mice to determine if knockout CA3 neuron activity returns to normal. In support, unstimulated and stimulated cFos expression in CA3 neurons is similar between P60 adult wild-type and knockout mice (***Figure 4K*** and ***Figure 4—figure supplement 1***). Thus, our data suggest a model in which a reduction in MF filopodia during development leads to hyper-activation of CA3 neurons that, with time, causes homeostatic mechanisms to decrease the size of the main DG-CA3 MF synapse and return overall CA3 activity levels to a set point. This model remains to be tested in more detail in future studies. Interestingly, a battery of behavioral tests was recently performed on adult Kirrel3 knockout mice (***Choi et al., 2015***). Kirrel3 knockout mice have only mild hyperactivity and a moderate impairment in novel object recognition compared to wild-type (***Choi et al., 2015***). Our results indicate CA3 neuron activity is significantly impaired in 14-day-old animals but returns to normal by 2 months of age. This may explain why adult Kirrel3 knockout mice have only moderate behavioral impairments and suggests that younger animals may have more severe behavioral problems.

Discussion

In summary, we demonstrate Kirrel3 is required for normal development of MF filopodia, the synaptic structures connecting DG and GABA neurons. Because Kirrel3 is a homophilic adhesion molecule expressed by DG neurons and calbindin-positive GABA neurons in hippocampal area CA3, our work suggests trans-cellular Kirrel3 interactions may stabilize MF filopodia contact and subsequent synapse formation between Kirrel3-expressing cells. Functionally, we demonstrate Kirrel3 is required to maintain feed-forward inhibition and constrain CA3 neuron activity in young animals. Although a few molecules have been shown to generally affect MF presynapse formation (***Danzer et al., 2008***; ***Williams et al., 2011***; ***Lanore et al., 2012***; ***Wilke et al., 2012***), Kirrel3 is among the first shown to selectively act on MF filopodia and our results provide evidence that main and filopodial MF synapse formation can be uncoupled. The role of calbindin-positive GABA neurons in the hippocampus is little studied, but our findings suggest they may receive a substantial fraction of DG MF input and be a critical component of feed-forward inhibitory circuits regulating CA3 activity.

Given that alterations in the Kirrel3 gene are associated with autism and intellectual disabilities, this work provides the first insight into cellular mechanisms that may underlie Kirrel3-dependent neurological disorders. Our work suggests Kirrel3 loss selectively reduces excitatory synapses made onto inhibitory neurons in hippocampal area CA3. Consequently, CA3 neurons are over-active in young Kirrel3 knockout animals. Altered E/I ratios are hypothesized to underlie neurodevelopmental disorders (***Rubenstein and Merzenich, 2003***; ***Baroncelli et al., 2011***; ***Fakhoury, 2015***), and our work suggests this may be an important circuit defect of Kirrel3-associated diseases. Interestingly, such a strong imbalance probably would not occur if all synapses were equally impaired. In this way, loss of synaptic specificity molecules can cause widespread circuit dysfunction. There is much evidence that hippocampal circuits are altered in autism and intellectual disabilities, but it is likely not the only brain region affected in these complex neurological disorders (***Philip et al., 2012***; ***Zoghbi and Bear, 2012***). Kirrel3 is also expressed by specific populations of neurons outside the hippocampus (***Lein et al., 2007***; ***Choi et al., 2015***). Thus, Kirrel3 may also regulate formation of other specific types of synapses throughout the brain, which may further contribute to its association with neurodevelopmental disorders.

Materials and methods

Mouse lines

Generation of the Kirrel3 knockout mouse line was recently reported (**Prince et al., 2013**). All animals and experiments were maintained and conducted in accordance with the NIH guidelines on the care and use of animals and approved by the University of Utah IACUC committee.

Kirrel3 cloning and RNA in situ hybridization

Kirrel3 cDNA was kindly provided by Dr Hitoshi Sakano and *Kirrel1* and *Kirrel2* cDNAs were obtained from OpenBiosystems. Standard PCR cloning was used to move cDNAs to the pBos vector and add an extracellular FLAG tag after the signal sequence. Full-length *Kirrel1*, *2*, and *3* cDNAs were used to generate sense and anti-sense probes. Standard DIG-labeled, non-radioactive in situ hybridization protocol was carried out using the Roche DIG-labeling kit on coronal cryosections of brain tissue.

Cell culture

Neurons: P0 rat cortical glia were cultured on PDL/collagen-coated coverslips to form a monolayer. 1 week later, P0 mouse or rat hippocampi were dissected in cold 4-(2-hydroxyethyl)-1-piperazineethanesulfonic acid (HEPES)-buffered saline solution, incubated in papain for 30 min, dissociated, and plated to glial monolayers at 4–5 $\times$ 10^4 cells/ml. All media was from Life Technologies (Carlsbad, CA, United States). Glia media: DMEM, 10% Fetal Bovine Serum (FBS), 75 mM glucose, and penicillin/streptomycin. Neuron-plating media: MEM, 10% horse serum, 50 mM glucose, 0.250 mM pyruvic acid, 2 mM Glutamax, 100 U/ml penicillin, 100 μg/ml streptomycin. Neuron-feeding media: Neurobasal A, B27, 30 mM glucose, 0.5 mM Glutamax, 20 U/ml penicillin, 20 μg/ml streptomycin. Neuron transfections were done using the calcium-phosphate method (**Dudek et al., 2001**). Cell lines: 293HEK media: DMEM, 10% FBS, and penicillin/streptomycin. CHO media: F12K media, 10% FBS, and penicillin/streptomycin. Cell line transfections were done using polyethylenimine (PEI, Polysciences, Warrington, PA, United States) at a ratio of 5 μg PEI/1 μg DNA.

CHO cell aggregation assay

CHO cells were co-transfected with FLAG-Kirrel3 pBOS (4 μg) and GFP pBOS (2 μg) using PEI. 48 hr later, cells were washed with HEPES Mg^{2+} free (HMF) buffer (137 mM NaCl, 5.4 mM KCl, 1 mM $CaCl_2$, 0.34 mM Na_2HPO_4, 5.5 mM glucose, 10 mM HEPES, pH 7.4 adjusted with NaOH) and detached from the dishes using 0.01% trypsin in HMF. Detached cells were spun down, resuspended in HMF, counted, and 100,000 cells were pipetted into single wells of 24-well plates precoated with 1% BSA in HMF. Subsequently, the plates were placed on a nutator for 90 min at 37°C. The cells were then fixed with paraformaldehyde (PFA) (4% final concentration), transferred to a 96-well glass bottom plate, and imaged in a Zeiss LSM 710 confocal microscope. The aggregation index was calculated by dividing the total GFP fluorescence in cell aggregates by the total GFP fluorescence in the well. Analysis was done using ImageJ.

Immunostaining

Cultured cells were fixed in 4% PFA for 10 min, washed with phosphate-buffered saline (PBS), and incubated in blocking solution (PBS with 3% bovine albumin and 0.1% Triton-X100) for 30 min. Primary antibody was diluted in blocking solution and incubated on cells for 1–2 hr. After three washes, secondary antibody was incubated for 45 min, washed, and cells were mounted for imaging using Fluoromount-G (Southern Biotech, Birmingham, AL, United States). For live labeling, cells were incubated with anti-FLAG antibody diluted 1:250 in serum-free media for 20 min in the culture incubator. Cells were washed, fixed with PFA, and immunostained as above. For tissue sections, mice were transcardially perfused with 4% PFA. Brains were post-fixed in PFA overnight and 50–100 μm vibratome sections were cut. Sections were incubated in blocking solution (PBS, 3% BSA, 0.2% Triton-X100) for more than 1 hr and incubated in primary antibody at 4°C overnight with gentle shaking. For VIP immunostaining, the blocking solution contained 0.3% triton +0.1% saponin. Secondary antibody incubation was done at room temperature for 2 hr. Sections were mounted in Fluoromount-G for imaging.

Antibodies

Primary antibodies were used as follows: rabbit anti-Kirrel3 1:2000 (this study, generated against C-terminal peptide), rabbit anti-GABA 1:5000 (Sigma, St. Louis, MO, United States), goat anti-GFP 1:5000 (Abcam, Cambridge, MA, United States), guinea pig anti-VGLUT1 1:10,000 (Millipore, Billerica, MA, United States), mouse anti-MAGUK 1:1000 (NeuroMab, UC Davis/NIH NeuroMAB Facility, Davis, CA, United States), mouse anti-FLAG M2 1:5000 (Sigma), rabbit anti-synapsin 1:1000 (Millipore), rabbit anti-cFos 1:500 (Santa Cruz Biotech, Dallas, TX), rabbit anti-GFP 1:1000 (Invitrogen, Waltham, MA, United States), chick anti-FLAG 1:1000 (Gallus Immunotech, Cary, NC, United States), mouse anti-PSD95 1:2000 (Thermo Scientific), mouse anti-GAPDH 1:5000 (Millipore), chick anti-MAP2 1:10,000 (Abcam), rabbit anti-calretinin 1:2000 (Swant, Switzerland), mouse anti-parvalbumin 1:5000 (Swant), mouse anti-CamKII 1:5000 (Millipore), rat anti-Somatostatin 1:500 (Chemicon), rabbit anti-calbindin d28k 1:2000 (Swant), rabbit anti-VIP 1:500 (Immunostar, Hudson, WI, United States). All secondary antibodies were obtained from Jackson ImmunoResearch (West Grove, PA, United States) and used at 1:1000.

F_c-binding assay

The extracellular domain of Kirrel3 was cloned in frame with human F_c protein. Kirrel3-F_c was transfected into HEK293 cells using PEI. Cells were incubated in OptiMEM (Life Technologies) media for 5 days. Then, the Kirrel3-F_c-conditioned media was harvested and concentrated using Amicon Ultra filter units (Millipore). Kirrel3-F_c concentration was estimated by Western blot using known concentrations of purified F_c (Jackson Immuno) as a standard. Kirrel3-F_c was pre-clustered by incubating it in OptiMEM plus anti-human Cy3 secondary antibodies at 1:100. Kirrel3-F_c and control F_c (used at ~1 μg/ml) were then tested for binding to transfected HEK293 cells using the live label immunostaining method described above.

Synaptosome preparation

Synaptosomes were prepared according to methods described by Jones and Matus with minor modifications (***Jones and Matus, 1974***). Briefly, hippocampi were dissected from mice. Tissue was homogenized with a Dounce homogenizer (20% wt/vol) in ice-cold 0.32 M sucrose +20 mM HEPES, pH 7.4 supplemented with protease inhibitors. Homogenates were cleared by spinning at 1000×*g* for 10 min at 4°C. The supernatant was spun at 17,000×*g* for 15 min. The pellet containing crude synaptosomes was resuspended in 0.32 M sucrose and 20 mM HEPES. Protein concentration was quantified with a BCA assay (Thermo Scientific). 2 μg of synaptosomal or cleared lysate proteins was loaded per lane for Western blot analysis.

Western blot

Proteins were run on Bis-Tris gradient acrylamide gels and transferred to nitrocellulose membranes using the iBlot system (Life Technologies). Membranes were incubated in blocking solution (50 mM Tris pH 7.5, 300 mM NaCl, 3% wt/vol dry milk powder, and 0.05% Tween-20) for 10–60 min, primary antibody overnight at 4°C, washed, incubated in HRP-conjugated secondary antibodies (Jackson Immuno) for 1 hr at room temperature and then detected using the Bio-Rad Clarity ECL kit on a Bio-Rad ChemiDoc XRS+ imaging system. To prepare hippocampal lysates, 100 mg of hippocampal tissue was homogenized in 1 ml of reducing sample buffer.

MF presynapse analysis

DiI crystals (Life Technologies) were placed in the DG of perfused hippocampi and incubated at 37°C in 2% PFA for 1 week. MF synapses from the suprapyramidal bundle in area CA3a/b were imaged, deconvolved in AutoQuant3 (Bitplane), and analyzed in ImageJ. Filopodia length was analyzed in 3D using the Simple Neurite Tracer plug-in, while area and perimeter of the main bouton were analyzed in 2D.

Microiontophoresis and spine analysis

Neurons were microinjected with fluorescent dye as described (***Dumitriu et al., 2011***). Briefly, P21 pups were perfused with 1% PFA in phosphate buffer (PB) for 1 min, followed by 4% PFA with 0.125% glutaraldehyde in PB for 9 min. The brains were extracted and post-fixed in 4% PFA for 30

min. 200 μm-thick coronal hippocampal slices were cut on a vibratome. Slices were submerged in 0.1 M PB and viewed through an Olympus BX51WI microscope coupled to a light source and fluorescent filters. High-resistance (150–250 MΩ) glass pipettes were pulled on a Flaming/Brown P-97 Sutter pipette puller and backfilled with 10 mM Alexa568 (dissolved in 200 mM KCl, Life Technologies). The pipettes were mounted on a micromanipulator connected to an S44 Grass square pulse stimulator. The pipette tip was gently advanced in tissue towards the cell of interest. On contact and penetration, a step stimulus of 1–5 V was used to inject the dye in the cell. Filled neurons were imaged on a Zeiss LSM710 confocal microscope.

cFos analysis

P14 and adult P60 wild-type and knockout mice were either removed from the home cage for immediate fixation by transcardial perfusion (unstimulated) or allowed to explore an enriched environment for 25 min prior to fixation (stimulated). The enriched environment consisted of mice placed individually into a 40 × 40 clear plastic box containing five novel objects spaced 10 cm apart. Mice were allowed to explore freely for 25 min. Immunostaining was conducted as described in the above methods.

Image analysis and statistics

When possible, experiments were conducted by an experimenter blind to condition or genotype. Sample sizes were based on previous experiments or power analysis. Statistics were calculated in Prism (GraphPad). Intensity levels of some images were adjusted for visibility in publication but if so, the entire field of view and all comparable conditions were adjusted similarly. All images and conditions from the same experiment were collected and analyzed using the same confocal and analysis settings.

Electrophysiology

Mice were rapidly decapitated and their brains carefully removed and kept in iced, artificial cerebrospinal fluid (aCSF) with sucrose (in mM—sucrose 200, KCl 3, Na_2PO_4 1.4, $MgSO_4$ 3, $NaHCO_3$ 26, glucose 10, and $CaCl_2$ 0.5). 300-μm thick transverse slices were cut on a Leica vibratome (Leica VT1200) and the slices were left at room temperature in the holding chamber, until recording. P14–P16 mice were used for E/I ratio experiments and P17–P21 mice were used for mEPSC experiments. Neurons were visualized by differential interference contrast using a bright light source and an infrared filter on an Olympus BX51WI microscope with attached Hitachi color CCD camera (KP-D20BU). For mEPSC recordings: slices were continuously superfused with aCSF containing (in mM) NaCl 126, $NaHCO_3$ 26, KCl 3, NaH_2PO_4 1.4, $CaCl_2$ 2.5, $MgSO_4$ 1, D-glucose 10, and TTX 1 bubbled with 95% O_2–5% CO_2. The intracellular pipette solution for mEPSC recordings contained (in mM) cesium methylsulfonate 80, CsCl 60, HEPES 10, EGTA 1 (adjusted with CsOH), $CaCl_2$ 0.5, glucose 10, and QX-314 5, adjusted to 290–300 mOsm/Lt at pH 7.3. For E/I ratio experiments, the aCSF was as above but without TTX and the intracellular solution was (in mM) cesium methylsulfonate 132, CsCl 8, HEPES 10, EGTA 1 (adjusted with CsOH), $CaCl_2$ 0.5, glucose 10, and QX-314 5, adjusted to 290–300 mOsm/Lt at pH 7.3. DCG-IV 0.5 μM (CAS no. 147782-19-2, TOCRIS) was perfused in the ACSF in some E/I ratio experiments to verify the specificity of stimulation. Unless noted, chemicals were sourced from Fisher Scientific (Pittsburgh, PA, United States).

Somatic whole-cell recordings were performed with Axon Multiclamp 700B amplifier (Molecular Devices, CA, United States) in voltage clamp mode at 34 ± 1°C bath temperature for mEPSC experiments and at room temperature (~22°C) for E/I ratio experiments. Data acquisition was performed via an Axon Digidata 1550 (Molecular Devices, CA, United States) with pClamp (Version 10, Molecular Devices, CA, United States). Current signals were sampled at 1 kHz and filtered with a 2-kHz Bessel filter. Patch pipettes with a tip resistance of 5–10 MΩ were pulled with a Flaming/Brown micropipette puller P-97 (Sutter Instruments and Co.) using borosilicate glass capillaries with filaments (1B150F-4, World Precision Instruments). Grass stimulator (S88, Grass Instruments) and bipolar tungsten electrodes (Harvard Apparatus, MA, United States, Ref. no. 72-0375) were used to deliver extracellular stimulation to the MF pathway at the hilus of the DG.

Acknowledgements

We thank Hitoshi Sakano's laboratory for the Kirrel3 cDNA, Jean-Francois Cloutier for mice, Dimitri Tränkner for Matlab assistance, Jason Shepherd for manuscript comments, and the entire Williams lab. This work was funded by grants to MEW from the Whitehall, Alfred P Sloan, and Edward Mallinckrodt Jr Foundations, a University of Utah seed grant, and NIH grant 1R01MH105426.

Additional information

Funding

Funder	Grant reference number	Author
National Institute of Mental Health	R01MH105426	Megan E Williams
Whitehall Foundation	3 year grant	Megan E Williams
Alfred P. Sloan Foundation	new investigator award	Megan E Williams
University of Utah	Seed grant	Megan E Williams

The funders had no role in study design, data collection and interpretation, or the decision to submit the work for publication.

Author contributions

EAM, Acquisition of data, Analysis and interpretation of data, Drafting or revising the article; SM, Acquisition of data, Analysis and interpretation of data, Drafting or revising the article; ZW, Acquisition of data, Analysis and interpretation of data; DCC, Acquisition of data, Analysis and interpretation of data; RB, Acquisition of data, Analysis and interpretation of data; MRT, Acquisition of data; JH, Acquisition of data; SAW, Acquisition of data; TC, Contributed unpublished essential data or reagents; AG, Conception and design; MEW, Conception and design, Acquisition of data, Analysis and interpretation of data, Drafting or revising the article

Ethics

Animal experimentation: This study was performed in strict accordance with the recommendations in the Guide for the Care and Use of Laboratory Animals of the National Institutes of Health. All of the animals were handled according to an approved Institutional Animal Care and Use Committee (IACUC) protocol (14-07004) from the University of Utah.

References

Acsády L, Kamondi A, Sík A, Freund T, Buzsáki G. 1998. GABAergic cells are the major postsynaptic targets of mossy fibers in the rat hippocampus. *Journal of Neuroscience* **18**:3386–3403.

Baroncelli L, Braschi C, Spolidoro M, Begenisic T, Maffei L, Sale A. 2011. Brain plasticity and disease: a matter of inhibition. *Neural Plasticity* **2011**:286073. doi: 10.1155/2011/286073

Bhalla K, Luo Y, Buchan T, Beachem MA, Guzauskas GF, Ladd S, Bratcher SJ, Schroer RJ, Balsamo J, DuPont BR, Lilien J, Srivastava AK. 2008. Alterations in CDH15 and KIRREL3 in patients with mild to severe intellectual disability. *American Journal of Human Genetics* **83**:703–713. doi: 10.1016/j.ajhg.2008.10.020

Chia PH, Chen B, Li P, Rosen MK, Shen K. 2014. Local F-actin network links synapse formation and axon branching. *Cell* **156**:208–220. doi: 10.1016/j.cell.2013.12.009

Choi SY, Han K, Cutforth T, Chung W, Park H, Lee D, Kim R, Kim MH, Choi Y, Shen K, Kim E. 2015. Mice lacking the synaptic adhesion molecule Neph2/Kirrel3 display moderate hyperactivity and defective novel object preference. *Frontiers in Cellular Neuroscience* **9**:283. doi: 10.3389/fncel.2015.00283

Danzer SC, Kotloski RJ, Walter C, Hughes M, McNamara JO. 2008. Altered morphology of hippocampal dentate granule cell presynaptic and postsynaptic terminals following conditional deletion of TrkB. *Hippocampus* **18**:668–678. doi: 10.1002/hipo.20426

Donoviel DB, Freed DD, Vogel H, Potter DG, Hawkins E, Barrish JP, Mathur BN, Turner CA, Geske R, Montgomery CA, Starbuck M, Brandt M, Gupta A, Ramirez-Solis R, Zambrowicz BP, Powell DR. 2001. Proteinuria and perinatal lethality in mice lacking NEPH1, a novel protein with homology to NEPHRIN. *Molecular and Cellular Biology* **21**:4829–4836. doi: 10.1128/MCB.21.14.4829-4836.2001

DudekH, GhoshA, GreenbergME. 2001. Calcium phosphate transfection of DNA into neurons in primary culture. *Current Protocols in Neuroscience* **Chapter 3: Unit 3**:11.
Dumitriu D, Rodriguez A, Morrison JH. 2011. High-throughput, detailed, cell-specific neuroanatomy of dendritic spines using microinjection and confocal microscopy. *Nature Protocols* **6**:1391–1411. doi: 10.1038/nprot.2011.389
Emes RD, Grant SG. 2012. Evolution of synapse complexity and diversity. *Annual Review of Neuroscience* **35**:111–131. doi: 10.1146/annurev-neuro-062111-150433
Fakhoury M. 2015. Autistic spectrum disorders: A review of clinical features, theories and diagnosis. *International Journal of Developmental Neuroscience* **43**:70–77. doi: 10.1016/j.ijdevneu.2015.04.003
Frotscher M. 1989. Mossy fiber synapses on glutamate decarboxylase-immunoreactive neurons: evidence for feed-forward inhibition in the CA3 region of the hippocampus. *Experimental Brain Research* **75**:441–445.
George B, Holzman LB. 2012. Signaling from the podocyte intercellular junction to the actin cytoskeleton. *Seminars in Nephrology* **32**:307–318. doi: 10.1016/j.semnephrol.2012.06.002
Gerke P, Huber TB, Sellin L, Benzing T, Walz G. 2003. Homodimerization and heterodimerization of the glomerular podocyte proteins nephrin and NEPH1. *Journal of the American Society of Nephrology* **14**:918–926. doi: 10.1097/01.ASN.0000057853.05686.89
Guerin A, Stavropoulos DJ, Diab Y, Chénier S, Christensen H, Kahr WH, Babul-Hirji R, Chitayat D. 2012. Interstitial deletion of 11q-implicating the KIRREL3 gene in the neurocognitive delay associated with Jacobsen syndrome. *American Journal of Medical Genetics. Part A* **158A**:2551–2556. doi: 10.1002/ajmg.a.35621
Jones DH, Matus AI. 1974. Isolation of synaptic plasma membrane from brain by combined flotation-sedimentation density gradient centrifugation. *Biochimica Et Biophysica Acta* **356**:276–287. doi: 10.1016/0005-2736(74)90268-5
Kamiya H, Shinozaki H, Yamamoto C. 1996. Activation of metabotropic glutamate receptor type 2/3 suppresses transmission at rat hippocampal mossy fibre synapses. *The Journal of Physiology* **493 (Pt 2)**:447–455. doi: 10.1113/jphysiol.1996.sp021395
Kawashima T, Okuno H, Bito H. 2014. A new era for functional labeling of neurons: activity-dependent promoters have come of age. *Frontiers in Neural Circuits* **8**:37. doi: 10.3389/fncir.2014.00037
Lanore F, Labrousse VF, Szabo Z, Normand E, Blanchet C, Mulle C. 2012. Deficits in morphofunctional maturation of hippocampal mossy fiber synapses in a mouse model of intellectual disability. *Journal of Neuroscience* **32**:17882–17893. doi: 10.1523/JNEUROSCI.2049-12.2012
Lein ES, Hawrylycz MJ, Ao N, Ayres M, Bensinger A, Bernard A, Boe AF, Boguski MS, Brockway KS, Byrnes EJ, Chen L, Chen L, Chen TM, Chin MC, Chong J, Crook BE, Czaplinska A, Dang CN, Datta S, Dee NR, et al. 2007. Genome-wide atlas of gene expression in the adult mouse brain. *Nature* **445**:168–176. doi: 10.1038/nature05453
McBain CJ. 2008. Differential mechanisms of transmission and plasticity at mossy fiber synapses. *Progress in Brain Research* **169**:225–240. doi: 10.1016/S0079-6123(07)00013-1
Michaelson JJ, Shi Y, Gujral M, Zheng H, Malhotra D, Jin X, Jian M, Liu G, Greer D, Bhandari A, Wu W, Corominas R, Peoples A, Koren A, Gore A, Kang S, Lin GN, Estabillo J, Gadomski T, Singh B, et al. 2012. Whole-genome sequencing in autism identifies hot spots for de novo germline mutation. *Cell* **151**:1431–1442. doi: 10.1016/j.cell.2012.11.019
Neale BM, Kou Y, Liu L, Ma'ayan A, Samocha KE, Sabo A, Lin CF, Stevens C, Wang LS, Makarov V, Polak P, Yoon S, Maguire J, Crawford EL, Campbell NG, Geller ET, Valladares O, Schafer C, Liu H, Zhao T, et al. 2012. Patterns and rates of exonic de novo mutations in autism spectrum disorders. *Nature* **485**:242–245. doi: 10.1038/nature11011
Philip RC, Dauvermann MR, Whalley HC, Baynham K, Lawrie SM, Stanfield AC. 2012. A systematic review and meta-analysis of the fMRI investigation of autism spectrum disorders. *Neuroscience and Biobehavioral Reviews* **36**:901–942. doi: 10.1016/j.neubiorev.2011.10.008
Prince JE, Brignall AC, Cutforth T, Shen K, Cloutier JF. 2013. Kirrel3 is required for the coalescence of vomeronasal sensory neuron axons into glomeruli and for male-male aggression. *Development* **140**:2398–2408. doi: 10.1242/dev.087262
Putaala H, Soininen R, Kilpeläinen P, Wartiovaara J, Tryggvason K. 2001. The murine nephrin gene is specifically expressed in kidney, brain and pancreas: inactivation of the gene leads to massive proteinuria and neonatal death. *Human Molecular Genetics* **10**:1–8. doi: 10.1093/hmg/10.1.1
Rubenstein JL, Merzenich MM. 2003. Model of autism: increased ratio of excitation/inhibition in key neural systems. *Genes, Brain, and Behavior* **2**:255–267. doi: 10.1034/j.1601-183X.2003.00037.x
Ruediger S, Vittori C, Bednarek E, Genoud C, Strata P, Sacchetti B, Caroni P. 2011. Learning-related feedforward inhibitory connectivity growth required for memory precision. *Nature* **473**:514–518. doi: 10.1038/nature09946
Serizawa S, Miyamichi K, Takeuchi H, Yamagishi Y, Suzuki M, Sakano H. 2006. A neuronal identity code for the odorant receptor-specific and activity-dependent axon sorting. *Cell* **127**:1057–1069. doi: 10.1016/j.cell.2006.10.031
Shen K, Bargmann CI. 2003. The immunoglobulin superfamily protein SYG-1 determines the location of specific synapses in C. elegans. *Cell* **112**:619–630. doi: 10.1016/S0092-8674(03)00113-2
Torborg CL, Nakashiba T, Tonegawa S, McBain CJ. 2010. Control of CA3 output by feedforward inhibition despite developmental changes in the excitation-inhibition balance. *Journal of Neuroscience* **30**:15628–15637. doi: 10.1523/JNEUROSCI.3099-10.2010
Toth K, Suares G, Lawrence JJ, Philips-Tansey E, McBain CJ. 2000. Differential mechanisms of transmission at three types of mossy fiber synapse. *Journal of Neuroscience* **20**:8279–8289.

Waters NS, Klintsova AY, Foster TC. 1997. Insensitivity of the hippocampus to environmental stimulation during postnatal development. *Journal of Neuroscience* **17**:7967–7973.

Wilke SA, Antonios JK, Bushong EA, Badkoobehi A, Malek E, Hwang M, Terada M, Ellisman MH, Ghosh A. 2013. Deconstructing complexity: serial block-face electron microscopic analysis of the hippocampal mossy fiber synapse. *Journal of Neuroscience* **33**:507–522. doi: 10.1523/JNEUROSCI.1600-12.2013

Wilke SA, Hall BJ, Antonios JK, Denardo LA, Otto S, Yuan B, Chen F, Robbins EM, Tiglio K, Williams ME, Qiu Z, Biederer T, Ghosh A. 2012. NeuroD2 regulates the development of hippocampal mossy fiber synapses. *Neural Development* **7**:9. doi: 10.1186/1749-8104-7-9

Williams ME, de Wit J, Ghosh A. 2010. Molecular mechanisms of synaptic specificity in developing neural circuits. *Neuron* **68**:9–18. doi: 10.1016/j.neuron.2010.09.007

Williams ME, Wilke SA, Daggett A, Davis E, Otto S, Ravi D, Ripley B, Bushong EA, Ellisman MH, Klein G, Ghosh A. 2011. Cadherin-9 regulates synapse-specific differentiation in the developing hippocampus. *Neuron* **71**:640–655. doi: 10.1016/j.neuron.2011.06.019

Yoshino M, Sawada S, Yamamoto C, Kamiya H. 1996. A metabotropic glutamate receptor agonist DCG-IV suppresses synaptic transmission at mossy fiber pathway of the guinea pig hippocampus. *Neuroscience Letters* **207**:70–72. doi: 10.1016/0304-3940(96)12486-1

Zoghbi HY, Bear MF. 2012. Synaptic dysfunction in neurodevelopmental disorders associated with autism and intellectual disabilities. *Cold Spring Harbor Perspectives in Biology* **4**:a009886. doi: 10.1101/cshperspect.a009886

CHAPTER 3

EXAMINING HIPPOCAMPAL MOSSY FIBER SYNAPSES BY 3D ELECTRON MICROSCOPY IN WILDTYPE AND KIRREL3 KNOCKOUT MICE

Reprint of: Martin et al. (2017). Examining hippocampal mossy fiber synapses by 3D electron microscopy in wildtype and Kirrel3 knockout mice. eNeuro.
Reprinted with permission.

eNeuro

New Research

Development

Examining Hippocampal Mossy Fiber Synapses by 3D Electron Microscopy in Wildtype and Kirrel3 Knockout Mice

E. Anne Martin, Derek Woodruff, Randi L. Rawson, and Megan E. Williams

DOI:http://dx.doi.org/10.1523/ENEURO.0088-17.2017

Department of Neurobiology and Anatomy, University of Utah School of Medicine, Salt Lake City, UT 84132

Visual Abstract

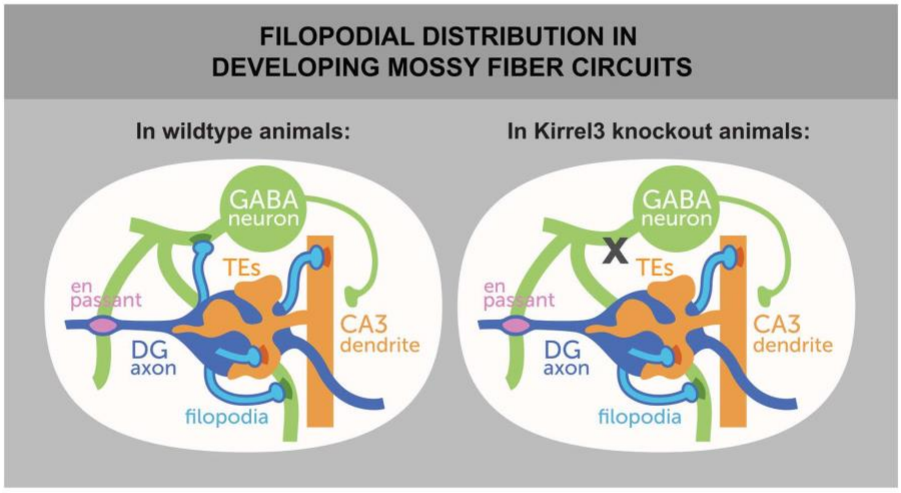

Neural circuits balance excitatory and inhibitory activity and disruptions in this balance are commonly found in neurodevelopmental disorders. Mice lacking the intellectual disability and autism-associated gene *Kirrel3* have an excitation-inhibition imbalance in the hippocampus but the precise synaptic changes underlying this functional defect are unknown. Kirrel3 is a homophilic adhesion molecule expressed in dentate gyrus (DG) and GABA neurons. It was suggested that the excitation-inhibition imbalance of hippocampal neurons in Kirrel3 knockout

Significance Statement

Point mutations and deletions in the gene *Kirrel3* are associated with neurodevelopmental disorders including autism, intellectual disability and Jacobsen's syndrome, a chromosomal disorder that frequently includes epilepsy, autism, and intellectual disability. We studied the effect of losing Kirrel3 on synaptic connections in the mouse hippocampus, a brain region critical for learning and memory. We find that not only are a specific subset of synapses missing in Kirrel3 knockouts, but we also discovered a new synaptic connection within the hippocampus. The synaptic changes we found in mice lacking Kirrel3 shed new light on how a defective *Kirrel3* gene could cause neurodevelopmental disorders in humans.

mice is due to loss of mossy fiber (MF) filopodia, which are DG axon protrusions thought to excite GABA neurons and thereby provide feed-forward inhibition to CA3 pyramidal neurons. Fewer filopodial structures were observed in Kirrel3 knockout mice but neither filopodial synapses nor DG en passant synapses, which also excite GABA neurons, were examined. Here, we used serial block-face scanning electron microscopy (SBEM) with 3D reconstruction to define the precise connectivity of MF filopodia and elucidate synaptic changes induced by Kirrel3 loss. Surprisingly, we discovered wildtype MF filopodia do not synapse exclusively onto GABA neurons as previously thought, but instead synapse with similar frequency onto GABA neurons and CA3 neurons. Moreover, Kirrel3 loss selectively reduces MF filopodial synapses onto GABA neurons but not those made onto CA3 neurons or en passant synapses. In sum, the selective loss of MF filopodial synapses with GABA neurons likely underlies the hippocampal activity imbalance observed in Kirrel3 knockout mice and may impact neural function in patients with Kirrel3-dependent neurodevelopmental disorders.

Key words: electron microscopy; hippocampus; Kirrel3; mossy fiber; reconstruction; synapse

Introduction

Mossy fiber (MF) presynaptic complexes are critical to hippocampal circuit function, especially for the mnemonic process of pattern separation (Rolls, 2013). Yet, the molecular mechanisms regulating their development are largely unknown. MF presynaptic complexes simultaneously connect glutamatergic DG neurons to glutamatergic CA3 pyramidal neurons (henceforth called "CA3 neurons") and GABAergic interneurons (henceforth called "GABA neurons"; Fig. 1*A*). MF presynaptic complexes consist of a giant main bouton that is up to 100 times larger in volume than a typical presynapse (Shepherd and Harris, 1998; Wilke et al., 2013) and they synapse onto multiheaded CA3 spines called thorny excrescences (TEs; Fig. 1*A*). Because of its large size, numerous active zones, and proximity to the CA3 soma, release at a single main bouton profoundly impacts activity of the connected CA3 neuron (McBain, 2008). In addition, the MF presynaptic complex extends protrusions called MF filopodia to synapse with nearby GABA neurons (Fig. 1*A*; Amaral, 1979; Claiborne et al., 1986; Acsády et al., 1998). This MF filopodial synapse provides feed-forward inhibition to CA3 neurons (Frotscher, 1985; Deller et al., 1994; Bragin et al., 1995; Penttonen et al., 1997; Torborg et al., 2010). Distinct from the MF presynaptic complex, DG axons also activate GABA neurons via more typical en passant synapses (Fig. 1*A*). The diversity of DG presynaptic structures made with distinct postsynaptic partners suggests that different molecular mechanisms might be involved in establishing each type of synaptic connection, however, the molecules regulating MF synapse specificity remain largely unknown.

Kirrel3 is an immunoglobulin superfamily member that mediates homophilic cell adhesion (Gerke et al., 2005; Serizawa et al., 2006; Martin et al., 2015). Point mutations, copy number variations, and deletions in Kirrel3 have been repeatedly identified in patients with intellectual disability (Bhalla et al., 2008; Kaminsky et al., 2011; Talkowski et al., 2012), autism spectrum disorders (Ben-David and Shifman, 2012; Iossifov et al., 2012; Michaelson et al., 2012; Neale et al., 2012; Talkowski et al., 2012; Cheng et al., 2013; De Rubeis et al., 2014), and Jacobsen's syndrome (Guerin et al., 2012). Given these associations with neurodevelopmental disorders affecting learning and memory, the role of Kirrel3 in the mouse hippocampus was recently investigated. Behaviorally, adult Kirrel3 knockout mice show a defective novel object recognition preference, as well as hyperactivity in a familiar environment (Choi et al., 2015). Molecularly, Kirrel3 is only expressed in DG neurons and a subset of GABA neurons in the hippocampus, yet functionally, Kirrel3 knockout mice have an increase in DG and CA3 neuron activity compared with wildtype mice (Martin et al., 2015; Roh et al., 2017). These functional defects could be explained by the morphologic observation that Kirrel3 knockout mice have fewer MF filopodia than wildtype mice (Martin et al., 2015), which may decrease feed-forward inhibition to CA3 neurons. These prior studies support the hypothesis that Kirrel3 acts via its homophilic extracellular domain to regulate synapse formation between DG MF filopodia and GABA neurons. However, hippocampal synapses in Kirrel3 knockout mice have not yet been directly examined.

Here, we define DG presynapse connectivity in wildtype and Kirrel3 knockout mice using serial block-face scanning electron microscopy (SBEM). Though several 3D electron microscopy (EM) studies of wildtype MF synapses exist (Rollenhagen et al., 2007; Faulkner et al., 2008; Wilke et al., 2013), none assessed MF filopodia or en passant synapse connectivity. Thus, our study not only provides a high-resolution analysis of hippocampal synaptic defects in Kirrel3 knockout mice but also provides

Received March 18, 2017; accepted May 17, 2017; First published May 22, 2017.

The authors declare no competing financial interests.

Author contributions: M.E.W. and E.A.M. designed research; M.E.W., E.A.M., D.W., and R.L.R. performed research; M.E.W. and E.A.M. analyzed data; M.E.W. and E.A.M. wrote the paper.

This work was supported by grants to M.E.W. from the Whitehall, Alfred P Sloan, and Edward Mallinckrodt Jr Foundations and by the NIH Grant 1R01MH105426. E.A.M. is funded by the Autism Speaks Dennis Weatherstone Predoctoral Fellowship 10116 and previously by the NIH Developmental Biology Training Grant NIH T32HD007491.

Acknowledgments: We thank Allison Schneggenburger, Jen Hunter, and Keegan Teeter for technical assistance and Michael Deans, Dimitri Tränkner, and the entire Williams lab for manuscript comments.

Correspondence should be addressed to Megan E. Williams, at the above address, E-mail: megan.williams@neuro.utah.edu.

DOI:http://dx.doi.org/10.1523/ENEURO.0088-17.2017

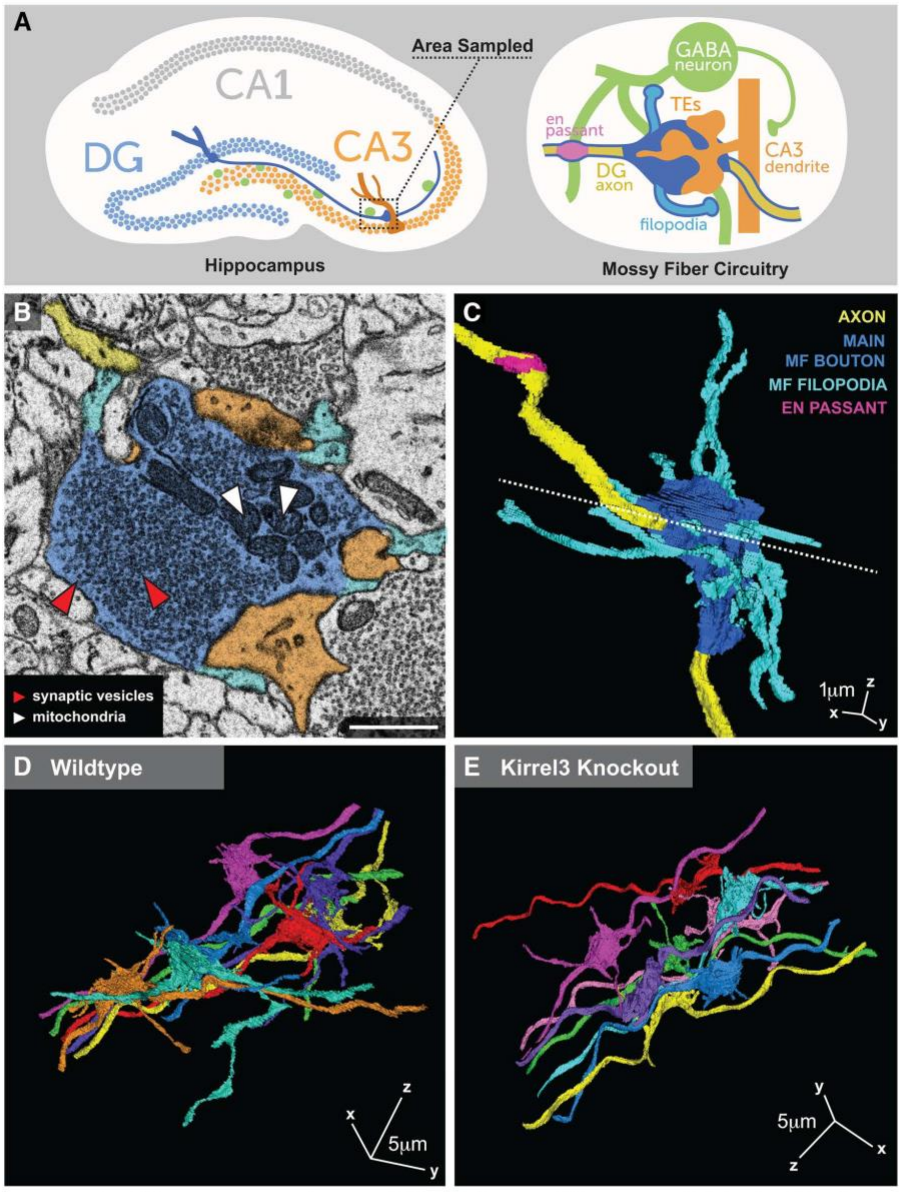

Figure 1. Reconstructing MF presynaptic complexes by SBEM. ***A***, Diagram of hippocampal MF circuitry. Boxed region notes the tissue area analyzed. On the right, the dark blue outline identifies the DG neuron. ***B***, Representative image of a wildtype SBEM section showing MF synapse components: main MF bouton (dark blue), MF filopodia (light blue), DG axon (yellow), TEs (orange), SVs (red arrows), and mitochondria (white arrows). Scale bar, 1 μm. ***C***, 3D reconstruction of the MF presynaptic complex in ***B***. The postsynaptic TEs are not shown. Dotted line in ***C*** shows the location of slice shown in ***B***. ***D***,***E***, Sample wildtype (***D***) and Kirrel3 knockout (***E***) 3D reconstructions showing eight MF presynaptic complexes each.

the first precise description of MF filopodia and en passant connectivity in wildtype mice.

Materials and Methods

Animals

Tissue from two different sets of wildtype and knockout littermate mice were imaged to create four independent SBEM datasets. P14 littermates consisting of a Kirrel3 wildtype (female) and a Kirrel3 knockout (female) were used for datasets 1 and 2 and P14 littermates from a different breeding pair consisting of a Kirrel3 wildtype (male) and a Kirrel3 knockout (female) were used for datasets 3 and 4. All animals and experiments were maintained and conducted in accordance with the NIH guidelines on the care and use of animals and approved by the University of Utah School of Medicine Institutional Animal Care and Use Committee. Generation of Kirrel3 knockout mice was previously described (Prince et al., 2013).

Tissue fixation and processing

Mice were anesthetized and perfused at a rate of 6 ml/min with 2.5% glutaraldehyde and 4% paraformaldehyde in 0.1 M sodium cacodylate buffer. The brains were removed and stored overnight at 4°C in perfusion solution. The next day the brains were sliced in cold PBS into 200-μm coronal sections and sent to Renovo Neural (RRID: SCR_001035) for processing and imaging on a Zeiss Sigma VP Scanning Electron Microscope with a Gatan 3View door.

Image stacks

Each dataset contains 400-500 serial images. In datasets 1 (wildtype) and 2 (knockout), images are 45 $\times$ 45 μm at 7 nm/pixel resolution with a z-depth of 70 nm to cover a volume of 56,700 μm^3. In datasets 3 (wildtype) and 4 (knockout), images are 37 $\times$ 37 μm at 6 nm/pixel resolution with a z-depth of 70 nm to cover a volume of 47,915 μm^3. Beam penetration for each was 25–30 nm. TrakEM2 software was used to assemble images for 3D reconstruction and analysis (Cardona et al., 2012; RRID: SCR_008954). All reconstruction and analysis was done blind to genotype. MF presynaptic complexes near the center of the dataset were randomly selected for reconstruction. MF presynaptic complexes with MF filopodia extending out of the dataset were not analyzed.

Determination of structures

Main MF boutons were identified as an axon enlargement filled with synaptic vesicles (SVs) adjacent to postsynaptic densities (PSDs) on CA3 TEs. MF filopodia were identified as a projection extending at least 0.5 μm off of the main MF bouton with a clear neck structure lacking SVs from the main MF bouton. SV clusters are defined as a group of 10 or more SVs. Synapse-free MF filopodia contained no SV clusters. Partial MF filopodial synapses are defined as SV clusters with no associated PSD. Complete MF filopodial synapses are defined as an SV cluster adjacent to a PSD. Complete and partial synapses could be located anywhere along the length of the MF filopodia. En passant synapses were identified by locating a main MF bouton and following its axon through the dataset. En passant synapses are defined as an SV cluster located in the DG axon with an adjacent PSD.

Dendrite classification

Synapses were classified as being made onto a CA3 neuron, GABA neuron, or unknown. GABA dendrites were identified as either aspiny or had simple protrusions that were not CA3 TEs. CA3 pyramidal neurons were identified by the presence of TEs (multiheaded spines that synapse with large main MF boutons. Some synapses were marked as having unknown partners because they were onto dendritic elements that could not be followed through the dataset.

Image measurements, statistics, and image presentation

Volumetric measurements were generated in TrakEM2 software. Statistics were calculated in Prism (GraphPad, RRID: SCR_002798). In all cases, data were tested for normality using the D'Agostino and Pearson test. If all datasets were normal, parametric tests were used to compare genotypes. Otherwise, nonparametric tests were used. For publication, EM images were adjusted for visibility using Photoshop, but the entire field of view and all images were always adjusted in the same manner. All analysis and quantification was done using raw image data.

Results

Reconstructing MF presynaptic complexes by SBEM

Because MF presynaptic complexes are giant structures with elaborate features, complete analysis of their ultrastructure requires 3D EM. SBEM excellently suits this task as it generates hundreds of well-aligned serial EM images at nanoscale resolution (Denk and Horstmann, 2004). Given that Kirrel3 is highly expressed in DG neurons and is associated with developmental disorders, we analyzed DG presynapses by EM during development at age postnatal day 14 (P14). We collected four SBEM datasets, each covering at least 47,915 μm^3 of tissue from two P14 wildtype and two P14 Kirrel3 knockout mice. Because Kirrel3 is selectively expressed in DG and GABA neurons and mediates homophilic adhesion, it suggests Kirrel3 will regulate DG-GABA synapses. Thus, in all datasets we sampled the stratum lucidum of the dorsal hippocampus, which contains DG axons, GABA neurons, and CA3 neurons (Fig. 1*A*).

TrakEM2 software (Cardona et al., 2012) was used to manually reconstruct synapses. We reconstructed 15 MF presynaptic complexes in each wildtype volume, 19 in one Kirrel3 knockout volume, and 15 in the other knockout volume for a total of 30 wildtype and 34 knockout MF complexes and all associated MF filopodia. All tracing and analysis was done blind to genotype to avoid selection biases. Main MF boutons were unambiguously identified by their large size, high density of SVs, and scattered mitochondria (Fig. 1*B*). After selection of a main MF bouton, all attached filopodia and the axon were fully traced and reconstructed in 3D (Fig. 1*B*,*C*; Movie 1). Representative images of eight reconstructed MF complexes from

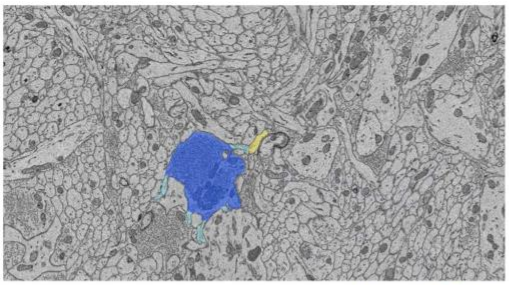

Movie 1. MF presynaptic complex shown in Figure 1*B*,*C*. [View online]

a wildtype mouse and a Kirrel3 knockout mouse are shown (Fig. 1*D*,*E*).

MF filopodia exist in three states during development

After reconstructing at least 30 MF presynaptic complexes from each genotype, we find that loss of Kirrel3 does not cause statistically significant differences in the volume of the main MF bouton (Fig. 2*A*) or the mean number of MF filopodia per main MF bouton (Fig. 2*B*) compared with wildtype mice. However, consistent with a previous report (Martin et al., 2015), a cumulative histogram of the data reveals that MF presynaptic complexes from Kirrel3 knockout mice tend to have fewer MF filopodia per main MF bouton (Fig. 2*C*).

It is currently unknown if MF filopodia density directly correlates with synapse density, which is ultimately the most critical factor impacting MF circuit function. Therefore, we next analyzed the density and postsynaptic targets of synapses housed in MF filopodia. We identified three states with which to classify MF filopodia. First, some MF filopodia contain no SV clusters nor are they adjacent to any PSDs anywhere along their length (Fig. 2*D*). We refer to these MF filopodia as "synapse free." Second, some MF filopodia contain clusters of 10 or more SVs but no visible corresponding PSD (Fig. 2*E*). Presynaptic elements are commonly found before postsynaptic elements are present (Amaral and Dent, 1981; Friedman et al., 2000; Wilke et al., 2013), and we postulate that these SV clusters either mark future synaptic sites or have PSDs that are not visible due to plane of sectioning. We refer to these as "partial synapses." Third, some MF

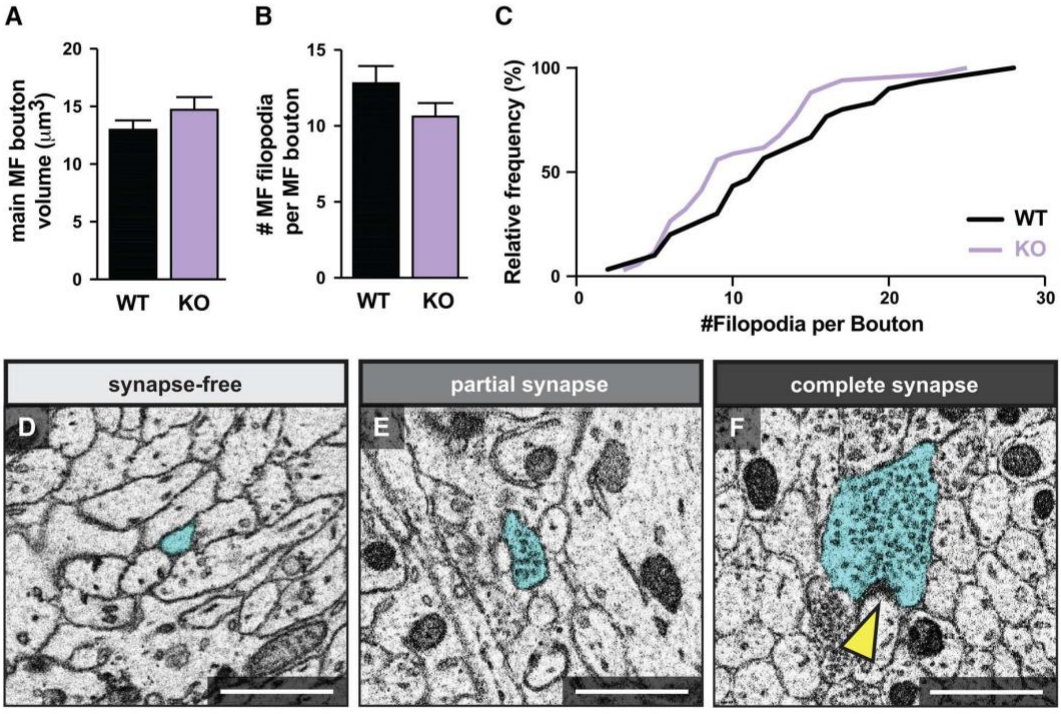

Figure 2. MF filopodia exist in three states during development. ***A***, The average volume of the main MF bouton per genotype. $p = 0.5102$. ***B***, The average number of MF filopodia per main MF bouton. $p = 0.1323$. ***C***, Cumulative histogram showing the number of MF filopodia per main MF bouton in each genotype. Note: Kirrel3 knockouts tend to have MF boutons with fewer filopodia. $p = 0.2360$. ***D–F***, Representative images of MF filopodia in each of the three synaptic states (synapse-free, partial, complete). Yellow arrow indicates PSD. For all graphs: sample size: WT = 30 and KO = 34 main MF boutons. Error bars show mean ± SEM. Scale bars, 1 μm.

A

	% MF filopodia	
	WT	KO
synapse-free	52.1% (200/384)	62.3% (225/361)
partial synapse	38.8% (149/384)	35.7% (129/361)
complete synapse	13.8% (53/384)	10.5% (38/361)

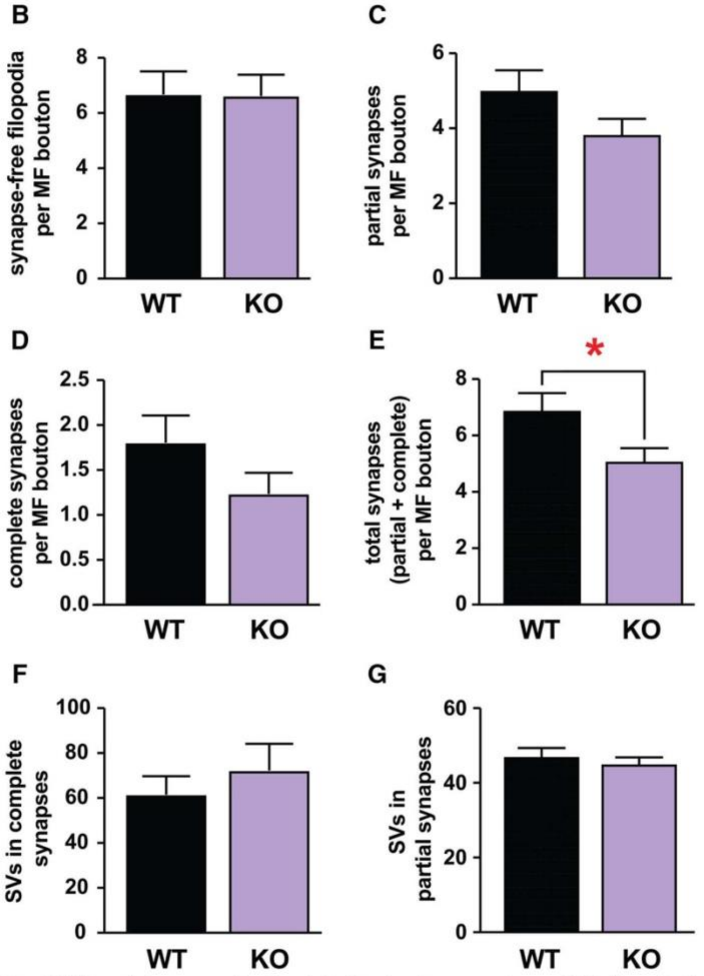

Figure 3. Kirrel3 regulates MF filopodial synapse density. ***A***, Table showing percentage of MF filopodia that are synapse-free, or contain partial or complete synapses. Note: An individual MF filopodia can have multiple synapses, thus the totals do not sum to 100%. ***B–D***, Quantification of the number of synapse-free MF filopodia (***B***), partial synapses (***C***), and complete synapses (***D***) per main MF bouton by genotype. ***E***, Quantification of total number of synapses (partial + complete) per main MF bouton. $*p = 0.0357$ using a two-tailed *t* test. Sample size for ***A–E***: WT = 30 and KO = 34 main MF boutons. ***F***, Quantification of the number of SVs in complete synapses. Sample size for ***F***: WT = 55 and KO = 42 synapses. ***G***, Quantification of the number of SVs in partial synapses. Sample size for ***G***: WT = 150 and KO = 131 synapses. For all graphs: Unless noted, $p > 0.05$ (Table 1). Error bars show mean ± SEM.

Table 1. Statistics

Graph	Data structure	Type of test	*p* value
Figure 2*A*	Nonparametric	Mann-Whitney test	0.5102
Figure 2*B*	Normal distribution	Unpaired *t* test	0.1323
Figure 2*C*	Normal distribution	Kolmogorov-Smirnov test	0.2360
Figure 3*B*	Normal distribution	Unpaired *t* test	0.9781
Figure 3*C*	Normal distribution	Unpaired *t* test	0.1140
Figure 3*D*	Nonparametric	Mann-Whitney test	0.2061
Figure 3*E*	Normal distribution	Unpaired *t* test	0.0357
Figure 3*F*	Nonparametric	Mann-Whitney test	0.2595
Figure 3*G*	Nonparametric	Mann-Whitney test	0.8720
Figure 4*J*	Nonparametric	Mann-Whitney test	0.0075
Figure 4*K*	Nonparametric	Mann-Whitney test	0.7906
Figure 4*M*	Nonparametric	Kruskal-Wallis test	0.0051
Figure 4*N*	Nonparametric	Kruskal-Wallis test	0.0153
Figure 4*O*	Nonparametric	Kruskal-Wallis test	0.0973
Figure 4*P*	Nonparametric	Kruskal-Wallis test	0.1268
Figure 6*E*	Nonparametric	Mann-Whitney test	0.5208

filopodia contain bona fide synapses with SV clusters adjacent to a PSD (Fig. 2*F*). We refer to these as "complete synapses."

Kirrel3 regulates formation of MF filopodial synapses

When comparing the total percentage of MF filopodia in each synaptic state by genotype, we find Kirrel3 knockout mice have a greater percentage of MF filopodia that are synapse-free and a lower percentage that contain partial and complete synapses compared with wildtype (Fig. 3*A*). Next, we analyzed the average number of MF filopodia that exist in each state per main MF bouton, which comprises the key functional unit for a DG neuron. When analyzed this way, the average number of synapse-free MF filopodia per main MF bouton is similar between wildtype and knockout (Fig. 3*B*). This suggests that the missing MF filopodia (Fig. 2*B*,*C*) are those that would normally contain a synapse. In support of this, we observe reductions in both synapse types per main bouton in Kirrel3 knockout mice (Fig. 3*C*,*D*), and when partial and complete synapses are combined, Kirrel3 knockout mice have significantly fewer synapses per main MF bouton than wildtype mice (Fig. 3*E*). The average number of SVs in synapses was similar between the genotypes (Fig. 3*F*,*G*). Thus, our data indicate that, compared with wildtype mice, Kirrel3 knockout mice have fewer MF filopodia with synapses, but the synapses that do form have normal ultrastructure.

Kirrel3 selectively regulates MF filopodial synapses onto GABA neurons

Next we determined the postsynaptic targets of MF filopodial synapses. Broadly defined there are two types of potential postsynaptic target neurons in the stratum lucidum; GABA neurons and CA3 neurons. The two target cell types can be readily identified by their dendritic morphology. GABA neurons can be aspiny or spiny but their dendrites always lack multiheaded TE spines (Fig. 4*A*,*B*). Conversely, CA3 dendrites always have multiheaded TE spines making multiple synapses with main MF boutons (Fig. 4*C*,*D*).

It is widely accepted that MF filopodia only synapse onto GABA neurons (Amaral, 1979; Claiborne et al., 1986; Acsády et al., 1998). Therefore, we were surprised to observe that, in P14 wildtype mice, MF filopodia form complete synapses with similar frequency onto GABA dendrites (Fig. 4*E*,*F*,*I*) as CA3 dendrites (Fig. 4*G*-*I*). Most GABA dendrites contacted by MF filopodia have simple spiny protrusions as previously observed (Acsády et al., 1998), and synaptic contacts are found on both GABA dendritic shafts (Fig. 4*E*) and spiny protrusions (Fig. 4*F*). Similarly, when MF filopodia synapse onto CA3 neurons, we observed synaptic contacts on CA3 dendritic shafts (Fig. 4*G*) and TE spines (Fig. 4*H*).

MF filopodia also synapse onto both GABA and CA3 neurons in Kirrel3 knockout mice. However, knockout mice have a clear shift in the distribution of postsynaptic partners. Compared with wildtype mice, Kirrel3 knockout mice develop significantly fewer complete synapses with GABA neurons (Fig. 4*J*). In contrast, the number of complete MF filopodial synapses made onto CA3 neurons is similar between wildtype and Kirrel3 knockout mice (Fig. 4*K*). The net effect of these changes is a dramatic decrease in the ratio of MF filopodial synapses made onto GABA versus CA3 neurons in mice lacking Kirrel3 compared with wildtype (Fig. 4*L*).

We then examined if filopodia synapsing with GABA neurons have a different morphological signature from filopodia synapsing with CA3 neurons, and if these characteristics change upon Kirrel3 loss (Fig. 4*M*–*P*). For this analysis, we only included only filopodia that have a complete synapse onto an identified GABA or CA3 neuron. Because Kirrel3 knockout mice have significantly fewer filopodia-GABA synapses than wildtype mice, the sample size for this category was small ($n = 4$ filopodia with five complete synapses). Nonetheless, this new analysis indicates that, on average, filopodia synapsing onto either GABA or CA3 neurons have a similar morphology and SV composition in wildtype mice (Fig. 4*O*,*P*). However, we did observe some differences in filopodia morphology between wildtype and Kirrel3 knockout mice. In particular, the total volume of both classes of filopodia (those connected to either GABA or CA3 neurons) is increased on Kirrel3 loss (Fig. 4*M*). For filopodia synapsing onto CA3 neurons, the increased volume is clearly due to increased length (Fig. 4*N*) and not an increase in cross-sectional area (Fig. 4*O*). For filopodia synapsing onto GABA neurons, the increased volume may be due to a combination of increased length and cross-sectional area but neither parameter is significantly different (Fig. 4*N*,*O*) and we hesitate to draw strong conclusions based on the low sample size of filopodia synapsing with GABA neurons in Kirrel3 knockout mice.

En passant connectivity is unperturbed by Kirrel3 loss

Next, we analyzed formation of DG en passant synapses in wildtype and Kirrel3 knockout mice. DG en passant synapses are readily identifiable by EM as clusters of SVs in the axon shaft adjacent to a PSD (Fig. 5*A*-*C*). Like MF filopodia, en passant synapses are thought to syn-

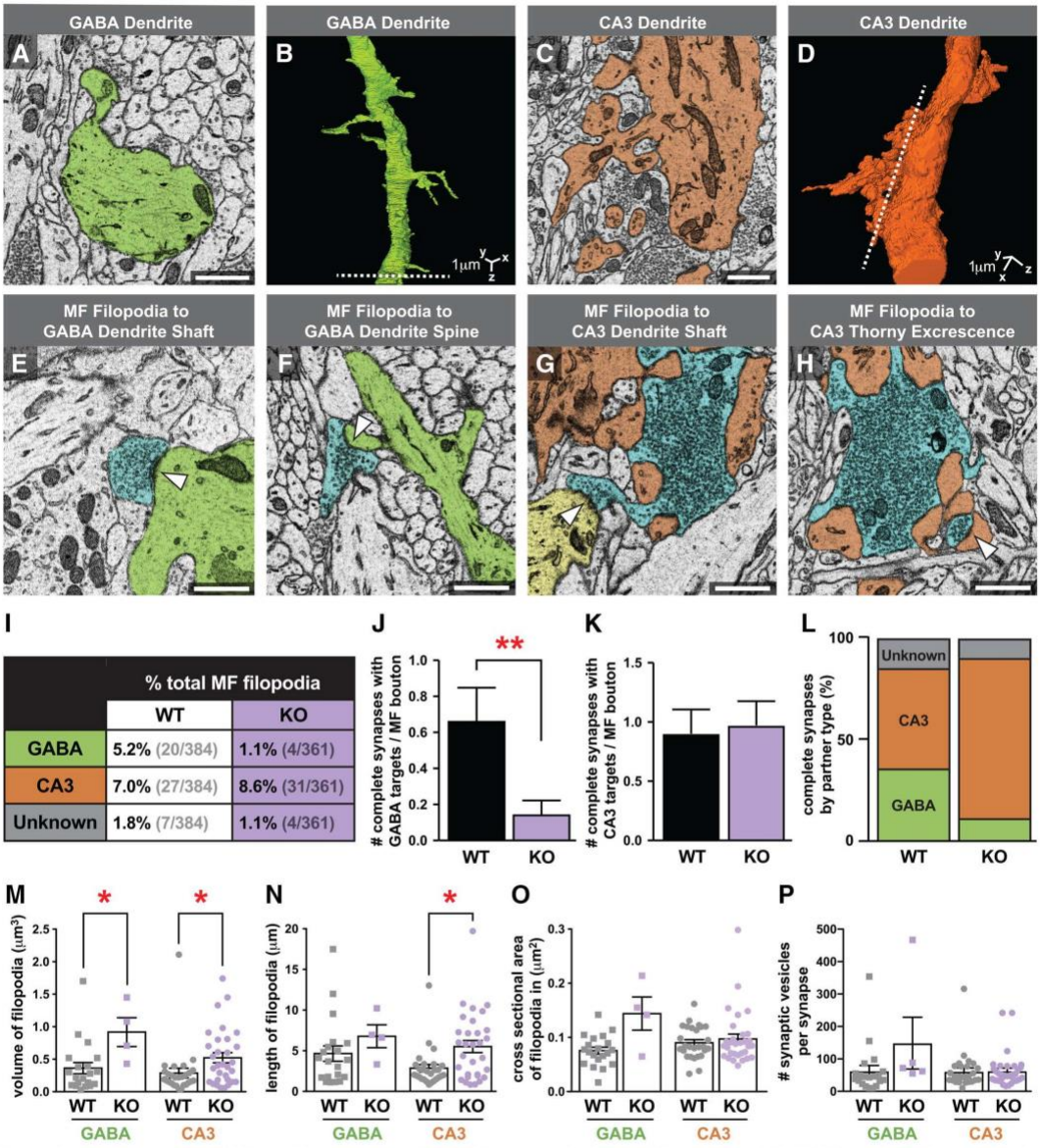

Figure 4. Kirrel3 regulates MF filopodial synapses with GABA neurons, but not CA3 neurons. ***A***,***B***, 2D (***A***) and 3D (***B***) example of a GABA dendrite (green) with simple spine-like protrusions and no PSDs with main MF boutons. Dotted line in ***B*** shows the location of slice shown in ***A***. ***C***,***D***, 2D (***C***) and 3D (***D***) example of a CA3 neuron (orange) with multiheaded TE spines and many PSDs with main MF boutons. Dotted line in ***D*** shows the location of slice shown in ***C***. ***E***,***F***, Representative images of complete MF filopodial synapses made onto a GABA dendritic shaft (***E***) and a GABA spine (***F***). MF filopodia (blue), GABA dendrite (green), synapses indicated by white arrows. ***G***,***H***, Representative images of complete MF filopodial synapses made onto a second CA3 dendritic shaft (***G***) and a CA3 TE (***H***). Main MF bouton and MF filopodia (blue), CA3 dendrite and TEs (orange), second CA3 dendrite (yellow), synapses indicated by white arrows. ***I–L***, Quantification of MF filopodial synapses onto different types of postsynaptic neurons. ***I***, Percentage of wildtype or Kirrel3 knockout MF filopodia making complete synapses with indicated postsynaptic partner type. ***J***, Number of complete MF filopodial synapses onto GABA neurons per main MF bouton. $^{**}p = 0.0075$ by Mann-Whitney test. ***K***, Number of complete MF filopodial synapses onto CA3 neurons per main MF bouton. ***L***, Including only the MF filopodia that make a complete synapse, the

continued
percentage of each partner type is shown. Sample size for ***I–L***: WT = 30 and KO = 34 main MF boutons. Unless indicated $p > 0.05$. ***M–P***, Comparison of the morphology of filopodia synapsing with GABA versus CA3 neurons in wildtype and Kirrel3 knockout mice using the Kruskal-Wallis test with multiple comparisons. ***M***, Volume of filopodia in μm^3. GABA WT to KO $*p = 0.0419$, CA3 WT to KO $*p = 0.0507$. ***N***, Length of filopodia in micrometers. $*p = 0.0299$. ***O***, Cross sectional area in square micrometers. $p > 0.05$. ***P***, Number of SVs per synapse. $p > 0.05$. Sample size for ***M–O***: WT GABA = 20, KO GABA = 4, WT CA3 = 27, KO CA3 = 31. Sample size for ***P***: WT GABA = 20, KO GABA = 5, WT CA3 = 27, KO CA3 = 33. For entire figure, error bars show mean ± SEM. Scale bars, 1 μm.

apse exclusively onto GABA neurons (Acsády et al., 1998). Given that Kirrel3 is expressed specifically by DG and GABA neurons, we reasoned that in addition to regulating DG MF filopodia to GABA synapses, Kirrel3 may also regulate formation of DG en passant to GABA synapses. Consistent with the existing literature, 100% of DG en passant synapses observed in our datasets synapse with GABA neurons (Fig. 5*D*). However, interestingly, the loss of Kirrel3 has no effect on the density of en passant synapses in DG axons (Fig. 5*E*). This indicates Kirrel3 has a highly specific function regulating DG MF filopodia to GABA neuron synapses but not DG axon to GABA neuron synapses.

Other morphologic features of MF filopodia

Given that this is the first in-depth 3D analysis of MF filopodia connectivity, we noted the presence of several unusual MF filopodia structures. First, we occasionally observed growth cone-like endings at the tips of MF filopodia (Fig. 6*A-C*). These structures had no synapses and few, if any, SVs along their length. Given that our data are from P14 mice that are near the peak of DG synaptogenesis, they likely represent newly formed MF filopodia in search of a target neuron. Second, we observe branched MF filopodia (Fig. 6*A*,*D*,*E*). We sought to determine if MF filopodia from Kirrel3 knockout mice have fewer branches because an ortholog of Kirrel3, SYG-1, regulates axonal branch generation in *Caenorhabditis elegans* motor neurons (Chia et al., 2014). However, we find little difference in filopodia branching between wildtype and Kirrel3 knockout mice (Fig. 6*E*). Third, though it is often assumed that MF filopodia contain only one terminal synapse at the MF filopodia tip, we observe that individual MF filopodia can house multiple synapses with some located in the MF filopodia shaft (Fig. 6*A*,*F-H*). It will be interesting to determine in a future study whether these features of growth cone-like ends, branches, and multiple synapses are developmental in origin or are dynamically maintained in adult mice to allow circuit flexibility.

Discussion

Here, we present a rigorous ultrastructural analysis of MF filopodial connectivity in the developing mammalian brain in wildtype and Kirrel3 knockout mice. First, we discovered contrary to previous reports, MF filopodia synapse with similar frequency onto GABA and CA3 neurons. Second, we show Kirrel3 is selectively required for normal synapse density between DG MF filopodia and GABA neurons but not CA3 neurons. Third, we discovered Kir-

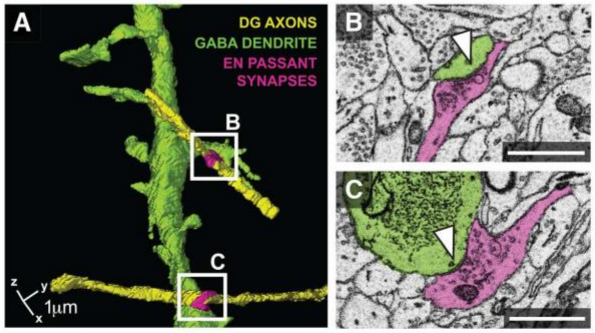

D	% en passant synapses	
	WT	KO
GABA	100% (21/21)	100% (20/20)
CA3	0% (0/21)	0% (0/20)

E	# en passants
WT	7.46 per mm axon
KO	7.84 per mm axon

Figure 5. Kirrel3 does not regulate en passant synapse density. ***A–C***, 3D example (***A***) of a spiny GABA dendrite targeted by en passant synapses from two separate DG axons. Synapses magnified in ***B***, ***C***. GABA dendrite (green), DG axon (yellow), en passant synapse (pink). ***D***, Percentage of en passant synapses made onto GABA and CA3 dendrites from 73 WT and 68 KO DG axon segments. ***E***, Table reporting the number of en passant synapses per millimeter axon. Scale bars, 1 μm.

A Observation	Wildtype	Kirrel3 Knockout
1) MF filopodia with growth cone-like endings	0.78% (3/384)	3.6% (13/361)
2) MF filopodia that branch	5.5% (21/384)	7.5% (27/361)
3) MF filopodia with multiple complete synapses	0.52% (2/384)	0.83% (3/361)

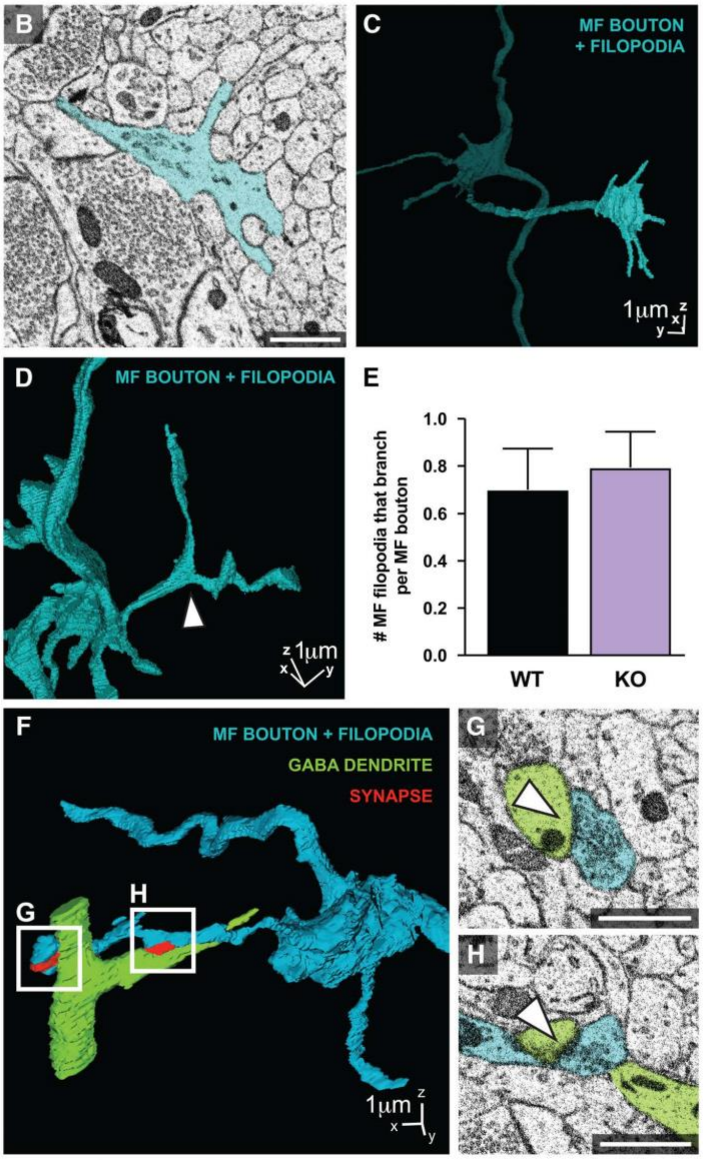

Figure 6. Additional morphologic features of MF circuits. ***A***, Table reporting the percentage of wildtype and Kirrel3 knockout MF filopodia with indicated features. ***B***, ***C***, Representative 2D (***B***) and 3D (***C***) example of a MF filopodia ending in a growth cone-like

continued

structure. ***D***, 3D example of a branched MF filopodia. White arrow indicates branch point. ***E***, Quantification of the number of branching MF filopodia per main MF bouton. Sample size: WT = 30 and KO = 34 main MF boutons. $p > 0.05$. Error bars show mean ± SEM. ***F–H***. 3D example of one MF filopodia making multiple synapses onto one GABA neuron (***F***), synapses magnified in ***G***, ***H*** shown in 2D. Main MF bouton with associated MF filopodia (blue), GABA dendrite (green), synapses (red). Scale bars, 1 μm.

rel3 does not regulate DG-GABA en passant synapse formation.

To our knowledge, this is the first report of MF filopodia synapsing with CA3 pyramidal neurons. Previous work indicated that MF filopodia only synapse onto GABA neurons (Acsády et al., 1998; McBain, 2008; Rollenhagen, 2010). However, prior work examined MF filopodia connectivity at an unspecified age without the use of current, high-throughput EM technologies (Acsády et al., 1998). In contrast, our study was done on juvenile P14 animals and we analyzed >350 MF filopodia per genotype, providing an improved sample size. Thus, it is possible MF filopodia-CA3 synapses exist in the adult and were previously missed due to factors such as sample size or imaging method. It is also possible MF filopodia-CA3 synapses are a developmental phenomenon that are selectively pruned by adulthood. Future studies on adult mice are needed to distinguish between these two possibilities. In addition, we observed that filopodia synapsing onto either GABA or CA3 neurons have a similar morphology and SV composition in wildtype mice, but those synapsing onto CA3 neurons in Kirrel3 knockout mice are significantly longer. Because Kirrel3 knockout mice have so few filopodia synapsing with GABA neurons, we postulate the increased length of filopodia synapsing with CA3 neurons could be due to the extra availability of resources, increased drive to search for a postsynaptic partner, or delayed maturity.

Why might the MF circuit benefit from having MF filopodia synapse onto both GABA and CA3 neurons? MF filopodia are highly plastic, motile structures (Tashiro et al., 2003) and are likely better suited to quickly adapt to changing circuit needs than the large anchored main MF bouton. Over time, circuits adapt to maintain a homeostatic balance of excitatory and inhibitory activity (Turrigiano, 2012; Nelson and Valakh, 2015) and having flexible MF filopodia that can increase or decrease input to GABA versus CA3 neurons may be one way the hippocampus maintains this balance. It was shown that MF presynaptic complexes and MF filopodia increase in response to enriched environment and learning tasks such as fear conditioning and the Morris water maze (Bednarek and Caroni, 2011; Ruediger et al., 2011). However, it is not known if and where these newly added MF filopodia make synapses. Knowing whether these newly added adult MF filopodia preferentially synapse onto GABA neurons or CA3 neurons would provide insight toward understanding hippocampal circuit changes underlying learning and memory.

In addition to more precisely defining MF connectivity in wildtype mice, our study suggests Kirrel3 is a highly selective target-specificity molecule. We show Kirrel3 is specifically required to establish the appropriate density of MF filopodia-GABA synapses, but not MF filopodia-CA3 synapses or DG en passant-GABA synapses during development. It is possible that loss of Kirrel3 causes a permanent reduction in filopodia-GABA synapses or, alternatively, the loss of Kirrel3 may cause a delayed maturation of filopodia-GABA synapses. The current study conducted at one developmental time point cannot distinguish between these possibilities but future work analyzing filopodial synapse development over time can address this mechanism. Nonetheless, Kirrel3 is a homophilic, transmembrane molecule selectively expressed in DG and GABA neurons (Martin et al., 2015). Thus, our results support the hypothesis that trans-cellular homophilic Kirrel3 binding selectively stabilizes MF filopodial contacts between DG axons and GABA dendrites. Kirrel3 may also provide a pre- and postsynaptic signal to actively induce synapse formation via its intracellular domain. In support, mammalian Kirrel3 was shown to interact with the synaptic molecules CASK (Gerke et al., 2006; Bhalla et al., 2008), PICK1 (Höhne et al., 2011), and recently PSD95 (Roh et al., 2017), but details of how Kirrel3 signals *in vivo* remain unknown.

It is noteworthy that not all MF filopodia-GABA synapses are eliminated in Kirrel3 knockout mice. Kirrel3 is widely expressed by DG neurons but is expressed only by a subpopulation of calbindin-positive GABA neurons. These Kirrel3-positive interneurons make up just 19% of all GABA neurons present in area CA3 (Martin et al., 2015). Thus Kirrel3 knockout mice may selectively lack all input to this subpopulation of GABA neurons and the MF filopodia-GABA synapses that remain may connect DG neurons to Kirrel3-negative GABAergic neurons via alternative mechanisms. Additionally, we observed no change in en passant synapse number on loss of Kirrel3. It is possible Kirrel3 does not localize along the DG axon or that en passant synapses selectively target Kirrel3-negative GABA neurons. The latter possibility would suggest DG neurons use MF filopodial and en passant synapses to differentially communicate with distinct types of GABA neurons.

In conclusion, our results indicate Kirrel3 is required for formation of a subset of hippocampal DG-GABA synapses. Loss of DG-GABA synapses is expected to reduce feed-forward inhibition to CA3 neurons and likely explains the prior observation that juvenile Kirrel3 knockout mice have over-active CA3 neurons (Martin et al., 2015). Selective loss of DG-GABA synapses may contribute to the etiology of Kirrel3-dependent neurodevelopmental disorders by causing an excitation/inhibition imbalance in hippocampal circuits and a better understanding of the precise synaptic defects caused by loss of Kirrel3 may ultimately lead to more effective treatments.

References

Acsády L, Kamondi A, Sík A, Freund T, Buzsáki G (1998) GABAergic cells are the major postsynaptic targets of mossy fibers in the rat hippocampus. J Neurosci 18:3386–3403. CrossRef

Amaral DG (1979) Synaptic extensions from the mossy fibers of the fascia dentata. Anat Embryol 155:241–251. CrossRef

Amaral DG, Dent JA (1981) Development of the mossy fibers of the dentate gyrus: I. A light and electron microscopic study of the mossy fibers and their expansions. J Comp Neurol 195:51–86. CrossRef

Bednarek E, Caroni P (2011) β-Adducin is required for stable assembly of new synapses and improved memory upon environmental enrichment. Neuron 69:1132–1146. CrossRef

Ben-David E, Shifman S (2012) Networks of neuronal genes affected by common and rare variants in autism spectrum disorders. PLoS Genet 8:e1002556. CrossRef

Bhalla K, Luo Y, Buchan T, Beachem MA, Guzauskas GF, Ladd S, Bratcher SJ, Schroer RJ, Balsamo J, DuPont BR, Lilien J, Srivastava AK (2008) Alterations in CDH15 and KIRREL3 in patients with mild to severe intellectual disability. Am J Hum Genet 83:703–713. CrossRef

Bragin A, Jando G, Nadasdy Z, Hetke J, Wise K, Buzsáki G (1995) Gamma (40-100 Hz) oscillation in the hippocampus of the behaving rat. J Neurosci 15:47–60.

Cardona A, Saalfeld S, Schindelin J, Arganda-Carreras I, Preibisch S, Longair M, Tomancak P, Hartenstein V, Douglas RJ (2012) TrakEM2 software for neural circuit reconstruction. PLoS One 7:e38011. CrossRef

Cheng Y, Quinn JF, Weiss LA (2013) An eQTL mapping approach reveals that rare variants in the SEMA5A regulatory network impact autism risk. Hum Mol Genet 22:2960–2972. CrossRef

Chia PH, Chen B, Li P, Rosen MK, Shen K (2014) Local F-actin network links synapse formation and axon branching. Cell 156:208–220. CrossRef

Choi S-Y, Han K, Cutforth T, Chung W, Park H, Lee D, Kim R, Kim M-H, Choi Y, Shen K, Kim E (2015) Mice lacking the synaptic adhesion molecule Neph2/Kirrel3 display moderate hyperactivity and defective novel object preference. Front Cell Neurosci 9:283. CrossRef

Claiborne BJ, Amaral DG, Cowan WM (1986) A light and electron microscopic analysis of the mossy fibers of the rat dentate gyrus. J Comp Neurol 246:435–458. CrossRef

De Rubeis S, He X, Goldberg AP, Poultney CS, Samocha K, Cicek AE, Kou Y, Liu L, Fromer M, Walker S, Singh T, Klei L, Kosmicki J, Shih-Chen F, Aleksic B, Biscaldi M, Bolton PF, Brownfeld JM, Cai J, Campbell NG, et al. (2014) Synaptic, transcriptional and chromatin genes disrupted in autism. Nature 515:209–215. CrossRef

Deller T, Nitsch R, Frotscher M (1994) Associational and commissural afferents of parvalbumin-immunoreactive neurons in the rat hippocampus: a combined immunocytochemical and PHA-L study. J Comp Neurol 350:612–622. CrossRef

Denk W, Horstmann H (2004) Serial block-face scanning electron microscopy to reconstruct three-dimensional tissue nanostructure. PLoS Biol 2:e329.

Faulkner RL, Jang M-H, Liu X-B, Duan X, Sailor KA, Kim JY, Ge S, Jones EG, Ming G-L, Song H, Cheng HJ (2008) Development of hippocampal mossy fiber synaptic outputs by new neurons in the adult brain. Proc Natl Acad Sci USA 105:14157–14162. CrossRef

Friedman HV, Bresler T, Garner CC, Ziv NE (2000) Assembly of new individual excitatory synapses: time course and temporal order of synaptic molecule recruitment. Neuron 27:57–69. CrossRef

Frotscher M (1985) Mossy fibres form synapses with identified pyramidal basket cells in the CA3 region of the guinea-pig hippocampus: a combined Golgi-electron microscope study. J Neurocytol 14:245–259. CrossRef

Gerke P, Benzing T, Höhne M, Kispert A, Frotscher M, Walz G, Kretz O (2006) Neuronal expression and interaction with the synaptic protein CASK suggest a role for Neph1 and Neph2 in synaptogenesis. J Comp Neurol 498:466–475. CrossRef

Gerke P, Sellin L, Kretz O, Petraschka D, Zentgraf H, Benzing T, Walz G (2005) NEPH2 is located at the glomerular slit diaphragm, interacts with nephrin and is cleaved from podocytes by metalloproteinases. J Am Soc Nephrol 16:1693–1702. CrossRef

Guerin A, Stavropoulos DJ, Diab Y, Chénier S, Christensen H, Kahr WHA, Babul-Hirji R, Chitayat D (2012) Interstitial deletion of 11q-implicating the KIRREL3 gene in the neurocognitive delay associated with Jacobsen syndrome. Am J Med Genet A 158A:2551–2556. CrossRef

Höhne M, Lorscheider J, Bardeleben v. A, Dufner M, Scharf MA, Gödel M, Helmstädter M, Schurek E-M, Zank S, Gerke P, Kurschat C, Sivritas SH, Neumann-Haefelin E, Huber TB, Reinhardt HC, Schauss AC, Schermer B, Fischbach KF, Benzing T (2011) The BAR domain protein PICK1 regulates cell recognition and morphogenesis by interacting with Neph proteins. Mol Cell Biol 31:3241–3251. CrossRef

Iossifov I, Ronemus M, Levy D, Wang Z, Hakker I, Rosenbaum J, Yamrom B, Lee Y-H, Narzisi G, Leotta A, Kendall J, Grabowska E, Ma B, Marks S, Rodgers L, Stepansky A, Troge J, Andrews P, Bekritsky M, Pradhan K, et al. (2012) De novo gene disruptions in children on the autistic spectrum. Neuron 74:285–299. CrossRef

Kaminsky EB, Kaul V, Paschall J, Church DM, Bunke B, Kunig D, Moreno-De-Luca D, Moreno-De-Luca A, Mulle JG, Warren ST, Richard G, Compton JG, Fuller AE, Gliem TJ, Huang S, Collinson MN, Beal SJ, Ackley T, Pickering DL, Golden DM, et al. (2011) An evidence-based approach to establish the functional and clinical significance of copy number variants in intellectual and developmental disabilities. Genet Med 13:777–784. CrossRef

Martin EA, Muralidhar S, Wang Z, Cervantes DC, Basu R, Taylor MR, Hunter J, Cutforth T, Wilke SA, Ghosh A, Williams ME (2015) The intellectual disability gene Kirrel3 regulates target-specific mossy fiber synapse development in the hippocampus. Elife 4:e09395. CrossRef

McBain CJ (2008) Differential mechanisms of transmission and plasticity at mossy fiber synapses. Prog Brain Res 169:225-240.

Michaelson JJ, Shi Y, Gujral M, Zheng H, Malhotra D, Jin X, Jian M, Liu G, Greer D, Bhandari A, Wu W, Corominas R, Peoples A, Koren A, Gore A, Kang S, Lin GN, Estabillo J, Gadomski T, Singh B, et al. (2012) Whole-genome sequencing in autism identifies hot spots for de novo germline mutation. Cell 151:1431–1442. CrossRef

Neale BM, Kou Y, Liu L, Ma'ayan A, Samocha KE, Sabo A, Lin C-F, Stevens C, Wang L-S, Makarov V, Polak P, Yoon S, Maguire J, Crawford EL, Campbell NG, Geller ET, Valladares O, Schafer C, Liu H, Zhao T, et al. (2012) Patterns and rates of exonic de novo mutations in autism spectrum disorders. Nature 485:242–245. CrossRef

Nelson SB, Valakh V (2015) Excitatory/inhibitory balance and circuit homeostasis in autism spectrum disorders. Neuron 87:684–698. CrossRef

Penttonen M, Kamondi A, Sik A, Acsády L, Buzsáki G (1997) Feed-forward and feed-back activation of the dentate gyrus in vivo during dentate spikes and sharp wave bursts. Hippocampus 7:437–450. CrossRef

Prince JEA, Brignall AC, Cutforth T, Shen K, Cloutier J-F (2013) Kirrel3 is required for the coalescence of vomeronasal sensory neuron axons into glomeruli and for male-male aggression. Development 140:2398–2408. CrossRef

Roh JD, Choi SY, Cho YS, Choi TY, Park JS, Cutforth T, Chung W, Park H, Lee D, Kim MH, Lee Y, Mo S, Rhee JS, Kim H, Ko J, Choi SY, Bae YC, Shen K, Kim E, Han K (2017) Increased excitatory synaptic transmission of dentate granule neurons in mice lacking PSD-95-interacting adhesion molecule Neph2/Kirrel3 during the early postnatal period. Front Mol Neurosci 10:81. CrossRef

Rollenhagen A (2010) The mossy fiber bouton: the "common" or the "unique" synapse? Front Synaptic Neurosci 2:2. CrossRef Medline

Rollenhagen A, Sätzler K, Rodríguez EP, Jonas P, Frotscher M, Lübke JHR (2007) Structural determinants of transmission at large hippocampal mossy fiber synapses. J Neurosci 27:10434–10444. CrossRef

Rolls ET (2013) The mechanisms for pattern completion and pattern separation in the hippocampus. Front Syst Neurosci 7:74. CrossRef

Ruediger S, Vittori C, Bednarek E, Genoud C, Strata P, Sacchetti B, Caroni P (2011) Learning-related feedforward inhibitory connectivity growth required for memory precision. Nature 473:514–518. CrossRef

Serizawa S, Miyamichi K, Takeuchi H, Yamagishi Y, Suzuki M, Sakano H (2006) A neuronal identity code for the odorant receptor-specific and activity-dependent axon sorting. Cell 127:1057–1069. CrossRef

Shepherd GMG, Harris KM (1998) Three-dimensional structure and composition of CA3→CA1 axons in rat hippocampal slices: implications for presynaptic connectivity and compartmentalization. J Neurosci 18:8300–8310.

Talkowski ME, Rosenfeld JA, Blumenthal I, Pillalamarri V, Chiang C, Heilbut A, Ernst C, Hanscom C, Rossin E, Lindgren AM, Pereira S, Ruderfer D, Kirby A, Ripke S, Harris DJ, Lee JH, Ha K, Kim HG, Solomon BD, Gropman AL, et al. (2012) Sequencing chromosomal abnormalities reveals neurodevelopmental loci that confer risk across diagnostic boundaries. Cell 149:525–537. CrossRef

Tashiro A, Dunaevsky A, Blazeski R, Mason CA, Yuste R (2003) Bidirectional regulation of hippocampal mossy fiber filopodial motility by kainate receptors. Neuron 38:773–784. CrossRef

Torborg CL, Nakashiba T, Tonegawa S, McBain CJ (2010) Control of CA3 output by feedforward inhibition despite developmental changes in the excitation-inhibition balance. J Neurosci 30:15628–15637. CrossRef

Turrigiano G (2012) Homeostatic synaptic plasticity: local and global mechanisms for stabilizing neuronal function. Cold Spring Harb Perspect Biol 4:a005736. CrossRef

Wilke SA, Antonios JK, Bushong EA, Badkoobehi A, Malek E, Hwang M, Terada M, Ellisman MH, Ghosh A (2013) Deconstructing complexity: serial block-face electron microscopic analysis of the hippocampal mossy fiber synapse. J Neurosci 33:507–522. CrossRef

CHAPTER 4

INVESTIGATING DISEASE-ASSOCIATED KIRREL3 VARIANTS FOR ALTERED FUNCTION IN SYNAPSE DEVELOPMENT

Co-authored by: Megan E. Williams[1]

1 – Department of Neurobiology and Anatomy, University of Utah School of Medicine, Salt Lake City, UT 84112

Abstract

Neurodevelopmental disorders are increasingly thought to be "synaptopathies" or disorders of the synapse. While many disease-associated changes are observed in the genome that encode synaptic proteins, we know little about how these mutations result in neural disease. Kirrel3 is a synaptic cell adhesion molecule and several protein coding variants of Kirrel3 are found in patients with mild to severe intellectual disability and autism spectrum disorders. We recently identified a role for Kirrel3 in hippocampal circuit formation. Kirrel3 loss reduces hippocampal mossy fiber DG-GABA filopodial synapses, which normally function to constrain CA3 pyramidal neuron activity. In addition, we found Kirrel3 knockout mice exhibit an increased excitation/inhibition ratio and evoked activity of CA3 neurons. Here, we examine rare Kirrel3 variants for altered function to identify critical regions of Kirrel3 and to determine if these variants are bona fide risk factors for disease. We find some Kirrel3 variants are unable to promote homophilic cell aggregation or induce synapse formation. These defects represent the first functional evidence that Kirrel3 variants could cause neural dysfunction and disease.

Introduction

Proteins involved in synaptic cell adhesion and synaptic scaffolding are the most prevalent genes identified in genome-wide association studies of neurodevelopmental disorders (Washbourne, 2014). This offers strong support to the current theory that most neurodevelopmental disorders are "synaptopathies" or disorders of the synapse. Studies of some synaptic proteins expressed by most neurons, such as Neurexins and Neuroligins, have led to valuable information about general synapse formation and function, and how

mutations found in disease can alter these processes (Sudhof, 2008; Zoghbi & Bear, 2012). However, few of these synaptic molecules function between specific subtypes of neurons to synthesize precise synapse types. Neurodevelopmental diseases vary greatly and any therapeutics will need to target specific synapse defects while avoiding general synapse function. Thus, it is critical to identify specific sets of synapses, the molecules that govern their development, and how these molecules fail to function in disease.

Kirrel3 is a homophilic transmembrane cell adhesion molecule of the immunoglobulin superfamily. Exonic missense point mutations, copy number variations, and deletions of Kirrel3 are repeatedly found in individuals with autism spectrum disorders (ASD), mild to severe intellectual disability (ID), and Jacobsen's syndrome (Ben-David & Shifman, 2012; Bhalla et al., 2008; Cheng, Quinn, & Weiss, 2013; De Rubeis et al., 2014; Guerin et al., 2012; Iossifov et al., 2012; Kalsner et al., 2017; Kaminsky et al., 2011; Michaelson et al., 2012; Neale et al., 2012; Talkowski et al., 2012). These alterations are typically identified through mass whole exome sequencing of patients, and rarely are comorbidities noted. However, it is likely Kirrel3 defects represent a particular subpopulation of ASD/ID codisorders, which is a valuable distinction as it is estimated that 70% of ASD cases also present with ID (Tuchman & Rapin, 2002).

Kirrel3 is composed of an extracellular region containing five immunoglobulin domains, a transmembrane domain, and an intracellular region terminating in a PDZ-binding domain, which implicates interaction with a number of different proteins such as PSD-95 and ZO-1 (Figure 4.1A, left). In the hippocampus, Kirrel3 is specifically expressed in DG neurons and GABA neurons (Martin et al., 2015). Previously, we

identified a role for Kirrel3 in specific hippocampal synapse development between DG and GABA neurons within the mossy fiber circuit (Figure 4.1B). We find reduced DG-GABA filopodial synapses in Kirrel3 knockout mice (Martin, Woodruff, Rawson, & Williams, 2017). In addition, we observed that loss of Kirrel3 results in an increase in the excitation/inhibition ratio and evoked activity of CA3 pyramidal neurons (Martin et al., 2015). Behaviorally, Kirrel3 knockout mice are consistently found to be hyperactive and also have defects in developmental vocalization, novel object preference, and social interaction (Choi et al., 2015; Hisaoka et al., 2018; Prince et al., 2013; Völker et al., 2018). Together, this work establishes Kirrel3 as a critical molecule for proper hippocampal mossy fiber circuit development.

Mutations are identified spanning the protein in both the extracellular and intracellular domains. However, no study has examined Kirrel3 variants for reduced function. We sought to identify critical regions of Kirrel3 important for its function in synapse development through analysis of disease-associated point mutations. For this investigation, we selected several point mutations that span the protein coding sequence (Figure 4.1A, left). Human and mouse kirrel3 proteins are 98% conserved and the point mutations selected target conserved residues. Each variant has a low minor allele frequency (MAF) score, which identifies them to be extremely rare variants within the population.

In addition, we questioned whether or not Kirrel3 functions during synapse development solely as a “molecular Velcro” to hold membranes together. This would imply that its extracellular region composed of IG domains is the critical component of the protein, and intracellular region is irrelevant to completing this function. To assess the

value of the intracellular domain, we chose to include in our assays a construct with the intracellular domain deleted (ΔICD). This protein is trimmed to four amino acids before the end of exon 14, just after the transmembrane domain (Figure 4.1A, right).

Here, we examine Kirrel3 variants spanning the protein and discover defects both in cell aggregation and synapse formation. Our results present the first mechanistic insight to Kirrel3-mediated pathophysiology within the developing brain.

Materials and methods

Rats and cell lines

Sprague dawley rats were ordered as timed pregnancies from Charles River. CHO cells from ATCC were kindly provided by the Nels Elde lab. All animals and experiments were maintained and conducted in accordance with the NIH guidelines on the care and use of animals and approved by the University of Utah IACUC committee.

Kirrel3 point mutation cloning

Standard PCR cloning was used to move Kirrel3 constructs to the pBos vector and add an extracellular FLAG tag after the signal sequence. Mutagenesis of the constructs was completed to introduce each point mutation. Separate constructs were synthesized to include mCherry-2A prior to each construct to achieve simultaneous labelling with a fluorophore within single cells.

Cell culture

Neurons: P0 rat cortical glia were cultured on PDL/collagen-coated coverslips to form a monolayer. One week later, P0 rat hippocampi were dissected in cold 4-(2-hydroxyethyl)-1-piperazineethanesulfonic acid (HEPES)-buffered saline solution, incubated in papain for 30 min, dissociated, and plated to glial monolayers at 4–5 × 104 cells/ml. All media was from Life Technologies (Carlsbad, CA, United States). Glia media: DMEM, 10% Fetal Bovine Serum (FBS), 75 mM glucose, and penicillin/streptomycin. Neuron-plating media: MEM, 10% horse serum, 50 mM glucose, 0.250 mM pyruvic acid, 2 mM Glutamax, 100 U/ml penicillin, 100 μg/ml streptomycin. Neuron-feeding media: Neurobasal A, B27, 30 mM glucose, 0.5 mM Glutamax, 20 U/ml penicillin, 20 μg/ml streptomycin. Neuron transfections were done using the electroporation method (ECM830 model, BTX, Harvard Apparatus) at time of plating using 10-20 ug DNA or by using calcium phosphate transfection on DIV5 using 1-2 ug DNA. Cell lines: CHO media: F12K media, 10% FBS, and penicillin/streptomycin. Cell line transfections were done using polyethylenimine (PEI, Polysciences, Warrington, PA, United States) at a ratio of 5 μg PEI/1 μg DNA in culture experiments.

CHO cell aggregation assay

CHO cells were transfected with 5 ug DNA of each construct of interest using PEI. Forty-eight hours later, cells were washed with HEPES Mg2+ free (HMF) buffer (137 mM NaCl, 5.4 mM KCl, 1 mM CaCl2, 0.34 mM Na2HPO4, 5.5 mM glucose, 10 mM HEPES, pH 7.4 adjusted with NaOH) and detached from the dishes using 0.01% trypsin in HMF. Detached cells were spun down, resuspended in HMF, counted, and

100,000 cells were pipetted into single wells of 24-well plates precoated with 1% BSA in HMF. Subsequently, the plates were placed on a nutator for 2 hours at 37°C. The cells were then fixed with paraformaldehyde (PFA) (2% final concentration) overnight, transferred to a 96-well glass bottom plate, and imaged in a Zeiss LSM 710 confocal microscope. The aggregation index was calculated by dividing the total fluorescence area in cell aggregates by the total fluorescence area in the well. Analysis was done using Fiji.

Immunostaining

All cultured cells were fixed in 4% PFA for 10 min, washed with phosphate-buffered saline (PBS), and incubated in blocking solution (PBS with 3% bovine albumin and 0.1% Triton-X100) for 30 min. Primary antibody was diluted in blocking solution and incubated on cells for 1.5 hours. After three washes, secondary antibody was incubated for 40-60 min, washed, and cells were mounted for imaging using Fluoromount-G (Southern Biotech, Birmingham, AL, United States). For live labeling, cells were incubated with anti-FLAG antibody diluted 1:250 in serum-free media for 25 min in the culture incubator. Cells were washed, fixed with PFA, and immunostained as above. For tissue sections, mice were transcardially perfused with 4% PFA. Brains were postfixed in 4% PFA overnight and 50 μm vibratome sections were cut. Sections were incubated in blocking solution (PBS, 3% BSA, 0.2% Triton-X100, 0.2% Saponin) for more than 1 hour and incubated in primary antibody at 4°C overnight while rocking. Secondary antibody incubation was done at room temperature for 2 hours. Sections were mounted in Fluoromount-G for imaging.

Antibodies

Primary antibodies were used as follows: goat anti-GFP 1:5000 (Abcam, Cambridge, MA, United States), chick anti-FLAG 1:250 livelabel, 1:1000 postfix (Gallus Immunotech, Cary, NC, United States), mouse anti-FLAG M2 1:5000 (Sigma), guinea pig anti-VGLUT1 1:10,000 (Millipore, Billerica, MA, United States), mouse anti-PSD95 1:500 (NeuroMAB, UC Davis/NIH NeuroMAB Facility, Davis, CA, United States), rabbit anti-2A peptide 1:1000 (Millipore, Billerica, MA, United States), rabbit anti-FoxP1 1:8000 (Abcam, Cambridge, MA, United States), mouse anti-GFP 1:100 (NeuroMab, UC Davis/NIH NeuroMAB Facility, Davis, CA, United States), goat anti-SPO 1:1000. All secondary antibodies were obtained from Jackson ImmunoResearch (West Grove, PA, United States) and used at 1:1000.

Image analysis and statistics

All experiments were conducted by an experimenter blind to condition. Sample sizes were based on previous experiments or power analysis. Statistics were calculated in Prism (GraphPad). All data were checked first for normality using the D'Agostino & Pearson normality test. If the data passed normality, *t*-tests or ANOVA were performed; if not, Mann Whitney or Kruskal-Wallis were performed. Post hoc multiple comparisons were run on ANOVA and/or Kruskal Wallis analyzed data to generate statistical significance between groups. Intensity levels of some images were adjusted for visibility in publication, but if so, the entire field of view and all comparable conditions were adjusted similarly. All images and conditions from the same experiment were collected and analyzed using the same confocal and analysis settings.

Variant selection

Kirrel3 variants were selected for this study based on their stratification across the protein. Beginning with R40W, this point mutation is linked with intellectual disability and is located on the extracellular side before IG domain 1, within the signal sequence. R161H has been identified in ASD patients, and is predicted to fall in between IG domains 1 and 2. R205 is linked with ASD and is also found between IG domains 1 and 2. All other point mutations selected are heterozygous, but R336Q was identified in a homozygous individual with ASD. In addition to extracellular point mutations, we also wanted to investigate mutations on the intracellular side. Thus, we selected both M673I and V731F, both of which have been identified in individuals with intellectual disabilities.

Results

Kirrel3 point mutations are present on the cell surface

For Kirrel3 to function as a cell adhesion molecule, it is necessary for the protein to be trafficked to the cell surface. A mechanism thought to contribute to other synaptopathies is a failure of mutated protein to escape quality control in the ER and traffic to the cell surface (Chih et al., 2004). To test each mutated protein's ability to make it to the cell surface, we co-transfected CHO cells, which do not have Kirrel3, with each of our variant constructs of interest and GFP to label the cell. Each Kirrel3 construct is tagged on the extracellular side with a Flag epitope (Figure 4.1A, left). We live labelled with a chick anti-Flag antibody to label extracellular Flag, and then after permeabilization, added a mouse anti-Flag antibody to label intracellular Flag (Figure

4.2A). Cells were selected by GFP and the ratio of extracellular to intracellular Flag calculated using Fiji. We observed no significant differences in the ratio of extracellular to intracellular Flag between any mutated proteins as compared with wildtype Kirrel3 (Figure 4.2B). Therefore, all mutated proteins, and the ΔICD construct, successfully pass quality control within the ER and traffic to the cell surface (Figure 4.2C).

Point mutations alter Kirrel3 homophilic binding

Previously, we identified a role for Kirrel3 in hippocampal mossy fiber synapse formation between DG filopodia and GABA dendrites (Martin et al., 2017). We hypothesize that transcellular Kirrel3 homophilic binding promotes synapse development between these structures. Thus, it is possible that extracellular Kirrel3 point mutations could prevent homophilic binding and subsequent synapse development. In addition, it is known that intracellular domains are necessary for transcellular protein binding in molecules such as the classical cadherins. The intracellular domains between cadherins are highly conserved and bind actin via auxiliary actin-binding proteins to create a tension without which homophilic binding does not occur (Kannan & Tang, 2018). Thus, is will be interesting to see if intracellular Kirrel3 point mutations or our ΔICD construct also restrict homophilic binding.

To determine if Kirrel3 variants can bind in trans, we used the CHO aggregation assay in which we transfect CHO cells with our construct of interest and then float the cells in suspension to allow for aggregates to form (Martin et al., 2015). We synthesized constructs containing mCherry followed by a 2A peptide followed by our flag-tagged wildtype Kirrel3 protein or Kirrel3 with each variant of interest. This allows for us to see

simultaneous expression of mCherry in cells that also have our Kirrel3 constructs (Figure 4.3A). We measured the total mCherry fluorescence in aggregate clumps over the total amount of mCherry fluorescence in the sample to create an aggregation index measurement. We observed clumping in our wildtype Kirrel3 samples, and we observed several mutated proteins that alter Kirrel3 aggregation (Figure 4.3B). Both R205Q and V731F significantly reduce Kirrel3 aggregation to levels near control. This offers a potential mechanism by which these two mutations could introduce disease and highlights two critical protein regions. Interestingly, our ΔICD construct actually tends to increase the ability of Kirrel3 to bind. This would imply the intracellular domain is not necessary for homophilic binding, yet one of the mutations that lessens cell aggregation is intracellular, V731F. This suggests a regulatory intracellular region exists, and extracellular protein-protein interactions are sufficient to induce cell aggregation.

Mutated Kirrel3 proteins localize to synapses

Overexpressed Kirrel3 protein localizes in and around synapses (Martin et al., 2015). We questioned whether or not each Kirrel3 variant is capable of localizing to synapses. We transfected each point mutation into cultured hippocampal neurons using our mCherry-2A-Flag-Kirrel3 constructs. Neurons were selected by staining for 2A and synapses identified by the colocalization of vGlut1, a presynaptic marker, and PSD-95, a postsynaptic marker (Figure 4.4A). Surface expressed Kirrel3 protein and its variants were identified by live-labeling with Flag antibody (Figure 4.4A). We observed no differences in the number of Kirrel3 puncta present with colocalizing synaptic proteins,

nor the number of Kirrel3 puncta per dendrite examined, nor in synapse density (Figure 4.4B-D). Thus, all Kirrel3 variants are properly trafficked in neurons to synapses.

Kirrel3 promotes synapse development

We hypothesize that homophilic binding of Kirrel3 is required for synapses to form between neurons expressing Kirrel3. To establish an in vitro assay of Kirrel3's synaptic function, we adapted the previously published SPO assay (Williams et al., 2011). Briefly, cultured hippocampal neurons largely retain their neuron-to-neuron specific connectivity as found in vivo (Williams et al., 2011). DG axons do not normally synapse onto CA1 neurons in vivo or in vitro. As Kirrel3 is endogenously expressed by DG neurons, we examined if Kirrel3 transfected into CA1 neurons could promote ectopic synapses to form between DG and CA1 neurons in culture. We reason that if ectopic DG synapses form onto Kirrel3-transfected CA1 neurons and not GFP-transfected neurons, then transcellular Kirrel3 signaling promotes synapse development. We can identify both CA1 neurons and DG synapses through combinatorial immunostaining with the following markers: CA1 neurons are identified by FoxP1 in developing cells (Figure 4.5A) (Ferland et al., 2003), CA synapses are identified by staining with presynaptic marker VGlut1 (vesicular glutamate transporter 1), a population of inhibitory synapses are identified by staining with presynaptic marker SPO (synaptophysin II), and DG synapses are identified by colocalization of VGlut1 and SPO (Figure 4.5B).

We first examined GFP-transfected neurons (Figure 4.5C) and Kirrel3 and GFP co-transfected neurons (Figure 4.5D) for the number of DG synapses made onto CA1 neurons. While we observed no difference in the number of CA synapses (VGlut1+ only)

or inhibitory synapses (SPO+ only), we found a significant twofold increase in the number of DG synapses onto Kirrel3-transfected CA1 neurons as opposed to GFP-transfected CA1 neurons (Figure 4.5E-G). We also observed no difference in the length of dendrite examined (Figure 4.5H). Total synapse density appears to increase in GFP and Kirrel3 co-transfected neurons, but the data do not reach significance (Figure 4.5I). These results support a role for Kirrel3 in targeted synapse development between neurons expressing Kirrel3.

Point mutations eliminate Kirrel3's ability to promote synapse development

We next examined if our point mutation constructs could eliminate Kirrel3's synaptic development function. This assay relies upon endogenous expression of full length Kirrel3 in DG neurons and thus tests for the ability of mutant Kirrel3 protein to bind with wildtype. We carried out the SPO assay for each point mutation of interest, co-transfected with GFP. Surprisingly several point mutations showed no increased DG synapse density (Figure 4.6A). Of all the point mutations tested, only R336Q and M673I appear to recapitulate Kirrel3's synapse development function. Also of interest is that the del-ICD construct is able to recapitulate Kirrel3's synapse development function. Upon reviewing the difference in total synapse density, GFP and Kirrel3 cotransfected neurons display an increased number of synapses that reaches significance in this assay, likely due to an increase in the number of neurons analyzed. However, none of the point mutations reflect this increase (Figure 4.6B). These results indicate that both extracellular and intracellular mutations can hamper Kirrel3-mediated synapse development. However, a

power analysis based off of previous assay results suggests the sample size is not yet large enough to draw conclusions. While currently, 18-46 neurons were sampled per construct, our power analysis suggests 30 neurons per condition. We will increase our sample size to this value.

Discussion

Here we offer the first examination of rare Kirrel3 variants and their impact on cell function. In summary, we find Kirrel3 variants do not show defects in cell surface expression nor neuronal trafficking to synapses, but instead, we find specific variants prevent cell aggregation and targeted synapse development. Fascinatingly, variants that prevent cell aggregation are located both on the extracellular and intracellular regions of the protein and our findings highlight the critical need to understand the function of the Kirrel3 intracellular domain. There is also evidence to support that the extracellular region of Kirrel3 is cleaved by metalloproteases; however, this has not yet been observed in the brain (Gerke et al., 2005). Our results could indicate differences in extracellular cleavage, protein turnover, or the timing of surface expression mediated through other protein interactors. It is also unknown if Kirrel3 is able to bind in cis, which could implicate additional levels of regulation between same-cell proteins. Several synaptic cell adhesion proteins of the immunoglobulin superfamily have been found to dimerize and their lateral assembly is necessary for synaptic function (Fogel et al., 2011).

Complete loss of the intracellular domain does not hamper cell aggregation; instead, it appears to enhance it. In addition, our ΔICD construct appears to mediate synapse development as well. We interpret these results as a loss of intracellular

regulation. Upon loss of regulatory elements, the molecule reverts into a simple "molecular velcro" that is able to promote synapse development through nonregulated homophilic binding. It will be of interest in the future to examine how loss of the intracellular domain affects protein management at the synapse.

In addition, we find Kirrel3 induces targeted synapse development onto other neurons also expressing Kirrel3. This supports our previous finding that Kirrel3 is necessary for formation of DG-GABA filopodial synapses (Martin et al., 2017). It will be important in the future to identify types of neurons expressing Kirrel3 in other brain regions that may similarly use this molecule to orchestrate synapse development.

Finally, we know Kirrel3 is an alternatively spliced protein with multiple isoforms found within the hippocampus. In particular, one form presents with a heavily truncated intracellular domain. This isoform is without the region that includes point mutation V731F, and is unable to increase DG synapses within the SPO assay (unpublished data). It would be of interest to add this region back into the protein to see if it rescues function.

Overall, our work further establishes Kirrel3 as a critical molecule in proper brain development. Our study highlights critical regions of the Kirrel3 molecule and offers the first mechanistic insight into how Kirrel3 alterations could result in disease.

Acknowledgements

We thank Yueqi Wang and Jennifer Hunter for their assistance in cloning point mutants, Matt Taylor for manuscript comments and insights, and Derek Woodruff for analysis of point mutation protein modifications.

References

Ben-David, E., & Shifman, S. (2012). Networks of neuronal genes affected by common and rare variants in autism spectrum disorders. *PLoS Genetics, 8*(3). doi:10.1371/journal.pgen.1002556

Betancur, C. (2011). Etiological heterogeneity in autism spectrum disorders: More than 100 genetic and genomic disorders and still counting. *Brain Research, 1380*, 42-77. doi:10.1016/j.brainres.2010.11.078

Bhalla, K., Luo, Y., Buchan, T., Beachem, M. A., Guzauskas, G. F., Ladd, S., . . . Srivastava, A. K. (2008). Alterations in CDH15 and KIRREL3 in patients with mild to severe intellectual disability. *The American Journal of Human Genetics, 83*(6), 703-713. doi:10.1016/j.ajhg.2008.10.020

Cheng, Y., Quinn, J. F., & Weiss, L. A. (2013). An eQTL mapping approach reveals that rare variants in the SEMA5A regulatory network impact autism risk. *Human Molecular Genetics, 22*(14), 2960-2972. doi:10.1093/hmg/ddt150

Chih, B., Afridi, S. K., Clark, L., & Scheiffele, P. (2004). Disorder-associated mutations lead to functional inactivation of neuroligins. *Human Molecular Genetics, 13*(14), 1471-1477. doi:10.1093/hmg/ddh158

Choi, S., Han, K., Cutforth, T., Chung, W., Park, H., Lee, D., . . . Kim, E. (2015). Mice lacking the synaptic adhesion molecule Neph2/Kirrel3 display moderate hyperactivity and defective novel object preference. *Frontiers in Cellular Neuroscience, 9*. doi:10.3389/fncel.2015.00283

De Rubeis, S., He, X., Goldberg, A. P., Poultney, C. S., Samocha, K., Cicek, A. E., . . . Buxbaum, J. D. (2014). Synaptic, transcriptional and chromatin genes disrupted in autism. *Nature, 515*(7526), 209–215. http://doi.org/10.1038/nature13772

Ferland, R. J., Cherry, T. J., Preware, P. O., Morrisey, E. E., & Walsh, C. A. (2003). Characterization of Foxp2 and Foxp1 mRNA and protein in the developing and mature brain. *The Journal of Comparative Neurology, 460*(2), 266-279. doi:10.1002/cne.10654

Fogel, A. I., Stagi, M., Arce, K. P., & Biederer, T. (2011). Lateral assembly of the immunoglobulin protein SynCAM 1 controls its adhesive function and instructs synapse formation. *The EMBO Journal, 30*(23), 4728-4738. doi:10.1038/emboj.2011.336

Gerke, P. (2005). NEPH2 is located at the glomerular slit diaphragm, interacts with nephrin and is cleaved from podocytes by metalloproteinases. *Journal of the American Society of Nephrology, 16*(6), 1693-1702. doi:10.1681/asn.2004060439

Guerin, A., Stavropoulos, D. J., Diab, Y., Chénier, S., Christensen, H., Kahr, W. H., . . . Chitayat, D. (2012). Interstitial deletion of 11q-implicating the KIRREL3 gene in the

neurocognitive delay associated with Jacobsen syndrome. *American Journal of Medical Genetics Part A, 158A*(10), 2551-2556. doi:10.1002/ajmg.a.35621

Hisaoka, T., Komori, T., Kitamura, T., & Morikawa, Y. (2018). Abnormal behaviours relevant to neurodevelopmental disorders in Kirrel3-knockout mice. *Scientific Reports ,8*(1). doi:10.1038/s41598-018-19844-7

Iossifov, I., Ronemus, M., Levy, D., Wang, Z., Hakker, I., Rosenbaum, J., . . . Wigler, M. (2012). De novo gene disruptions in children on the autistic spectrum, *74*(2), 285–299. http://doi.org/10.1016/j.neuron.2012.04.009

Kalsner, L., Twachtman-Bassett, J., Tokarski, K., Stanley, C., Dumont-Mathieu, T., Cotney, J., & Chamberlain, S. (2017). Genetic testing including targeted gene panel in a diverse clinical population of children with autism spectrum disorder: Findings and implications. *Molecular Genetics & Genomic Medicine, 6*(2), 171-185. doi:10.1002/mgg3.354

Kaminsky, E. B., Kaul, V., Paschall, J., Church, D. M., Bunke, B., Kunig, D., . . . Martin, C. L. (2011) An evidence-based approach to establish the functional and clinical significance of CNVs in intellectual and developmental disabilities. *Genetics in Medicine, 13*, 777–784. doi: 10.1097/GIM.0b013e31822c79f9

Kannan, N., & Tang, V. W. (2018). Myosin-1c promotes E-cadherin tension and force-dependent recruitment of α-actinin to the epithelial cell junction. *Journal of Cell Science, 131*(12). doi:10.1242/jcs.211334

Martin, E. A., Muralidhar, S., Wang, Z., Cervantes, D. C., Basu, R., Taylor, M. R., . . . Williams, M. E. (2015). The intellectual disability gene Kirrel3 regulates target-specific mossy fiber synapse development in the hippocampus. *ELife, 4*. doi:10.7554/elife.09395

Martin, E. A., Woodruff, D., Rawson, R. L., & Williams, M. E. (2017). Examining hippocampal mossy fiber synapses by 3D electron microscopy in wildtype and Kirrel3 knockout mice. *Eneuro, 4*(3). doi:10.1523/eneuro.0088-17.2017

Michaelson, J., Shi, Y., Gujral, M., Zheng, H., Malhotra, D., Jin, X., . . . Sebat, J. (2012). Whole-genome sequencing in autism identifies hot spots for de novo germline mutation. *Cell, 151*(7), 1431-1442. doi:10.1016/j.cell.2012.11.019

Neale, B. M., Kou, Y., Liu, L., Ma'ayan, A., Samocha, K. E., Sabo, A., . . . Daly, M. J. (2012). Patterns and rates of exonic de novo mutations in autism spectrum disorders. *Nature, 485*(7397), 242–245. doi: 10.1038/nature11011

Prince, J. E., Brignall, A. C., Cutforth, T., Shen, K., & Cloutier, J. (2013). Kirrel3 is required for the coalescence of vomeronasal sensory neuron axons into glomeruli and for male-male aggression. *Development, 140*(11), 2398-2408. doi:10.1242/dev.087262

Südhof, T. C. (2008). Neuroligins and neurexins link synaptic function to cognitive disease. *Nature, 455*(7215), 903-911. doi:10.1038/nature07456

Talkowski, M., Rosenfeld, J., Blumenthal, I., Pillalamarri, V., Chiang, C., Heilbut, A., . . . Gusella, J. (2012). Sequencing chromosomal abnormalities reveals neurodevelopmental loci that confer risk across diagnostic boundaries. *Cell, 149*(3), 525-537. doi:10.1016/j.cell.2012.03.028

Völker, L. A., Maar, B. A., Guevara, B. A., Bilkei-Gorzo, A., Zimmer, A., Brönneke, H., . . . Hoehne, M. (2018). Neph2/Kirrel3 regulates sensory input, motor coordination, and home-cage activity in rodents. *Genes, Brain and Behavior*. doi:10.1111/gbb.12516

Washbourne, P. (2014). Synapse assembly and neurodevelopmental disorders. *Neuropsychopharmacology, 40*(1), 4-15. doi:10.1038/npp.2014.163

Williams, M., Wilke, S., Daggett, A., Davis, E., Otto, S., Ravi, D., . . . Ghosh, A. (2011). Cadherin-9 regulates synapse-specific differentiation in the developing hippocampus. *Neuron, 71*(4), 640-655. doi:10.1016/j.neuron.2011.06.019

Zoghbi, H. Y., & Bear, M. F. (2012). Synaptic dysfunction in neurodevelopmental disorders associated with autism and intellectual disabilities. *Cold Spring Harbor Perspectives in Biology, 4*(3). doi:10.1101/cshperspect.a009886

Figure One

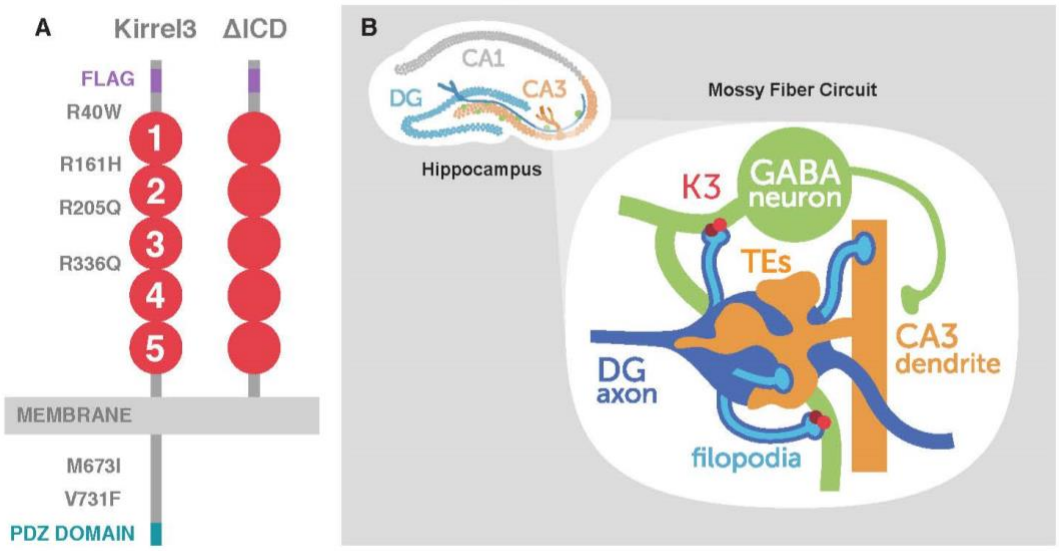

Figure 4.1: Kirrel3 is a transmembrane cell adhesion molecule in the immunoglobulin superfamily. (A) (left) Diagram of Kirrel3 protein and location of inserted FLAG tag, PDZ binding domain, and tested point mutations. Numbers identify separate immunoglobulin domains. (right) Diagram of synthesized Kirrel3 without the intracellular domain. (B) Diagram of hippocampal mossy fiber circuit location and morphology. Abbreviations: deleted intracellular domain, ΔICD; Kirrel3, K3

Figure 4.2: Kirrel3 variants are surface expressed. (A) Diagram explaining surface expression assay. Extracellular protein (purple) and intracellular protein (beige) are shown. (B-C) Cultured CHO cells were cotransfected with GFP and each Flag-Kirrel3 variant construct of interest and immunostained for indicated markers. Chick anti-FLAG antibody was added prior to fixation to label only surface Kirrel3. Mouse anti-FLAG antibody was added postfixation to label intracellular Kirrel3. Hoescht was used post-immunostain to label cell nuclei. Cells selected by presence of GFP and Integrated Density (IntDen) measured in EC and IC channels. Extra/Intracellular Ratio calculated by dividing Extracellular IntDen by Intracellular IntDen. Quantification shown in (B) normalized to wildtype Kirrel3 shows no significant differences as measured by Kruskal-Wallis test. Line demarcates normalized value of 1. Mean ± SEM shown. $N = 3$ cells per construct per culture, 3 cultures total. P value = 0.4410. Representative images shown for each construct in (C). Abbreviations: deleted intracellular domain, ΔICD; Extracellular, EC; Intracellular, IC

Figure Two

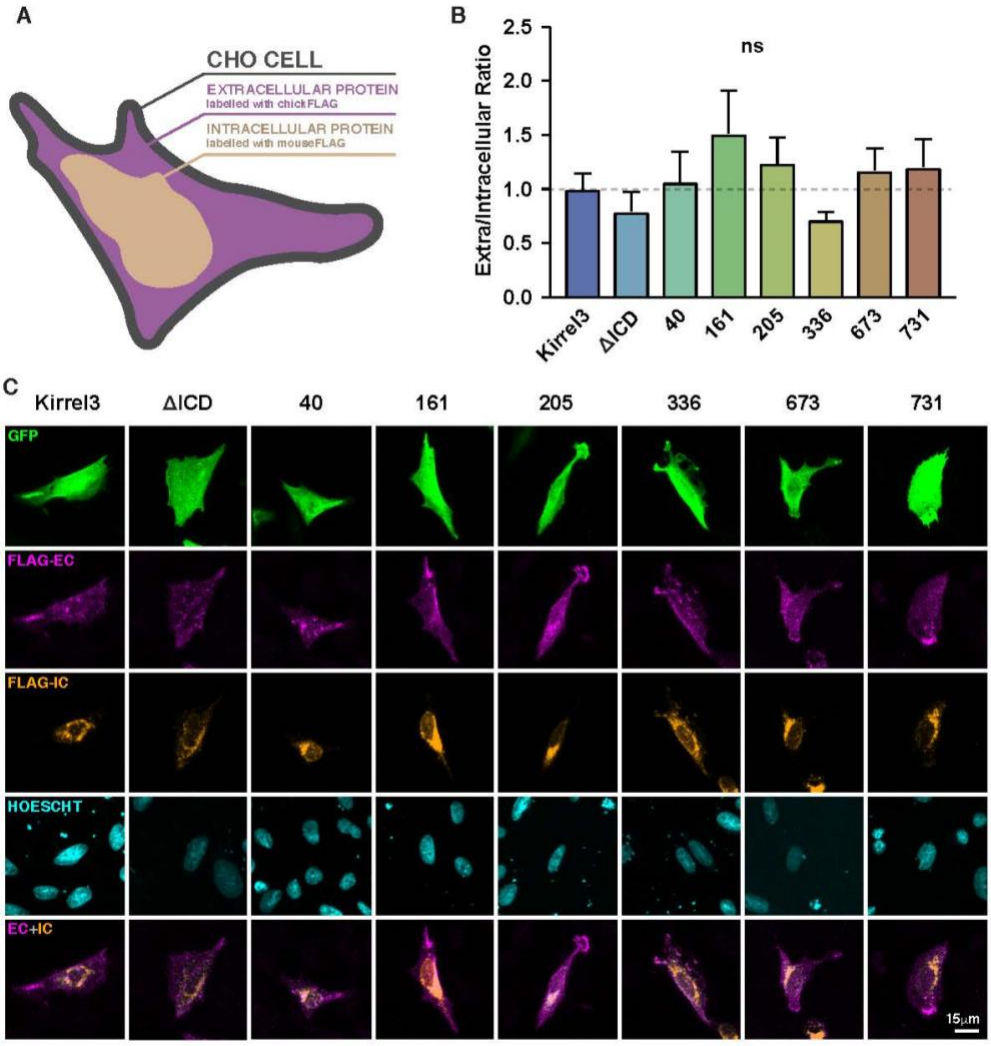
A
CHO CELL
EXTRACELLULAR PROTEIN
labelled with chickFLAG
INTRACELLULAR PROTEIN
labelled with mouseFLAG
B
Extra/Intracellular Ratio
2.5
2.0
1.5
1.0
0.5
0.0
ns
Kirrel3
ΔICD
40
161
205
336
673
731
C
Kirrel3
ΔICD
40
161
205
336
673
731
GFP
FLAG-EC
FLAG-IC
HOESCHT
EC+IC
15μm

Figure Three

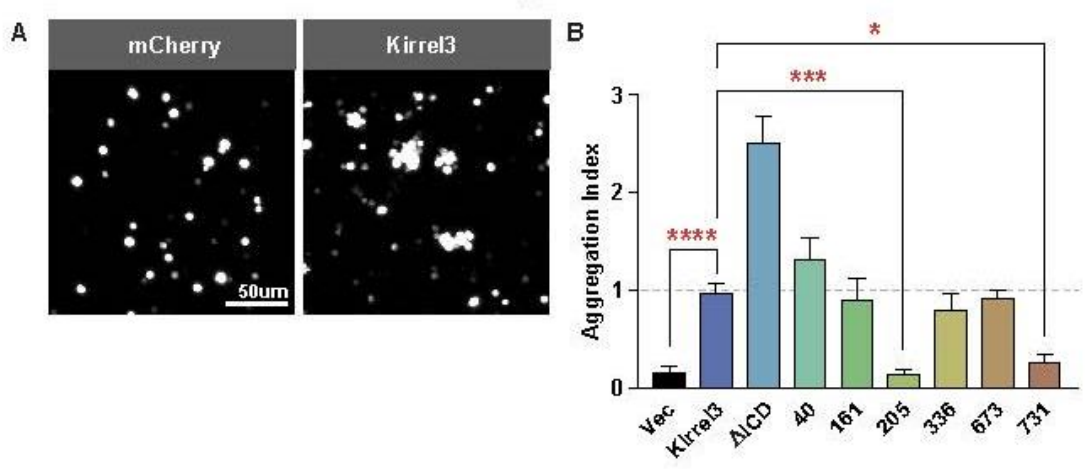

Figure 4.3: Cell aggregation is altered by some Kirrel3 variants. (A-B) CHO cells were transfected with mCherry or mCherry-2A-Flag-Kirrel3 variant constructs and then tested for adhesion. Representative images show CHO cells transfected with mCherry or mCherry-2A-Flag-Kirrel3 and imaged for mCherry. (A) Aggregation index calculated by dividing the total mCherry fluorescence in aggregated cells by total mCherry fluorescence in the sample well. mCherry, R205Q, and V731F each showed reduced aggregation when compared to wildtype Kirrel3. Line demarcates normalized value of 1. (D) Mean ± SEM shown. $N = 3$ wells per construct per culture, 3 cultures total normalized to Kirrel3. **** indicates $p < .0001$, *** indicates $p = .0004$, * indicated $p = .0109$ by Kruskal-Wallis test followed by post hoc test to Kirrel3. Abbreviations: vector, Vec; deleted intracellular domain, ΔICD

Figure Four

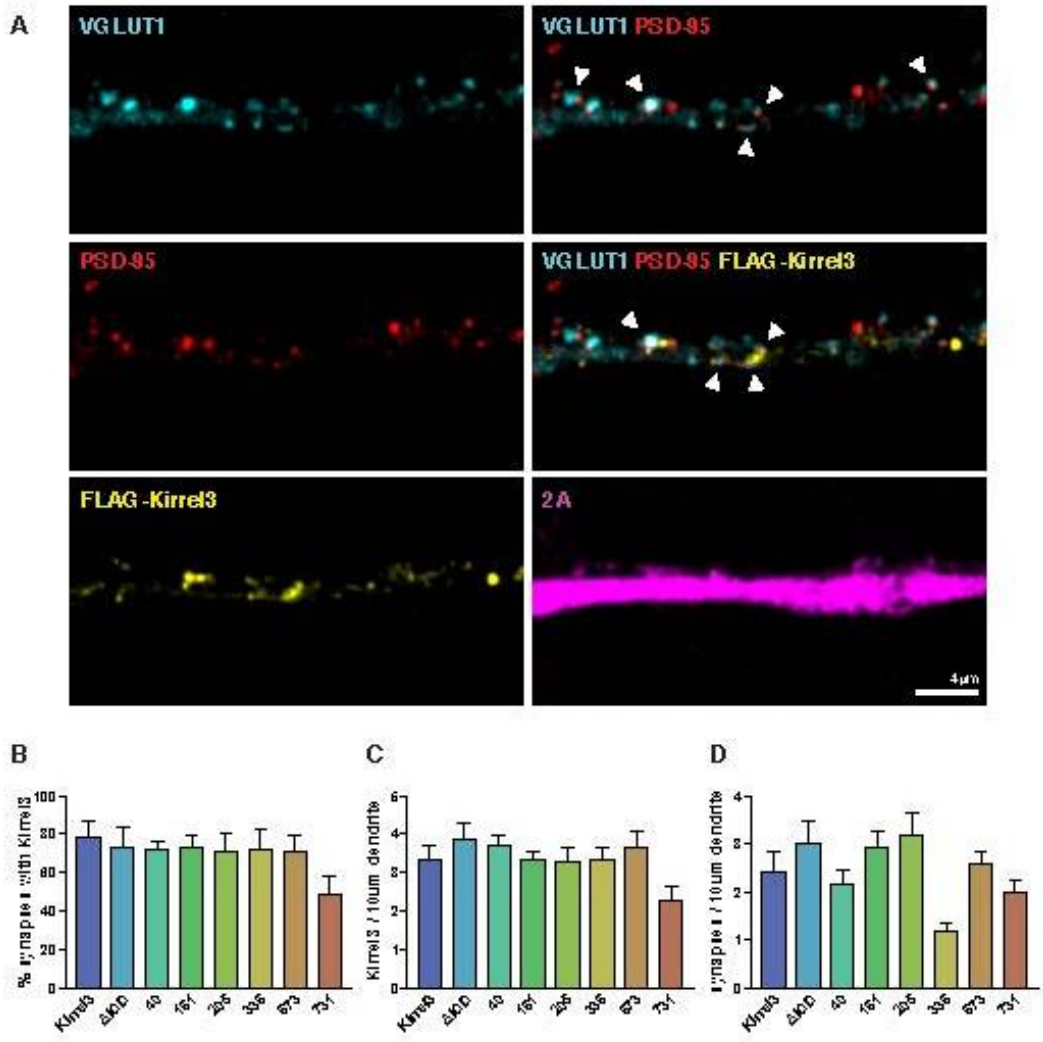

Figure 4.4: Kirrel3 variants are similarly expressed at synapses. (A) Cultured hippocampal neurons were transfected with mCherry-2A-Flag-Kirrel3 variant constructs. At DIV21, Anti-FLAG antibodies were added prior to fixation to label only surface Kirrel3 (yellow). Cells were subsequently immunostained with vGlut1 (cyan) to mark presynaptic puncta, PSD-95 (red) to label postsynaptic puncta, and 2A (magenta) to identify transfected neurons. White arrows indicate synapses found by co-localization of vGlut1 and PSD-95 along transfected dendrites. No significant difference was found in the percent of synapses with Kirrel3 (B), the density of Kirrel3 puncta per 10um dendrite (C), nor the density of synapses per 10um dendrite (D). Mean ± SEM shown. *N* = 9-19 neurons from one culture. Abbreviation: days in vitro, DIV; deleted intracellular domain, ΔICD

Figure 4.5: Kirrel3 induces DG synapse formation onto transfected CA1 neurons. (A) Diagram showing a Kirrel3-transfected CA1 neuron with representative synaptic markers: vGlut1 identifying excitatory synapses (red), SPO identifying dg mossy fiber synapses and some inhibitory synapses (green), and vGlut1+SPO+ co-localized puncta identifying dg mossy fiber synapses (yellow). (B) P8 rat was perfused in 4% PFA and brain removed. Tissue was sliced into 100um slices and immunostained with FOXPI (red). (C-H) Cultured hippocampal neurons were electroporated with GFP (C) or co-electroporated with GFP and Kirrel3 (D). At DIV14, cells were immunostained for GFP (purple), SPO (red), vGlut1 (green), and FoxP1 (not shown). White arrows indicate DG synapses identified by colocalization of vGlut1 and SPO (D). Kirrel3-transfected CA1 neurons had significantly more DG synapses than GFP-transfected CA1 neurons (E). No significant differences were found in CA synapse density (F), spo+ only synapse density (G), or in the dendrite length examined (H). Total synapse density trends towards significance (I). Mean ± SEM are shown. N = 48 GFP transfected neurons and 38 GFP + Kirrel3 cotransfected neurons from three separate cultures normalized to GFP. ** indicates p = .0020 by Mann Whitney test.

Figure Five

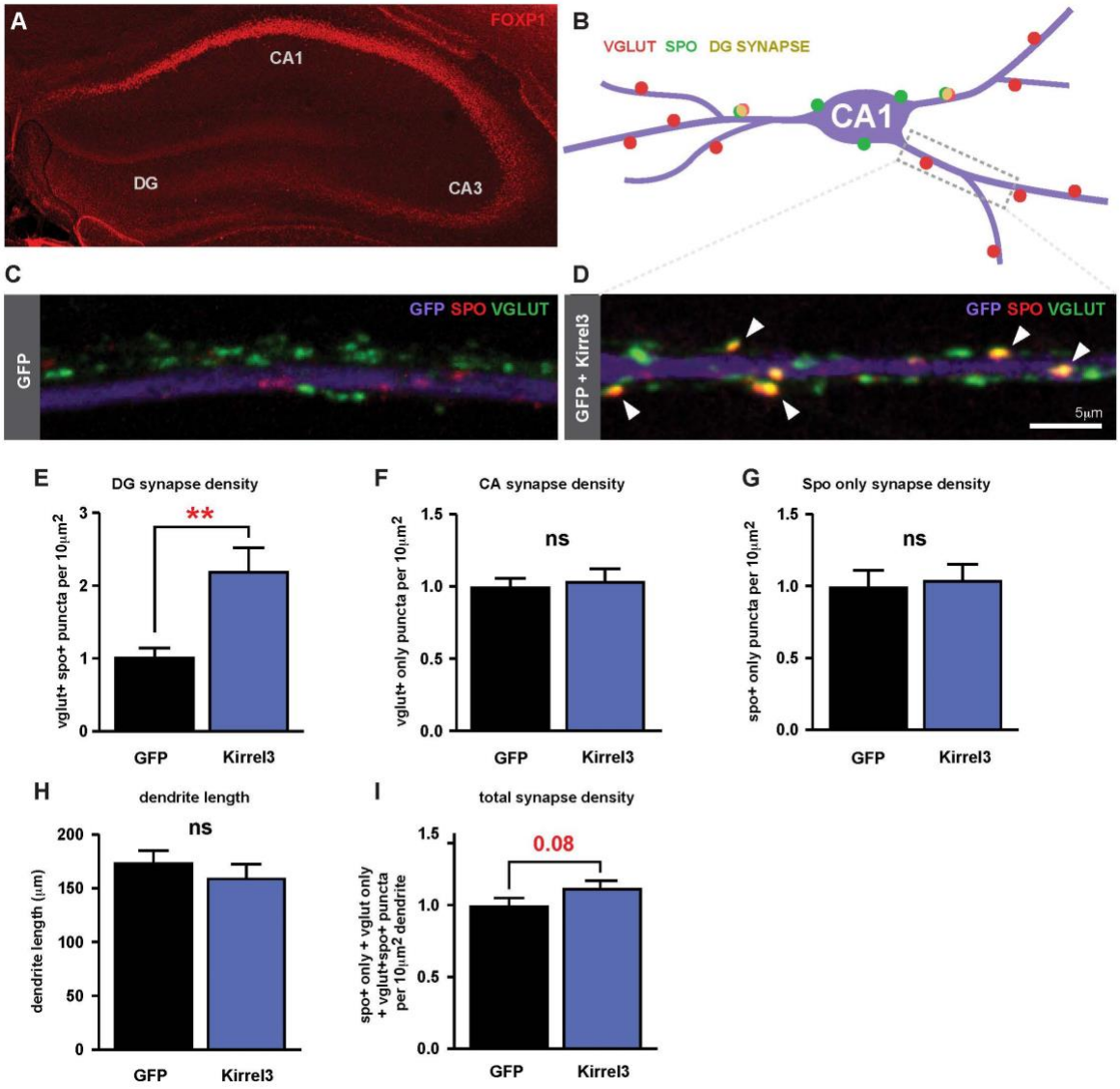
A
FOXP1
CA1
DG
CA3
B
VGLUT SPO DG SYNAPSE
CA1
C
GFP
GFP SPO VGLUT
D
GFP + Kirrel3
GFP SPO VGLUT
5µm
E
DG synapse density
**
vglut+ spo+ puncta per 10µm2
GFP
Kirrel3
F
CA synapse density
ns
vglut+ only puncta per 10µm2
GFP
Kirrel3
G
Spo only synapse density
ns
spo+ only puncta per 10µm2
GFP
Kirrel3
H
dendrite length
ns
dendrite length (µm)
GFP
Kirrel3
I
total synapse density
0.08
spo+ only + vglut only + vglut+spo+ puncta per 10µm2 dendrite
GFP
Kirrel3

Figure Six

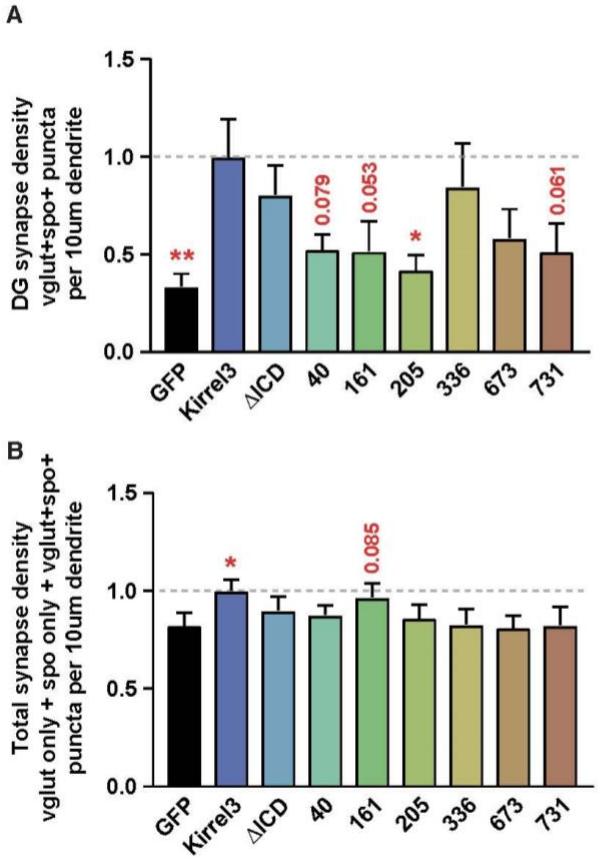

Figure 4.6: Kirrel3 variants impair synapse formation (A-B) Cultured hippocampal neurons were electroporated with GFP or co-electroporated with GFP and Kirrel3 construct of interest. At DIV14, cells were immunostained. Kirrel3-transfected CA1 neurons had significantly more DG synapses than GFP-transfected CA1 neurons (A). ΔICD-transfected CA1 neurons had near significantly more DG synapses than GFP-transfected neurons (A). No significant differences were found in total synapse density, though trends followed those observed in Figure 4.5 (B). Mean ± SEM are shown. *N* = 18-46 neurons from two-four separate cultures normalized to Kirrel3. * indicates *p* </= .05 ** indicates *p* </= .01 by pairwise Kruskal Wallis test followed by an uncorrected Dunn's post hoc test to Kirrel3 in A and GFP in B.

CHAPTER 5

DISCUSSION

Overview

In Chapter 2, we described the first investigation of immunoglobulin superfamily member Kirrel3 at mammalian synapses. We found Kirrel3 is a homophilic, synaptic protein and loss of Kirrel3 results in a reduction of mossy fiber filopodia, the structures that facilitate DG synapses onto GABA neurons. Furthermore, we found that loss of Kirrel3 translated into perturbation of the excitation/inhibition ratio via increased activity of CA3 neurons. In Chapter 3, we looked closer at these mossy fiber filopodia by electron microscopy and found the loss of mossy fiber filopodia in Kirrel3 knockout mice resulted in fewer DG-to-GABA filopodial synapses during development, but no change in the number of en passant synapses. Here we also made several novel observations about wildtype mossy fiber filopodia including a change in their synaptic targets. We found that slightly more than 50% of mossy fiber filopodia synapse onto CA3 pyramidal neurons instead of 100% onto GABA neurons as previously described in literature (Acsády, Kamondi, Sík, Freund, & Buzsáki, 1998). In Chapter 4, we looked closer at the functional regions of Kirrel3 and tested if rare Kirrel3 variants found in humans attenuate Kirrel3 function. We found several point mutations that compromise Kirrel3 function in both cell aggregation and synapse development in culture.

While my work in graduate school has provided answers to many of our initial questions about Kirrel3, many important questions remain and several more have been introduced. Is Kirrel3 just a cell adhesion molecule or is it doing more? What does Kirrel3 bind? How does Kirrel3 function at synapses? Why does Kirrel3 function at DG-GABA filopodial synapses and not en passant synapses? In this chapter, I will propose

ideas for future studies of Kirrel3 and its role in neural circuit development to address these questions.

How does Kirrel3 function at synapses?

Through our investigations of Kirrel3 in synapse formation, we observed reductions in filopodia density, filopodial synapse density, and CA3 neuron activity upon Kirrel3 loss. We also discovered defects in cell aggregation and synapse development in Kirrel3-transfected neurons upon introduction of Kirrel3 variants. However, these analyses were conducted without visualizing Kirrel3 and its exact location in vivo. We have some clues to Kirrel3 localization through overexpression experiments in which we used epitope-tagging to see Kirrel3 localized at synapses. However, to understand how Kirrel3 contributes to synapse formation over time, we need an in vivo examination of Kirrel3 localization.

It would be informative to conduct immuno electron microscopy work to see if Kirrel3 localizes to en passant synapses as well as filopodial synapses. If Kirrel3 localizes to both synapses, it would suggest that a critical Kirrel3 partner protein is not present at en passant synapses, but present at filopodial synapses to promote synapse formation. Alternatively, en passant synapses could form earlier in development than filopodial synapses, at a time when Kirrel3 is not at high enough levels to promote synapse formation. In support, while the timeline of en passant synapse formation is unknown, en passant synapses visualized in our analyses were generally larger and more mature than filopodial synapses. Secondly, in our eLife publication, we included a synaptosome preparation examining Kirrel3 levels at postnatal day (P) 9, P21, and adult (Martin et al.,

2015). Kirrel3 expression was low at P9 and increased at P21; however, we do not know about the expression of Kirrel3 at earlier time points. It is also possible that Kirrel3 does not localize to filopodial synapses at all, but instead orchestrates filopodial synapse formation through interactions with other proteins. For instance, Kirrel3 could interact with actin-binding proteins to motivate filopodia extension and motility to create a structure for synapse formation to occur. Or, Kirrel3 could manage synapses downstream of synapse formation and instead provide scaffolding for synapse stabilization. Time-dependent localization assays will help narrow down these possibilities.

What are Kirrel3's binding partners?

Particularly in Chapter 4, we questioned if Kirrel3 acted more as a pure cell adhesion molecule or if the intracellular domain also plays an important role in the molecule's ability to promote synapse formation. We used a construct with the intracellular domain deleted (ΔICD) to determine if the extracellular IG domains were the only necessary factor for cell adhesion and synapse formation. While the ΔICD construct showed no defect in cell aggregation as expected, it instead aggregated more than other Kirrel3 constructs. Interestingly, in our SPO synapse formation assay, the ΔICD construct also showed no loss of function. This would support the idea that the intracellular domain is not necessary for synapse formation, and instead, Kirrel3 is acting purely as a cell adhesion molecule to hold the membranes together. However, in our analyses, we did find that one intracellular mutation did reduce Kirrel3's synapse formation function. This contradicts the pure cell adhesion hypothesis, and instead leads us to think that there is an important regulatory region on the intracellular side that manages protein turnover or

posttranslational modification to impact Kirrel3 function. Upon deleting this domain, we have reduced the construct to a simple molecular glue.

These results highlight the need to identify the intracellular binding partners of Kirrel3. Now that we know some of the critical functional domains through our variant analysis, we can identify key Kirrel3 binding partners and subsequent downstream signaling pathways. Some in vitro support exists for Kirrel3 to bind other synaptic molecules by its PDZ domain such as calmodulin-associated serine/threonin kinase calmodulin-associated serine/threonin kinase (CASK), Fyn kinase, PICK1, and ZO-1 (Bhalla et al., 2008; Harita et al., 2008; Höhne et al., 2011; Huber et al., 2003). Another study used a yeast two-hybrid screen to identify extracellular binding partners MAP1B and MYO16, and intracellular binding partners ATP1B1, UFC1, and SHMT2 (Liu et al., 2015). They verified these partners by completing immunoprecipitations with transfected 293 cells; however, their only evidence for interaction in neurons was through co-localization in immunostaining experiments. It would be of value to complete an unbiased examination of Kirrel3 binding partners through proteomics. Completing pull downs followed by mass spectrometry would be a much more thorough and robust analysis of Kirrel3 binding partners.

Finally, we know from our aggregation assays that Kirrel3 can accomplish homophilic binding in trans. However, we do not know if Kirrel3 can bind in cis. Synaptic cell adhesion molecules such as SynCAM1 can oligomerize together in cis via its immunoglobulin domains. This lateral formation of SynCAM1 is shown to increase adhesion, promote clustering of axo-dendritic contact points in neurons, and removing this oligomerization reduces synaptogenesis (Fogel, Stagi, de Arce, & Biederer, 2011).

These findings could also be relevant for Kirrel3 and explain some of the defects observed in Kirrel3 variants in Chapter 4.

What GABA neurons express Kirrel3?

Earlier in this discussion, I suggested Kirrel3 might govern DG-GABA filopodial synapses but not en passant synapses because Kirrel3 might selectively localize to DG filopodia. Another qualifying factor are the types of GABA neurons that make en passant and filopodial synapses. There could be distinct populations of GABA neurons that synapse with DG neurons at en passants as opposed to filopodia, potentially governed by Kirrel3 expression. We did not examine in Chapter 3 if filopodia and en passant synapses ever occurred on the same GABA neuron. We can now return to this dataset to answer this question.

In Chapter 2, we described the population of GABA neurons expressing Kirrel3. Using a number of antibodies for GABA neuron markers, we found that 67% and 19% of Kirrel3 positive interneurons in the CA3 region of the hippocampus colabel with Calbindin and Somatostatin, respectively. This identifies an unknown population of GABA neurons in which we do not know their synaptic partners nor other properties. Further analysis will need to be performed on these interneurons to determine their role within the hippocampus.

Why do mossy fiber filopodia synapse with both GABA and CA3 neurons?

Perhaps the most surprising finding we made was discovering that wildtype mossy fiber filopodia synapse with both GABA and CA3 neurons in development. This was unanticipated due to the fact that it is established in the field that DG filopodia solely synapse with GABA neurons to facilitate feed forward inhibition onto CA3 neurons. However, upon review, this finding is attributed solely to a single study in which only four filopodia were examined of 52.7% that were not observed to synapse with substance P receptor-positive GABA neurons (Acsády et al., 1998). Our findings highlight the importance of being open minded with regards to established dogma in the field.

It is possible that our observation of DG filopodia synapsing with both GABA and CA3 pyramidal neurons is a developmental phenomenon that disappears in adulthood. Our datasets capture young mice at P14 and we have not analyzed adult mice for defects. Further analysis will need to be done to discover if this phenomenon exists in adult animals as well. Regardless, it is a curious finding from the perspective of efficiency. Why might a DG axon utilize filopodial synapses to connect to CA3 neurons when thorny excrescences already exist to connect these structures? It is known that thorny excrescences, the postsynaptic spines connecting DG axons to CA3 dendrites, form early in development at P7 in rodents, prior to filopodia eruption at P14 (Wilke et al., 2013). Perhaps because filopodia are more plastic and motile, they can more easily manage shifting circuit needs between excitation and inhibition. But what feedback properties determine these shifts? Otherwise, some filopodial structures could also

function as extensions of the main bouton as a way of exploring the direction the main bouton will move in the near future.

Regardless, this finding makes our previous discovery of reduced filopodial density in Kirrel3 knockouts more significant. Previously we had assumed only 30% of DG-to-GABA filopodia were lost in Kirrel3 knockouts as observed by our DiI light microscopy experiments in Chapter 2. Instead, we find that 30% represents a much larger chunk of the DG-to-GABA filopodia as more than 50% of the filopodia contact CA3 neurons. This further explains the large increases we see in CA3 neuron activity in Kirrel3 knockouts.

Conclusion

In this dissertation, I have presented the first examination of Kirrel3 at mammalian synapses and made a number of novel insights. These results will help guide the course of future research in the lab to further uncover the mechanisms of Kirrel3 function.

References

Acsády, L., Kamondi, A., Sík, A., Freund, T., & Buzsáki, G. (1998). GABAergic cells are the major postsynaptic targets of mossy fibers in the rat hippocampus. *The Journal of Neuroscience, 18*(9), 3386-3403. doi:10.1523/jneurosci.18-09-03386.1998

Bhalla, K., Luo, Y., Buchan, T., Beachem, M. A., Guzauskas, G. F., Ladd, S., . . . Srivastava, A. K. (2008). Alterations in CDH15 and KIRREL3 in patients with mild to severe intellectual disability. *The American Journal of Human Genetics, 83*(6), 703-713. doi:10.1016/j.ajhg.2008.10.020

Fogel, A. I., Stagi, M., Arce, K. P., & Biederer, T. (2011). Lateral assembly of the immunoglobulin protein SynCAM 1 controls its adhesive function and instructs synapse formation. *The EMBO Journal, 30*(23), 4728-4738. doi:10.1038/emboj.2011.336

Harita, Y., Kurihara, H., Kosako, H., Tezuka, T., Sekine, T., Igarashi, T., & Hattori, S. (2008). Neph1, a component of the kidney slit diaphragm, is tyrosine-phosphorylated by the Src family tyrosine kinase and modulates intracellular signaling by binding to Grb2. *Journal of Biological Chemistry, 283*(14), 9177-9186. doi:10.1074/jbc.m707247200

Hohne, M., Lorscheider, J., Bardeleben, A. V., Dufner, M., Scharf, M. A., Godel, M., . . . Benzing, T. (2011). The BAR domain protein PICK1 regulates cell recognition and morphogenesis by interacting with Neph proteins. *Molecular and Cellular Biology, 31*(16), 3241-3251. doi:10.1128/mcb.05286-11

Huber, T. B., Schmidts, M., Gerke, P., Schermer, B., Zahn, A., Hartleben, B., . . . Benzing, T. (2003). The carboxyl terminus of Neph family members binds to the PDZ domain protein Zonula Occludens-1. *Journal of Biological Chemistry, 278*(15), 13417-13421. doi:10.1074/jbc.c200678200

Liu, Y. F., Sowell, S. M., Luo, Y., Chaubey, A., Cameron, R. S., Kim, H., & Srivastava, A. K. (2015). Autism and intellectual disability-associated KIRREL3 interacts with neuronal proteins MAP1B and MYO16 with potential roles in neurodevelopment. *Plos One, 10*(4). doi:10.1371/journal.pone.0123106

Wilke, S. A., Antonios, J. K., Bushong, E. A., Badkoobehi, A., Malek, E., Hwang, M., . . . Ghosh, A. (2013). Deconstructing complexity: Serial block-face electron microscopic analysis of the hippocampal mossy fiber synapse. *Journal of Neuroscience, 33*(2), 507-522. doi:10.1523/jneurosci.1600-12.2013